FRACTIONAL – DYNAMIC INFILTRATION IN WATER REPLLENT SOIL

THE HYDROLOGICAL EFFECTS OF FRACTIONAL WETTABILITY AND CONTACT ANGLE DYNAMICS IN WATER REPELLENT POROUS MEDIA

By

SARAH M.B. BEATTY, B.Sc.

A Thesis

Submitted to the School of Graduate Studies

in Partial Fulfilment of the Requirements

for the Degree

Master of Science

McMaster University

MASTER OF SCIENCE (2009)
(Earth and Environmental Sciences)

McMaster University
Hamilton, Ontario

TITLE: The Hydrological Effects of Fractional Wettability and Contact Angle Dynamics in Water Repellent Porous Media

AUTHOR: Sarah M.B. Beatty, B.Sc. (Brock University)

SUPERVISOR: Professor James E. Smith

NUMBER OF PAGES: xiv, 169

ABSTRACT

Soil water repellency is a spatially and temporally variable near surface phenomenon most often associated with reduced or impeded infiltration into porous media. In recent years, soil water repellency (hydrophobicity) has garnered much attention in the literature due to its detrimental effects on soil water processes and its widespread observance all over the world in both rural and urban settings. While previous work has developed our understanding of these inherently complex systems, insight into their dynamic and variable nature is still lacking. Having utilized existing technologies in a new way, in this study we present a series of systematic field and laboratory based investigations that clarify the roles of fractional wetting and contact angle dynamics on soil water processes using hydrophobic materials found at a wildfire site approximately 1.5 years post-fire. The robust and fundamental approach taken in investigating water repellency in these materials provided the foundation to develop two conceptual models based on our observations and with respect to existing and emerging theory. These models better explain soil water behaviour in hydrophobic systems than is currently afforded by the literature. We found that wetting and infiltration processes are contingent upon the functional relationship between wettable fractions of materials and the rate of contact angle change in non-wettable fractions.

ACKNOWLEDGEMENTS

To my dad Bill Beatty (in memoriam) and my brother John.

I have an amazing group of individuals around me. My family and friends have done far more than could be expressed in words, but I would like to thank my mom Margaret Battles, sister Rachel, and brother Lincoln for being my first and most committed teachers. So much of who I am is because of them. My cousin Katharine Beatty is a remarkable woman who quietly encourages me to be remarkable in my own way. I am indebted to Marg Theisen and the Balasak's (Holly, John, Karen, Kelly, and Jennie) for their uncompromising encouragement, curiosity, and willingness to help in any way possible. Scott, my partner and best friend is a function of all things great and good and reminds me regularly that I am those things too.

This project found its legs through Halfway Lake Provincial Park and the Ontario Ministry of Natural Resources (Sudbury). I would like to specifically thank Ryan Gardner (HLPP) and Ed Morris (OMNR) for their instrumental role in accommodating this research from beginning to end through their promptness, professionalism, and helpful comments.

Jennie Kirby is a pleasure to work with and has added days to my life. Her assistance in the lab (and in general) was indispensable throughout this project. I am also grateful to Denis O'Carroll and Jason Gerhard at the University of Western Ontario for training (provided by Ian Molnar) and the unrestricted use of their drop shape analysis equipment. We were able to learn so much more about these systems because of the work carried out in their lab.

I consider it a real luxury to have had two amazing lab mates with such large (and enjoyable) personalities. Maricris Marinas and Heather McLeod broke up the monotony, listened to me gripe, helped me in the lab, and made me laugh on many occasions.

I would like to express my gratitude to my review committee (Doctors Jim Roy and Altaf Arian) and thesis defence Chair (Dr. Walt Peace) for their thoughtful comments, questions, and suggestions. The time and care took in reviewing my work is wholly appreciated. Throughout the review process I felt I was respected as a colleague, but also nurtured as a young scientist. I cannot express how much I value that.

The role of my supervisor, Dr. James E. Smith, in the success of this project cannot be overstated. In short, I won the supervisor lottery with Dr. Smith. Through his consistent guidance and generosity, this work became so much more than I could have ever imagined. Dr. Smith has been a true mentor who has supported, challenged, and listened to my ideas and has taught me to be a better scientist, educator, and person. I will be eternally grateful of the perspective I've developed in working with him.

I am so fortunate to live in a country that is able and willing to support science research and education. This research was backed financially by the Ontario Graduate Scholarship program and the National Sciences and Engineering Research Council of Canada and I would like to express my gratitude to Canadian Taxpayers for supporting these programs.

CONTENTS

ILLUSTRATIONS

TABLES

Chapter 1: Introduction

1.1 Soil Water Repellency: Overview

Soil water repellency is a near surface phenomenon that has received much attention in recent years, most notably for its adverse effects on vadose zone processes. Its most distinguishing characteristic being impeded infiltration into porous media, a water repellent soil is one into which water will not spontaneously infiltrate (Letey, 2001; Roy and McGill, 2002). The implications for systems where hydrophobic (water repellent) soils exist are numerous and significant. Water repellent soils can contribute to the development and propagation of unstable wetting fronts and preferential flow paths, increased aquifer contamination, reduced agricultural productivity and seed germination, increased soil degradation (i.e. erosion and rill formation), enhanced overland flow, and reduced soil-water redistribution (Leighton-Boyce et al., 2007; Taumer et al., 2005; Ritsema and Dekker, 1994; Doerr et al., 2000). Soil water repellency can develop both naturally and anthropogenically in soils of varied textural composition and structural properties, and have been found all over the world.

Hydrophobic soils develop where hydrophobic compounds are able to enter the soil through natural and/or anthropogenic processes and remain either as interstitial matter (Franco et al., 1995) or as coatings on particle surfaces (Bisdom et al., 1993). Hydrophobic compounds are often attributed to the presence of polar waxes and long chain fatty acids (Horne and McIntosh, 2003) which may be derived from one or more of the following: humic acids (Bisdom et al., 1993), plant material (Rodriguez-Alleres et al., 2007; Mataix-Solera et al., 2007; Franco et al., 1995; Ellerbrock et al., 2005), biological activity (Schaumann et al., 2007; Fidanza et al., 2007), and contamination sources (Diehl and Schaumann, 2007). At the molecular level, hydrophobic compounds impart repellency as a reduced affinity to water due to the spatial arrangement of functional groups i.e. the orientation of polar groups (Bayer and Schaumann, 2007; Doerr et al., 2000; Diehl and Schaumann, 2007).

In water repellent soil the surface energy of the porous media is such that the cohesive forces of water (i.e. surface tension) are greater than those of the porous media (Douglas et al., 2007). Because of this, water preferentially beads on soil surfaces in water repellent media (i.e. in air-water systems). Comparatively, in water wettable soil, porous media will have a greater attractive force than the cohesive forces of the water and cause the water to spontaneously spread and enter pore spaces (Roy and McGIll, 2002).

In addition to the various sources of hydrophobic compounds, a host of variables can further influence the expression of water repellency in porous media. Soil moisture (Taumer et al., 2005; MacDonald and Huffman, 2004), soil texture (Bisdom et al., 1993), temperature (Diehl and Schaumann, 2007), pH (Bayer and Schaumann, 2007; Mataix-Solera et al., 2007), biological activity (Fidanza et al., 2007), fire (Pierson et al., 2008; Debano, 2003; Doerr et al., 2006; Dlapa et al., 2008), and relative humidity (Goebel et al., 2004) alone will not induce repellency, but can affect its expression. Temporal processes and conditions introduce even greater complexity in porous media expressing repellency (Debano, 2003; Doerr et al., 2007).

Water repellency is regarded as a spatially and temporally variable phenomenon in fire-affected materials (Doerr et al., 2000; Debano, 2003). The role of fire in water repellent media is unique in that it can both remove pre-existing repellency and induce repellency (Debano, 2003). The establishment or removal of repellency is highly contingent upon the nature of burning at particular sites (e.g. Huffman et al. 2001; Martin and Moody, 2001, Lewis et al., 2006). Doerr et al. (2004) identified that repellency was removed in Australian top soils burned at temperatures between 260 and 340°C. Debano (2003) has noted that hydrophobicity is destroyed in materials burned between 280 and 400°C while lower temperature, longer duration burning can contribute to the development of water repellency in soils. Debano (2003) also describes the often cited mechanism by which repellency is thought to develop deeper in the soil profile.

He explains that surface burning of litter and duff layers provides a supply of volatilized organic substances that can move freely along steep temperature gradients between the fire and more insulated mineral soil. As these volatilized substances move along these temperature gradients into cooler regions (i.e. deeper in the soil profile), they are then able to coalesce onto soil particles thus creating a hydrophobic 'layer' at depth. While there are *many* proposed sources and mechanisms of repellency in materials, this mechanism is most often associated with post fire repellency in *mineral* soils. We investigate repellency in *organic* soils throughout this document, but the effect of burning / heating / drying of organic materials is critical to the expressed repellency of many soils (Debano, 1981; Bisdom et al., 1993; Valat et al., 1991; Franco et al., 1995); both in terms of fractional wettability and contact angle dynamics.

In spatially and chemically heterogeneous media, particularly for post-fire environments where large differences may exist in the wettability of adjacent surfaces, what is most likely to occur is a combination of both wettable and non-wettable materials coexisting. Bisdom et al. (1993) found that water repellency was caused by 'combinations' of interstitial particles. Additionally, when hydrophobic interstitial soil particles and particles with hydrophobic coatings are mixed, repellence is enhanced in porous media (Franco et al., 1995; Bradford et al., 1997). Conversely, the existence of wettable particles in hydrophobic media facilitates wetting (Imeson et al., 1992; Doerr and Thomas, 2003) by creating breaks in hydrophobic connections (Quyum et al., 2002).

Moisture also has a complex functional relationship with water repellent media. While hydrophobic soils affect the distribution and movement of water in porous media (Ritsema and Dekker, 1994), soil moisture has a variable effect on repellency expression. Increased water content can both increase and decrease repellency (Bayer and Schaumann, 2007). Under relatively low moisture contents in organic soils (<0.5kg/kg), repellence severity (i.e. contact angle) has been found to increase with increasing moisture content (Regalado and Ritter, 2009).

Taumer et al. (2005) found that the persistence of repellency increased with decreasing gravimetric water content (0.0-0.3g/g) (and organic matter content).

Because of their inherent complexity (re: forming processes, temporal and spatial dependence, influences), water repellent systems have proven difficult to represent theoretically, investigate quantitatively, and model accurately.

1.2 Measuring Water Repellency: Contact Angles and Infiltration

Since soil water repellency has the potential to influence so many hydrological processes, it is essential to quantify hydrophobicity in porous media so we can better understand the manner in which these systems respond to various hydrological events. At the most elemental level, the tendency to wet ideal surfaces is determined by the contact angle at which an air-water interface meets a solid surface (Gilboa et al., 2006; Murray and Darvel., 1990). While the measurement of contact angles is the most fundamental approach to characterizing the wettability of surfaces, measuring contact angles in real world systems is not straightforward. Because of this, many investigations employ secondary measures of contact angle in attempts to quantify this essential information (Letey, 2001).

The fundamental importance of understanding the nature and behaviour of contact angles is at the root of secondary methods such as the Critical Surface Tension (CST) test and Water Drop Penetration Time (WDPT) test. These tests are based on a binary premise of whether drops will infiltrate or not when placed on the surface of porous media. The CST test is referred to as a measure of the initial *severity* of repellence (Letey, 2001). The test is based on the assumption that water will not spontaneously infiltrate into porous media with contact angles >90° and that ethanol wets all soil materials at a contact angle of 0° (Letey et al., 2003). By adding ethanol to water, the surface tension of the aqueous-ethanol solution progressively decreases with increasing ethanol concentration (Huffman et al., 2001). The greater the ethanol concentration required to induce wetting, the more severe the water repellence. By identifying the surface tension of a

particular ethanol concentration at which water repellent media will spontaneously wet (with an assumed 90° contact angle), it is thought that initial contact angle information can be discerned. Other forms of this test (e.g. Molarity of Ethanol (MED) and Volumetric Ethanol Percentage (VEP)) vary only in the way results are reported and not in the manner with which tests are conducted (Letey, 2001). The WDPT test is commonly referred to as an approximate measure of the *persistence* of repellency (Cerda and Doerr, 2007; Douglas, 2007; Dekker and Ritsema, 1994; Scott, 2003), stability of repellence (Letey, 2003), or the time to infiltration initiation (Wang et al., 2000). It measures the time required for drops placed on a surface to disappear via infiltration. It is based on the premise that water repellent media have contact angles greater than 90°; WDPT measures the time required for the contact angle to change from a non-wetting angle to a (theoretically) wetting one (<90°) (Letey, 2001). Put another way, the intent of the WDPT test is to measure the temporal dependence of water repellency or the dynamic change of contact angles in porous media.

To say that researchers in soil water repellency investigations are most interested in contact angle information would be misleading. While there is a heavy reliance on CST and WDPT tests (e.g. Huffman et al., 2001; MacDonald and Huffman, 2004; Feng et al., 2001; Mataix-Solera et al., 2007; Verheijen and Cammeraat, 2007), they do not provide a reliable measure of repellence in many investigation scenarios (Cerda and Doerr, 2007; Lewis et al., 2006); nor do they capture the information we truly seek. It is not contact angles or contact angle dynamics as subjects per se that are most relevant to many researchers, but rather their combined effects on infiltration and moisture distribution in unsaturated media.

Infiltration and moisture distribution processes in water repellent media are not fully understood (Doerr and Moody, 2004). Much of our understanding about infiltration processes in these systems has come from research using forced wetting techniques (e.g. rainfall simulations, ponded infiltration) (e.g. Martin and

Moody, 2001; Pierson et al., 2008; Cerda and Doerr, 2007; Leighton-Boyce et al., 2007; Scott, 2003; Ferreira et al., 2003; Shakesby et al., 2003). While providing insight into hydrological processes under high intensity, low frequency precipitation events, these tests rely on a fundamentally different flow mechanism that masks any temporal dependencies existing within these systems. As a result, little is known about temporal infiltration processes / controls in hydrophobic media. This is particularly problematic given that temporal processes and contact angle dynamics are so often recognized in these systems (e.g. Letey, 2001; Wang et al., 2000; Doerr et al., 2000; Douglas et al., 2007; Cerda and Doerr, 2007).

1.3 Problem Statement and Thesis Overview

There is an overwhelming reliance on WDPT tests to discern temporal changes in these systems and a relative absence of time-dependent infiltration testing (that is sensitive to changes in contact angles) in the literature. This discrepancy highlights the necessity for more thorough and systematic research on these dynamic systems so that even basic hydrologic controls (e.g. contact angles) and processes (e.g. infiltration) can be better understood. To this end, this study presents systematic laboratory and field investigations conducted on water repellent natural materials collected from a wildfire site approximately 1.5 years post-fire. We sought to identify, discern, and measure the effects of static controls and dynamic processes on infiltration and moisture distribution in a more robust manner than is presented in most of the literature.

In chapter 2, we outline and report upon the measure of advancing contact angles collected on naturally occurring hydrophobic materials using Axisymmetric Drop Shape Analysis (ADSA). This was done to 1) systematically identify differences between materials of greater / lesser hydrophobicity in a reliable manner and 2) gauge the importance of fractional wettability on measured contact angles with respect to larger scale processes. We applied ADSA techniques on post-fire repellent materials to incorporate this method in the

measure of repellency in naturally occurring repellent soils. To our knowledge this is the first ADSA study of its kind.

Chapter 3 scales up spatially and temporally (re: chapter 2) and reports on the temporal dynamics of contact angles through a series of tension disc infiltration experiments carried out using two different sized 1D laboratory columns. In these experiments, we sought to determine the effectiveness of the tension disc infiltrometer as a tool for measuring 1) dynamic changes in contact angle for fractionally wettable media and 2) infiltration processes under conditions that better mimic low intensity, higher frequency rainfall events. Time dependent changes in contact angle are evaluated with respect to observations of infiltration and moisture content.

Chapter 4 builds upon the initial contact angle measurements of fractionally wettable materials from chapter 2 and the measure of dynamic contact angles from chapter 3 by scaling up spatially though 3D (field) infiltration tests conducted at Halfway Lake Provincial Park in Fall, 2008. Tension disc infiltration experiments were carried out to 1) determine the usefulness and constraints of this instrument for *in situ* water repellency investigations and 2) to better understand the nature of infiltration into these water repellent media under field conditions.

In chapter 5, we present a conceptual model to better represent the nature of wetting in fractionally-dynamic repellent media. In the model we relate static controls and temporal processes observed in chapters 2-4 to infiltration processes in 1D and 3D.

Chapter 6 provides a summary of the thesis and concludes with an assessment of the techniques used and a discussion on how these unique methodologies could be improved upon.

Chapter 2: Measuring Contact Angles and Wettability

2.1 Introduction

At the essence of measuring the wettability or energy of surfaces is the measurement of interfacial tensions and contact angles. In water repellence investigations especially, contact angle information is highly sought after for it provides researchers with fundamental information about small scale conditions that control larger scale, more easily observable phenomena. In discerning the contact angle at which an air-water interface meet a surface, one can better understand the nature of water movement in hard to wet systems.

2.1.1 Theory

Regardless of the measurement technique employed, the determination of contact angle is often based on the premise stated in Young's (1805) contact angle (CA) equation (eq. 2.1). The equation describes an equilibrium force balance between three acting forces; the interfacial tensions between two immiscible fluids, and an ideal solid (Marmur, 2006) (Fig. 2.1). The equilibrium angle at which these three forces converge is considered the contact angle (θ).

$$\sigma_{LV} \cos\theta_i = \sigma_{SV} - \sigma_{SL} \qquad \text{(eq. 2.1)}$$

Where σ_{LV} is the liquid-vapour interfacial tension, σ_{SV} the solid-vapour interfacial tension, and σ_{SL} the solid-liquid interfacial tension (Bachmann et al., 2000). The relation between these three interfacial tensions is the cosine of θ_i, or the intrinsic contact angle. Experimentally however, the surface energies of solid surfaces are not directly measurable and so with two unknowns (σ_{SV} and σ_{SL}) the relationship is unsolvable (de Gennes, 1985). Measured contact angles using multiple fluids with known surface tensions has traditionally served the purpose of indirectly

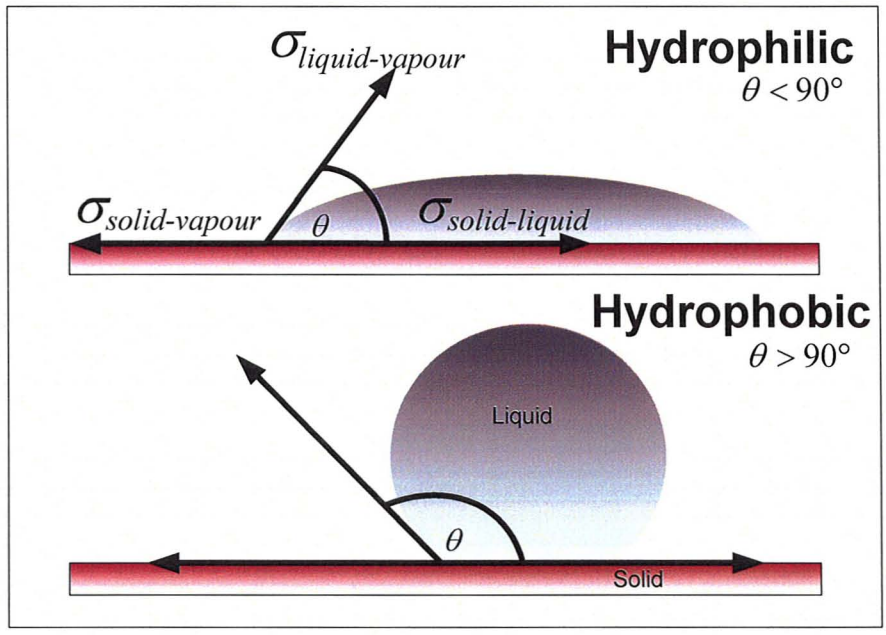

Fig. 2.1 Hydrophilic and hydrophobic drops resting on planar surfaces

isolating the energy contribution of solid surfaces (Marmur, 2006; Kwok et al., 1998; Dussan, 1979; (Arye) Gilboa et al., 2006).

The nature of repellency in air-water systems is, according to Young's equation, imparted by the surface energy of the solid (Roy and McGIll, 2002). On a *completely* wetting substrate, the interfacial tension (IFT) of the solid-vapour interface is sufficiently high compared to that of the liquid-vapour interface. In this condition, water spontaneously spreads and the contact angle is 0° (Roy and McGill, 2002; de Gennes, 1985). Conversely, on water repellent or hard to wet substrates, water will not spontaneously spread as the surface energy of the substrate (solid-vapour IFT) is lower than that of water (liquid-vapour IFT). In this condition, water acts as a non-wetting fluid and will rest on the surface at some angle greater than 90°. Bachmann et al. (2003) notes that natural soils have contact angles that vary between 0 and 140°.

Young's equation, however, describes contact angles under ideal conditions where the solid phase is smooth, flat, rigid, chemically homogeneous, non reactive, and insoluble (Marmur, 2006; de Gennes, 1985); and where the liquid is a pure phase liquid in which vapour adsorption to the solid phase is

negligible (Chibowski, 2007). Since soils, for example, are typically not flat, smooth, or chemically homogeneous, these assumptions are often violated when Young's equation is applied in real world systems. Surface roughness, while having no affect on intrinsic contact angles at the microscopic level, can result in highly complex *apparent* or *observed* contact angles macroscopically (Murray and Darvell, 1990; Kwok et al., 1997; Johnson and Dettre, 1964). Local asperities on rough surfaces can pin the interface of a moving drop on a surface such that a 'stick-slip' motion is observed; resulting in a range of apparent contact angles on both advance and retreat of drops (Marmur, 2006; de Gennes, 1985). These deviations from a single, unique contact angle (for a given material and fluid pair) have given rise to a body of literature attempting to address the uncertainty in contact angle measures on rough surfaces (Meiron et al., 2004; Chibowski, 2007). Chemical heterogeneity further complicates the measurement of contact angles on surfaces by contributing to deviations from a unique contact angle. For surfaces where chemical heterogeneity occurs, two or more intrinsic contact angles simultaneously exist, relative to the surface energy contribution of each chemical input (Murray and Darvel, 1990).

To deal with the roughness and chemical heterogeneity of surfaces, theoretical arguments have been made in order to derive some notion of ideal or intrinsic contact angles from measured advancing and receding angles. The often-observed variation within and between advancing and angles is termed contact angle hysteresis and has been dealt with, at least theoretically via Wenzel and Cassie equations.

The Wenzel equation relates the observed or (θ_{obs}) apparent contact angle to the intrinsic contact angle (θ) through a roughness term (r) (eq. 2.2) (Bachmann et al., 2000). The roughness term is defined as the ratio between the (real) 3D surface area and 2D planar or projected surface area (Good, 1992). For

$$\cos(\theta_{obs}) = r\cos(\theta) \qquad \text{eq. 2.2}$$

smooth surfaces r =1 and for rough surfaces r > 1(Marmur, 2006). When in a Wenzel state, drops completely penetrate and conform to the microtopographical variations of a rough surface (Fig. 2.2) (Yeh et al., 2008). The equation predicts that roughness will increase contact angle for intrinsic angles greater than 90°, and decrease contact angle for intrinsic angles less than 90° (Bachmann et al.,

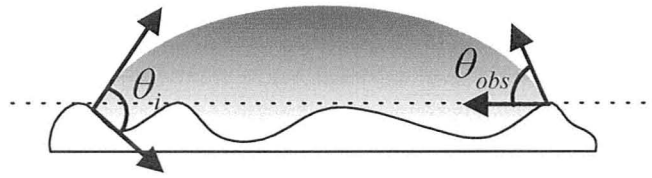

Fig. 2.2 Intrinsic (θ) and observed (θ_{obs}) contact angles on hypothetical, hydrophilic rough surface (after Marmur, 2006).

2000). McHale et al., (2004) have also shown that the magnitude of increases for CA>90° (decreases for CA<90°) is not linear and amplified in larger (smaller) angles i.e. angles farther from 90°. Rough surfaces are thought to contribute to contact angle hysteresis in advancing and receding drops due to pinning and slipping as the interface moves over rough areas (since drops conform to the undulations of rough surfaces) (Merion et al., 2004; Yeh at al., 2008).

The Cassie (or Cassie-Baxter) equation (eq. 2.3) states that for a chemically heterogeneous surface, the resultant observed contact angle (θ_{obs}) will be determined by the summation of the proportional contributions of each chemical component (φ_i), multiplied by the cosine of the component specific contact angle (θ_T) (Murray and Darvel, 1990). When applied to 'rough' surfaces, drops behave as though they rest on a planar surface composed of an air and solid fraction (Yeh et al., 2008) (Fig. 2.3). Stick and slip mechanisms observed in these systems are directly related to the energy barriers of non-inert surfaces and not because of microtopographical variations (Kwock et al., 1997); the effect

$$\cos(\theta_{obs}) = \varphi_1 \cos(\theta_{T1}) + \varphi_2 \cos(\theta_{T2}) \qquad \text{eq. 2.3}$$

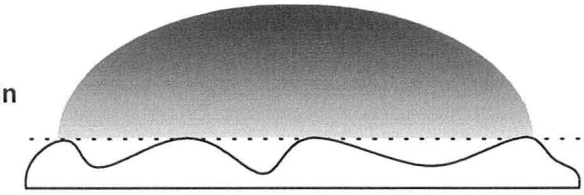

Fig. 2.3 Drop on hypothetical rough surface in Cassie state (after Yeh et al., 2008).

on contact angle heterogeneity is less than in the Wenzel case. When in the Cassie state, angles are independent of surface roughness (Yeh et al., 2008); so while differences may exist between advancing and receding contact angles, divergences are attenuated.

Murray and Darvel (1990) present a generalized form of the Cassie equation for more than two phases (eq. 2.4). They note that it is still a weighted average and tells very little of local variations in contact angle at each drop perimeter-chemical component interface. However, for the purposes of this investigation, we find this generalized form superior to eq. 2.3 as it better represents natural media; where a large number of surfaces with different chemistries can coexist. For fractional wettability systems in particular, eq. 2.4 facilitates the conceptualization of a system that includes air and (at least) two distinct heterogeneous chemical inputs.

$$\cos(\theta_{obs}) = \sum_{i=1}^{n} \varphi_i \cos\theta_{Ti} \qquad \text{eq. 2.4}$$

2.1.2 Methods of Measurement

Because measuring contact angles is not straightforward, various techniques have developed out of a need to better understand the wettability of surfaces. As a widely used and powerful tool for the determination of contact angle, Axisymmetric Drop Shape Analysis (ADSA) has been developed and in practice over the last 20+ years (Hoorfar and Neuman, 2004). The technique is

used to analyze both sessile (resting on a surface) and pendant (hanging) drop shapes by fitting a Laplacian curve to digitally captured drop profiles (Hoorfar and Neumann, 2004; del Rio and Neumann, 1997; Cheng et al., 1990). ADSA has an added advantage over other methods such as the Wilhelmy Plate Method (WPM), Capillary Rise Method (CRM) and the Modified Sessile Drop Method (MSDM) because instantaneous measurements of contact angles can be captured for real drop shapes on materials that express dynamic behaviour (i.e. contact angles changing with time).

That is not to say that the techniques noted above have not revealed important and insightful information about non-wetting contact angles in water repellent soils and/or the methodologies used to acquire them. Variations on the CRM have been used by many authors to evaluate contact angles using reduced surface tension fluids and the application of forced wetting via ponding water on surfaces (e.g. Scott, 2003; Czachor, 2007; Feng et al., 2001; Diehl and Schaumann, 2007; Gilboa et al., 2006; Wang et al., 2003; Bachmann et al., 2006). This technique however, has been significantly criticized because of exposure time requirements (Letey et al., 2003; Feng et al., 2001) and the application of positive hydrostatic pressures (Bachmann et al., 2000). Czachor (2007) also found the CRM overestimated contact angle when used in conjunction with the Washburn equation, while Scott (2003) found that the test was only applicable for a narrow range of contact angles (i.e. 67-94°). Further limiting the widespread application of this method is the difficulty in approximating effective contact angles in water repellent media using ethanol as a reduced-surface tension fluid ((Ayre)Gilboa et al., 2006); a fluid commonly used in the assessment of repellency in other applications.

The Modified Sessile Drop Method (MSDM) as proposed by Bachmann et al. (2000) has been used to measure contact angles on small sieved fractions of water repellent soils with reproducible results. The technique relies on the measurement of static drops using a microscope fitted with a goniometer scale.

Although they present a novel technique to preparing soil surfaces for sessile drop shape analysis by fixing soil materials to a glass slide using 2-sided tape, the measure of static contact angles is limited in that reference angles are unknown. Good (1992) also notes that static measures of contact angles are not as scientifically useful as advancing (and retreating) measures. Diehl and Schaumann (2007), however, use the 2-sided tape technique to monitor time-dependent changes in drop shapes on water repellent soils to isolate the effects of wetting and evaporation. The WPM is one of the methods more commonly used to measure contact angles in contact angle – soil water repellency investigations (e.g. Goebel et al., 2007; Bachmann et al., 2000; Schaumann et al., 2007; (Arye) Gilboa et al., 2006; Diehl and Schaumann, 2007). The WPM derives advancing contact angles by immersing a glass slide coated with hydrophobic media into a container filled with water and measuring weight changes as a function of submersion depth; where weight changes are determined by plate mass, buoyancy, and the wetting force (Diehl and Schaumann, 2007; Bachmann et al., 2006). Decker et al. (1999) and Good (1992) raise a practical concern over notions of scale in relation to single drops on surfaces, particularly for advancing contact angles measured using the WPM, which are averaged over the length of a (larger) wetted sample.

In terms of contact angle measurements in water repellent systems, advancing initial contact angles are thought to be superior in that constant humidity and temperature can be maintained over relatively short time intervals and exposure to fluids is limited; prolonged exposure can affect the surface tension of solid surfaces and liquids and the resultant contact angle ((Arye) Gilboa et al., 2006; Roy and McGill, 2002). For fractionally wetting materials, the maximum observed value in advancing angle measures is associated with hydrophobic (low-energy) surfaces (Good, 1992). This might be an overly simplistic generalization for porous materials; where complex chemical and spatial heterogeneity can be observed in a range of potentially valid advancing

angles. In this investigation we use ADSA to determine advancing contact angles for both hydrophilic and hydrophobic materials collected at a wild fire site approximately 1.5 years post-fire. Though ADSA has been used in a broad range of wettability investigations (e.g. biological, industrial) (Rodrigues-Valverde et al., 2002; Kwok et al., 1997; Hoorfar and Neumann, 2006), to our knowledge, it has not been used to measure initial advancing contact angles on naturally occurring hydrophobic soils until now.

In this chapter we report upon our success in determining 1) whether differences in hydrophilic and hydrophobic organic materials collected at a post fire site could be reliably identified 1.5 years post fire, 2) whether differences in hydrophobicity (i.e. >90° or >>90°) could be discerned for materials where fractionally wettable particles were suspected to exist and affect measures, and 3) the extent to which measures of advancing contact angle could contribute to our understanding of wetting behaviour (of these materials) in a larger context (i.e. at the pore scale). In addition to our analysis, practical limitations of the method relative to these materials will be addressed in concluding sections.

2.2 Equipment and Materials

2.2.1 ADSA Equipment

The basic hardware components of axisymmetric drop shape analysis (ADSA) are shown in Fig. 2.4. For this investigation, all measurements were carried out using a First Ten Angstroms: Model FTA200 (Fig. 2.5) which included a computer-controlled step motor (1) that pumped water in and out of a 3 ml syringe (2). Lighting preferences (i.e. backlit using blue light or full lighting) were handled both manually and remotely via the software (FTA32 video 2.0) installed on the computer. This software also controlled camera / frame grabber functions and the pump rate and direction. A flat tipped stainless steel needle (B-D 23G1; maker: Becton-Dickinson) was used throughout the investigation on prepared samples.

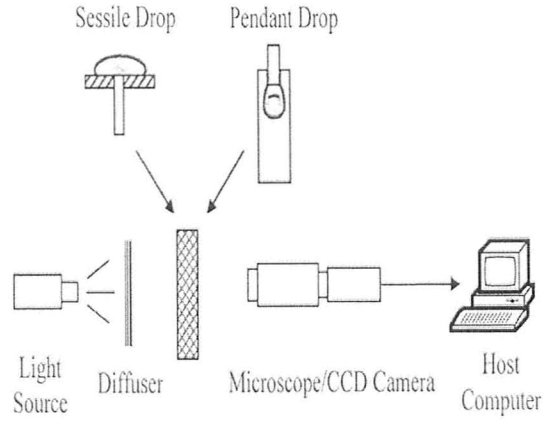

Fig. 2.4 Schematic diagram of typical ADSA set up (from Hoorfar and Neumann, 2004)

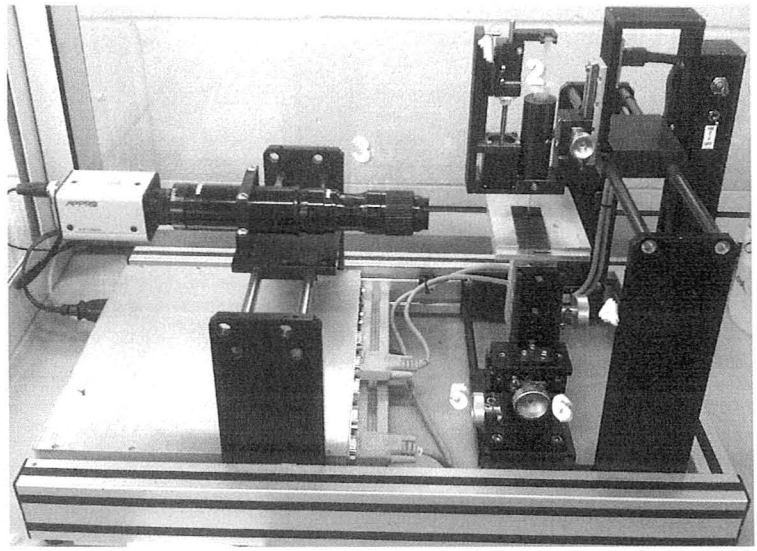

Fig. 2.5 Actual ADSA equipment and prepared slide with step motor (1), syringe (2), CCD camera (3), stage, and stage adjustment dials (4,5,6); host computer out of frame

2.2.2 Hydrophilic and Hydrophobic Materials

Hydrophilic and hydrophobic organic soil materials used in this investigation were collected from a post-wildfire site approximately 1.5 years following the fire. These materials were identified during field tests conducted in Fall, 2008 using WDPT and MED drop tests.

The nature of tests conducted in this investigation evolved during the course of study, and as a result, so did sample preparation. Initially, all samples used in ADSA were prepared as air-dried, undisturbed surfaces so that contact angle *and* drop infiltration information could be captured. Undisturbed surfaces were prepared minimally to permit a clear field of view between the camera lens and the 3-phase (i.e. air, water, soil) contact on sample surfaces. Drop infiltration behaviour and other complex water-material interactions could be observed using this set up. However, capturing contact angles proved more problematic as loose surface materials would often adhere and skate up the sides of the drop surface, thus distorting drops and obscuring the contacts required for contact angle measurement (Fig. 2.6). McHale et al. (2007) explain that this phenomenon is energetically favourable for contact angles <180°. Since this range includes contact angles of interest in soil water repellency investigations, using undisturbed samples was abandoned as a primary means of capturing contact angles, and utilized only for the (secondary) drop infiltration / wetting information it provided.

Fig. 2.6 Drop on undisturbed hydrophobic surface. Loose surface materials adhered to drop surface indicated by arrows.

Materials were grouped into two broad categories. The first group being "Charred Surface Materials" or surface materials that showed more (relative) complete consumption by fire; these materials were black, unconsolidated, organic materials presumed to be originating from mosses and pine needles. The second group consisted of "Brown Surface Materials" that had been burned, but to a much lesser degree relative to the Char materials. These materials were brown, cohesive materials which were again, made up of mosses and pine needles. These two surface materials were found to be ubiquitous at the site in varying amounts according to the nature of the fire mosaic, and representative of the materials that were tested in infiltration tests (as will be discussed in chapters 3 & 4).

These two broad representative categories were selected so that a spectrum of possible contact angles for these materials could be established for the site. For the majority of samples, a depth variable was also added so that differences between initial contact angle in surface materials (0cm) and at-depth (2cm) materials could be considered. *In situ* post-infiltration test excavations showed that for many tests, depth of wetting existed within a 5cm interval. It should be noted that characterizing soil water repellency over depth intervals using contact angles was not a primary aim of this investigation as it has been elsewhere (e.g. Keizer et al., 2007 used Molarity of Ethanol and Dekker et al., 2003 evaluated persistence over depth intervals via Water Drop Penetration Time tests.).

Samples for axisymmetric drop shape analysis were first air dried at 21-25 °C with variable Relative Humidity ranging from 3 to 23% (averaging 10%) for a minimum of 3 weeks and then passed through a 500µm sieve by hand. While there are various approaches to preparing samples (e.g. field moist, air-dry, oven-dry), air drying has become the preferred method of drying samples (Doerr et al., 2000). The effect of drying on water repellency expression is variable (i.e. drying can both increase and decrease repellency) (e.g. Leelamanie and Karube,

2007; Bayer and Schaumann, 2007; Doerr and Thomas, 2003). This 500µm sieve size fraction represented a smaller proportion of the overall sample, but facilitated measurements using ADSA. In contrast, measures on *unsieved* prepared slides, displayed highly complex drop behaviour due to the random orientation of large particles. The inability to obtain clear observance of 3-phase contacts because of these large particles also restricted measurements. These combined effects impeded the establishment of measurable drops on unsieved slides using ADSA. We acknowledge that sieving would not only bias the grain sizes found on the slide, but could also alter hydrophobic coatings (Bisdom et al., 1993; King, 1981). If for these materials hydrophobic coatings were in fact the cause of repellency, one could expect a decrease in contact angle measures. The apparent uncertainty involved in measures on sieved samples vs. unsieved samples was investigated to a limited degree via using two slides of the same material; one slide prepared with material passed through a 500µm sieve, and one slide prepared with unsieved material.

All slides were prepared by attaching double-sided tape (Bachmann et al., 2000) to one side of a (1x3inch) glass slide. Materials were then poured into a mounded layer on the exposed side of the tape and gently pressed onto the slide to ensure complete coverage of tape. Excess materials were removed by tapping the slide while vertical in orientation. Slides were then covered in aluminium foil and sealed in Ziploc bags for transport the following day. All samples were transported in a cooler between McMaster University and the University of Western Ontario (where the experiments were conducted). During transport, samples were exposed to cold (winter) temperatures, so upon arrival were allowed to equilibrate to room temperature prior to use. A significant number of measures were made over a 3 day period at UWO. Samples for this series of measurements were prepared the night before the first day of experimentation. During this period, samples remained in the lab.

2.3 Methods

Once prepared, slides were placed on the stage and brought into focus manually using the ADSA camera and stage dials (Fig. 2.5). Before data capture, a flat-tipped dispensing needle (diameter =0.635mm) was lowered so that it was close to the slide, but not touching (Fig. 2.7). Before formal data capture, a snapshot image was taken before each experiment under full lighting conditions. When the blue light was activated, drops appeared as silhouette images. The purpose of the snapshot image preceding formal data capture was to acquire images showing the surfaces / particles under normal lighting conditions for reference. When initiated, the software captured sequential images as deionized water was pumped out of the needle and onto the surface. Drops were grown using the captive needle / captive drop approach (Woodward, 2008a; Good, 1992) to an approximate width of 2mm (or 50% the width the field of view); at which point water was then pumped back into the needle. Two more pump in / pump out cycles were then carried out, each time doing so to advance the

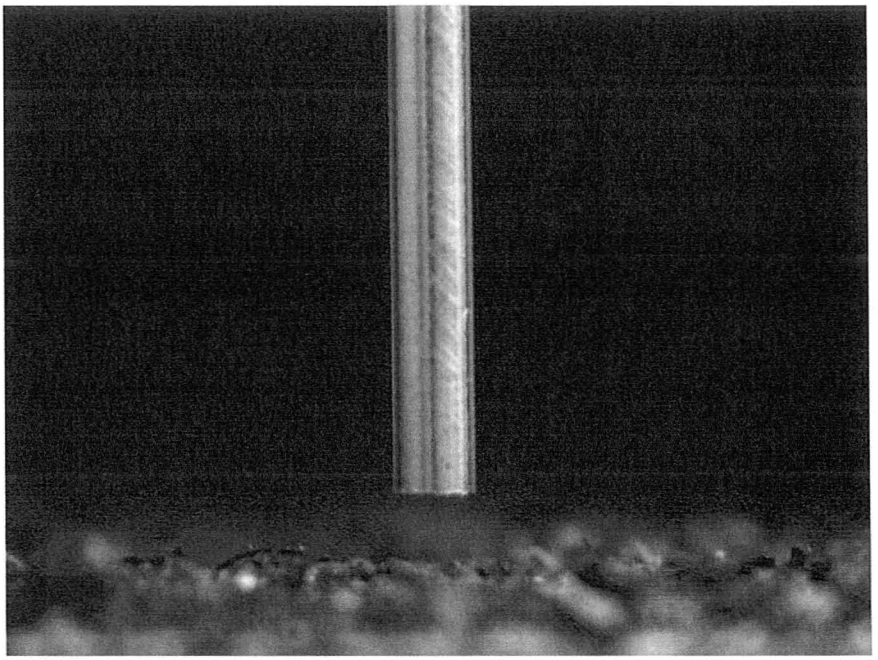

Fig. 2.7 Snapshot of pre-data collection surface with full lighting; dispensing needle (diameter = 0.635mm) at representative height (for all tests)

wetting perimeter of the drop beyond the previous cycle's drop perimeter and onto new material (Fig. 2.8-2.10). Once 3 pump in / pump out cycles were complete, a series of pendant drop images were captured to measure the (water-air) interfacial tension of the (used) water by raising the needle and pumping out enough water to create a small hanging drop (approx. 10µl on average) (Fig. 2.11) (Woodward, 2008b).

Each movie lasted approximately three minutes. This time interval was desirable because any influence on observed contact angles due to evaporation would not affect measures significantly (Diehl and Schaumann, 2007). Roy and McGill (2002) indicate further that since water repellent soils have a high capacity for vapour adsorption, in the absence of a vacuum, it is desirable to keep relative humidity constant between measures as this can affect contact angle measures. Although changes in relative humidity during the course of data capture for a single slide could be presumed to be negligible, changes within the laboratory over the course of all tests (on multiple days) could not. Since a vacuum could not be employed in this investigation, RH and temperature measurements were recorded at 10 minute intervals throughout the duration of the experiments using a HOBO data logger (model: HOBO U12) with built-in relative humidity / temperature sensors. Temperature fluctuated ±1 around 22 °C, while RH was more variable between days (i.e. 16-36% for all days, with a max standard deviation on any particular day of 1.75%).

After each movie, water was purged from the needle and the slide was repositioned to a new location to capture another set of advance / retreat cycles and interfacial tension measurements. This was done once more before a slide was retired and a between-samples interfacial tension measurement was made. In total, each slide underwent 9 total growth / retreat cycles consisting of 3 pump in / pump out cycles at each of 3 drop locations. Interfacial tension measures of the water were taken at regular intervals between samples and each time the syringe was re-filled.

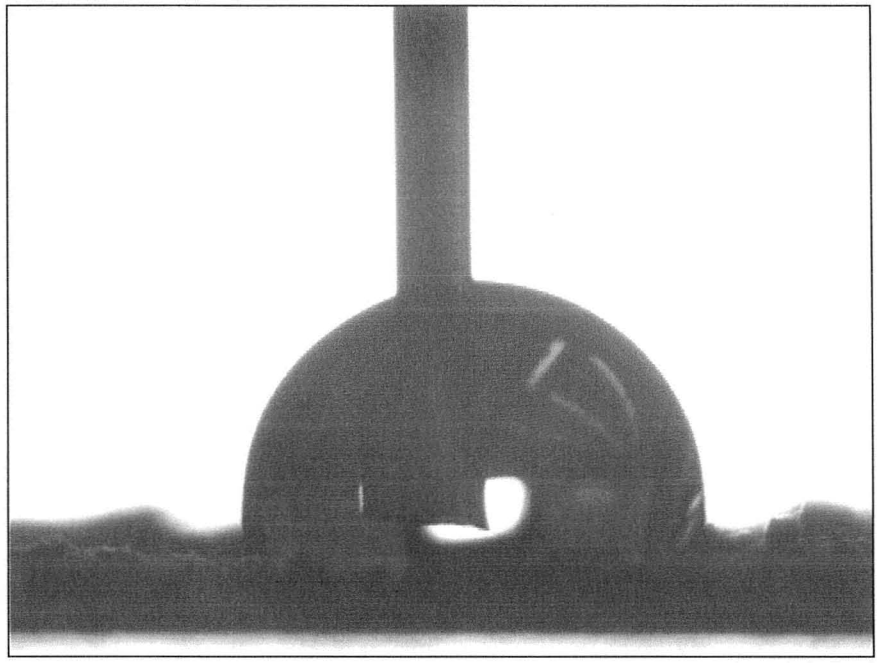

Fig. 2.8 Example of: silhouette image of maximum initial drop width (i.e. cycle 1)

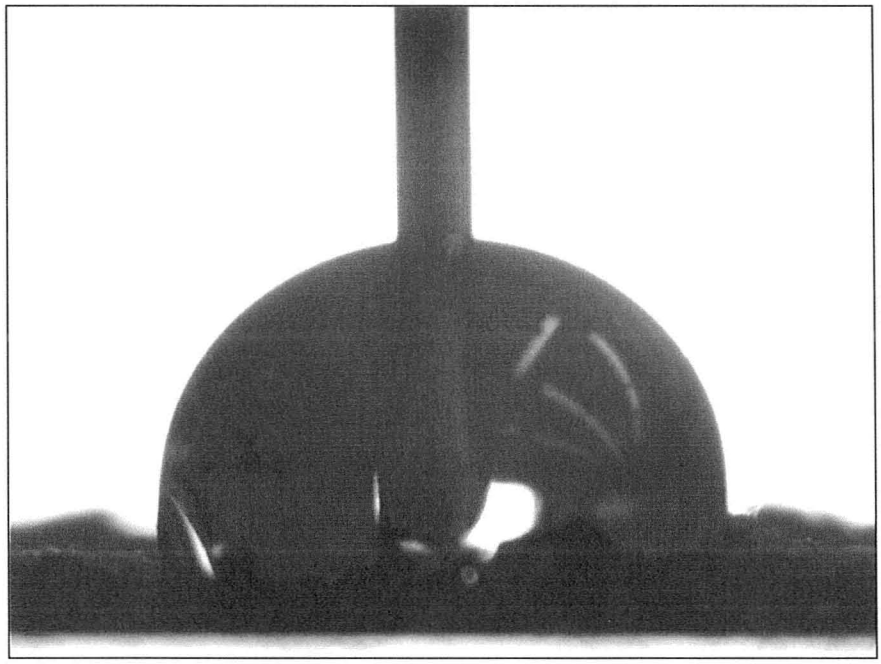

Fig. 2.9 Example of: silhouette image of maximum drop width on cycle 2

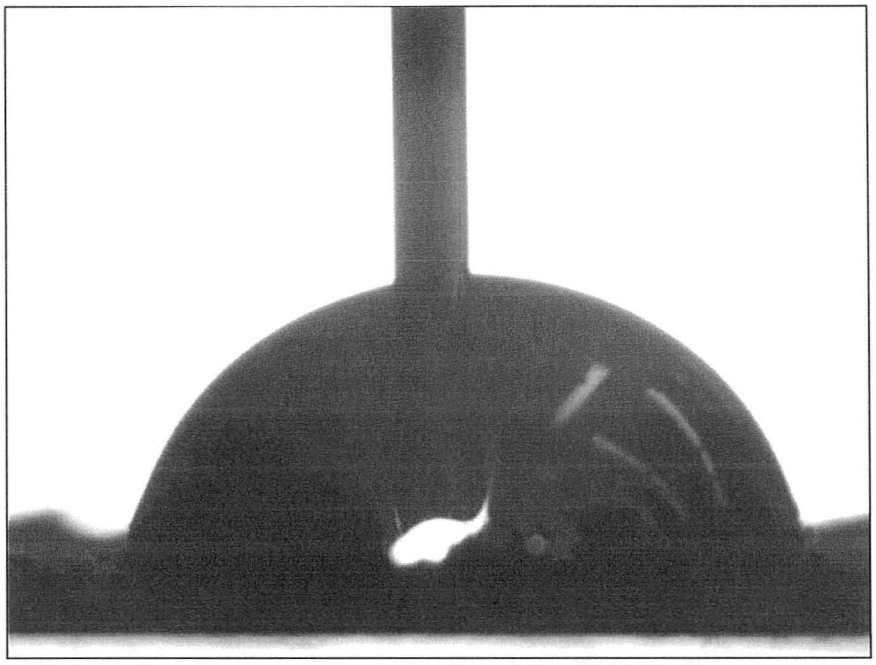

Fig. 2.10 Example of: silhouette image of maximum drop width on cycle 3

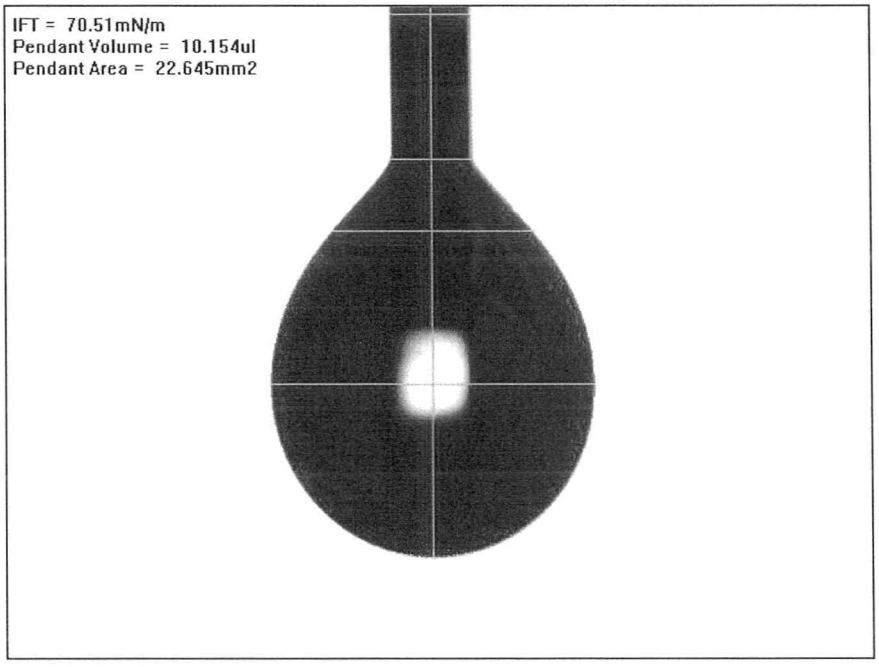

Fig. 2.11 Example of: silhouette image of pendant (hanging) drop captured at end of 3 cycles

Following data capture for all samples, movies were scanned visually for images that permitted clear observance of the 3-phase contact between the soil, water and air while the drop was in a state of advance. Once sufficiently large such that the needle at the centre of the drop did not affect the 3-phase contact, advancing contact angles were analysed semi-automatically using the FTA32 2.0 video software by 1) manually selecting points to draw a horizontal baseline where the drop contacted the sample surface (Fig. 2.12) and 2) manually tracing the drop interface / profile on images (Fig. 2.13). The software then calculated the line tangent to the drawn profile using a 'non-spherical fit' with an intersection at the end of the baseline for right or left sides (or both) of the water drop (Fig. 2.14). Each analytical contact angle result was then scanned visually for accuracy; for computed results that did not fit drop profiles well, images were re-analysed.

The selection to analyse the right, left or both sides of the drop was entirely dependent on the nature of advance of drops. In most instances only one

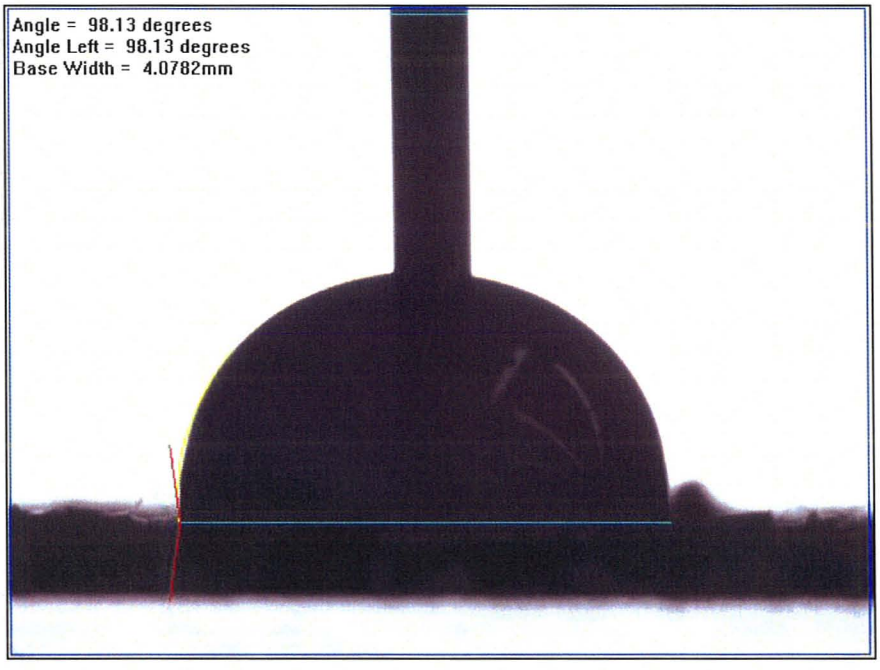

Fig. 2.12 Example of: calculated contact angle using non-spherical fit on left side of drop. Shows drawn baseline (blue), profile tracing (yellow), and tangent line (red).

side of the drop profile would be in a state of advance for a particular image. As much as was possible, measures were made on left and right sides of drops throughout movies.

Fully automated analysis using the software yielded inadequate baselines for these natural materials due to shadows from particles blocking light sources. The system recognizes significant changes in pixel intensity values (i.e. 0-255) as an indication of surfaces. When baselines are drawn using the automated system, surface roughness and the tops of particles in the background are often (wrongly) recognized as the planar reference surface itself. One way to get around this is to perform what are known as tilting plate experiments. However, in this study, attempts to use that methodology did not result in significantly better observation of the 3-phase line. As a result, using the program's internal method for detecting interfaces was abandoned early on in favour of the manual method.

Images were distance-calibrated iteratively to within ±0.0005mm using the outer needle diameter (0.635mm) and all contact angle measures were made through water. For all samples, contact angles were captured while in a state of advance, and as such all measures can be regarded as advancing apparent contact angles (AACA's). As many measures as possible were taken during the course of each movie; variability in the number of measures captured was due entirely to the visibility and reliable identification of the *advancing* 3 phase contact.

In the final stage of data capture, contact angle and interfacial tension measures (to 2 decimal places) were exported to a text file. In a separate text file, contact angle and interfacial tension sample statistics for each movie were exported. Receding contact angles were observed during the course of data capture, though were not measured in the analytical stage of investigation because of difficulty in the clear observance of the receding air-water interface. This highlights a potential weakness of ADSA for these materials. Receding angles will not be discussed further in this work.

All measurements used the software's internal surface tension database, which set the interfacial tension of water at 72.80 dynes/cm. Interfacial tension measurements taken at the end of each movie were used to identify differences in the calculation of contact angle using FTA32 Video 2.0. No differences in contact angles were reported in IFT measures observed vs. the predetermined 72.80 dynes/cm.

2.4 Results and Discussion

2.4.1 Interfacial Tension (IFT) measurements

Although noticeable differences in interfacial tension (IFT) measures were observed at times during the course of investigation, no identifiable trends in behaviour could be observed for either hydrophilic or hydrophobic materials. Where deviations from typical values (i.e. 70.5-72.0 dyne/cm) did occur, they were sporadic and often associated with Char samples. Secondary in nature to the objectives of this study, looking at changes in IFT of interstitial water in materials using the method of measure similar to that outlined here might prove to be an interesting study. Overall, IFT measures were primarily observed during this study to ensure consistency between samples. These measures were consistent throughout the course of study and stayed within an acceptable range (i.e. 70-72.5 dyne/cm).

2.4.2 Contact Angles

Sample statistics for measured air/water/soil contact angles (θ) are shown in Table 2.1. This table also reports statistics for $\cos(\theta)$ values (without standard deviations or COV's) as suggested by Murray and Darvell (1990). Ayre et al. (2007) have also been successful in scaling constitutive relationships using $\cos(\theta)$.

Much of the uncertainty surrounding contact angles is focused primarily around the interpretation of practical measures on real surfaces (Marmur, 2006).

Table 2.1 Apparent Advancing Contact Angles for 0 and 2cm depth intervals.

Sample ID	Depth (cm)	# of measures	Mean (θ)	Mean Cos (θ)	Standard Deviation (θ)	%Coefficient of Variance (θ)	Minimum (θ)	Maximum cos (θ) – re: Min (θ)	Maximum (θ)	Minimum cos (θ) – re: Max (θ)
Charred Surface Materials										
FSL (18): ACM	**0**	63	79.68	*0.1791*	12.06	15.13	62.62	*0.4599*	101.08	*-0.1922*
FSH (19): ACM	**0**	45	89.84	*0.0028*	16.55	18.42	44.23	*0.7165*	115.76	*-0.4346*
TRAN (13) MM	**0**	23	69.57	*0.3491*	14.27	20.51	39.04	*0.7767*	90.02	*-0.0003*
	2	22	99.73	*-0.1690*	6.71	6.73	92.40	*-0.0419*	116.06	*-0.4393*
FSL (16,13): MM	**0**	51	100.26	*-0.1781*	15.33	15.29	71.73	*0.3135*	121.78	*-0.5267*
	2	42	139.72	*-0.7629*	8.29	5.93	118.63	*-0.4792*	152.62	*-0.8880*
FSH (16): MM	**0**	22	78.41	*0.2009*	14.57	18.58	57.17	*0.5421*	96.23	*-0.1085*
	2	45	116.28	*-0.4428*	6.26	5.39	99.41	*-0.1635*	126.86	*-0.5999*
TRAN (14): CM	**0**	21	84.69	*0.0925*	12.79	15.11	71.28	*0.3209*	99.53	*-0.1656*
	2	38	94.63	*-0.0807*	10.73	11.34	73.52	*0.2837*	110.89	*-0.3566*
FSH (12): CM	**0**	22	71.81	*0.3122*	10.50	14.62	54.28	*0.5838*	89.82	*0.0031*
	2	88	116.33	*-0.4435*	4.72	4.05	106.79	*-0.2889*	127.12	*-0.6035*
Brown Surface Materials										
TRAN (-3,-2): BRM	**0**	89	96.00	*-0.1045*	11.62	12.10	70.05	*0.3412*	116.12	*-0.4403*
	2	20	107.44	*-0.2997*	5.91	5.50	88.42	*0.0276*	116.75	*-0.4501*
FSL (7,8): BRM	**0**	45	93.18	*-0.0555*	6.96	7.47	80.75	*0.1607*	111.14	*-0.3606*
	2	53	97.88	*-0.1371*	9.30	9.50	80.73	*0.1611*	118.89	*-0.4831*
FSH (15): BRM	**0**	55	97.44	*-0.1295*	12.03	12.35	70.50	*0.3338*	119.83	*-0.4974*
	2	19	91.47	*-0.0257*	7.18	7.84	80.32	*0.1681*	111.30	*-0.3633*
FSH (25): BRM	**0**	67	92.23	*-0.0389*	9.65	10.13	74.73	*0.2634*	110.85	*-0.3559*
	2	58	121.54	*-0.5231*	4.41	3.63	112.28	*-0.3791*	130.38	*-0.6479*
TRAN (11): BRM	**0**	12	102.33	*-0.2135*	4.80	4.69	95.38	*-0.0938*	111.17	*-0.3611*
FSH (1,7)	**0**	75	94.23	*-0.0738*	9.91	10.52	71.49	*0.3175*	116.62	*-0.4481*

Since non-ideal surfaces often display a range of contact angles within and between advancing and retreating drops, contact angles are often reported in terms of mean, weighted means, or maximum values (Merion et al., 2004; O'Carroll et al., 2005; Murray and Darvel, 1990; Kwok et al., 1997). Murray and Darvell (1990) point out that the biggest hurdle in properly assessing the validity of contact angle measurements comes not from the methodologies employed, but rather the reproducibility of measures for a given surface, further stating that multiple drops on surfaces is exceedingly rare. It seems only appropriate then to present a range of statistics based on a sufficient number of measures. While measures are reported here to 2 decimal places as generated by the software, it is in our view from operational experience that individual measures are reliable to approximately ±1°.

Also of importance is the fact that the contact angle threshold between wettable and non-wettable (90°) is only theoretical in nature, and applicable for microscopic, ideal systems. Since observations made here are macroscopic in nature, there is some inherent uncertainty in terms of what has been classified as 'hydrophobic / non-wettable' and 'hydrophilic / wettable'. Given that the theoretical understanding of macroscopic CA's is limited in terms of being able to predict wetting and non-wetting CA's for real surfaces, here we adopt the convention of using 90° as a hydrophobic / hydrophilic threshold reference point (Bachmann et al., 2007).

Charred Surface Materials

While Accumulated Char Materials (ACM), Char Materials (CM) and Mixed Materials (MM) at the 0 cm depth have mean contact angles <90° in all but one case (Table 2.1), visual similarities in surface condition are not necessarily reflected in contact angle measures. These combusted surface materials exhibit variable behaviour in mean contact angles between samples as well as maximum and minimum values. Both hydrophilic and hydrophobic contact angles were observed in 0 cm samples. Further, no samples wetted at 0° - the often

assumed contact angle for wettable media. Standard deviations are relatively high for 0cm charred surface materials (CSM's) with a range of 10.5-16.55°. Coefficients of variance are also high for these materials (14.62-20.51%) This indicates that these wettable materials exhibit the greatest range of wetting behaviour at the site (as expressed through initial contact angles); i.e. both hydrophilic and hydrophobic wetting behaviour. This is important considering that, in many applications, wetting soils are often assigned a singular hydrophilic contact angle of 0°.

It may be the case that higher standard deviations and COV's (relative to the 2 cm depth where standard deviations are in the range of 4.72-10.73° and COV's are between 4.05 and 11.34%) observed in these more wettable surface samples are actually more indicative of the exposure of these surface samples to external effects; whereas subsurface samples having been more protected both during and post fire, are thus less variable in their composition and exposure to various natural processes. For charred materials that showed no repellency in the field (i.e. WDPT of 0s), one might expect less variability in measures, particularly if the fire effectively volatilized and removed hydrophobic compounds from these materials. The fact that the greatest variation in contact angle occurs for these very samples is significant and worthy of further investigation.

At the 2cm depth, these materials exhibit a different kind of wettability altogether. At-depth mean contact angles are much higher (by +10-44°) than near surface (0cm) samples. Coupled with these non-wetting angles are much lower standard deviations and coefficients of variance than observed at the 0cm depth. What is similar is that ranges are quite large and variable within and between samples. This indicates that these at-depth materials also have the potential to exhibit a range of wetting behaviours; of which insight is not readily garnered through visual inspection of surface burn condition.

In addition to the fractional wettability observed within depth intervals (i.e. in the maximum hydrophobic and minimum hydrophilic measures), these

materials exhibit layered (wettability) heterogeneity as measured through advancing contact angles. From these measures, it can be discerned that Charred (wettable) surface materials are underlain by hydrophobic materials of varied severity (i.e. 111-153°). It seems incongruous that visually similar wettable surface materials (i.e. 0 cm - Charred Surface Materials) would show such significant variation between maximum and minimum measures of contact angle, particularly when the same kinds of differences are not observed at depth (e.g. standard deviation, coefficient of variation). However, if we consider that more hydrophobic materials below the surface (i.e. 1-2cm) could 'contaminate' surface materials as interstitial matter, then perhaps it is reasonable that a relatively small amount of highly hydrophobic material could impart the resistance to wetting observed in the contact angle measurements of these materials. Work by Franco et al. (1995) has shown that even relatively small amounts of interstitial organic matter can elicit significant changes in wettability.

Brown Surface Materials

Samples statistics for the second group of materials show surface samples (0cm depth) with relatively weak hydrophobic contact angles. Where Char materials were identified as hydrophilic in the field, these materials were identified as hydrophobic. There is very little variation in mean values between sample locations (i.e. Fire Sites 1 & 2, and the Transition site). Not only does this indicate that similarly burned materials can be visually identified between sites, but that materials at Halfway Lake show quite similar non-wetting angles. This information is unique in that soil water repellency is often regarded as highly variable in natural systems (e.g. Hallet et al., 2004). These data indicate that for these materials, under a visibly identifiable burn condition, similar surface soil water repellency (as measured through advancing contact angles) can be observed in locations where this material is found.

Similar to the Charred surface materials, Brown surface materials also showed variation between surface statistics and at-depth statistics. In three of

four cases contact angle increased with depth (i.e. all but Sample ID FSH (15): BRM). This singular (decreasing CA with depth) case may be significant, but in terms of analysis, the difference is small and the minimum value observed for the 0cm depth is 10° lower than the 2cm depth. Increases between the two depths for all brown surface materials were overall however, much smaller than those observed in the Char surface materials. Standard deviations tend to behave similarly, with decreasing standard deviation with depth, although the differences between 0cm samples and 2cm samples are not as large as in char materials. This implies that a less-heterogeneous and more predictable repellency occurs in these lesser burned materials.

Maximum and minimum values for each material are one of the more identifiable differences in the statistics. Brown surface materials show a relatively small range of minimum values (70-95°). Complimentary to this is the even smaller range of values observed in the maximum values (111-119°). The apparent similarity between samples is not observed for the Char surface materials. Noting previously the unanticipated variation between hydrophilic contact angle measurements, a large range of values can be observed in minimum (39-119°) and maximum (90-153°) measures for these apparently hydrophilic surface materials.

Charred vs. Brown Surface Materials: 0cm and 2cm depths

When considering the effect of depth on both charred and brown surface materials, it is interesting to note that at the 2cm depth, higher relative contact angles are found for char materials than for brown surface materials. While it is not an uncommon phenomenon to observe increased repellency at depth (Huffman et al., 2001; Doerr et al., 2006) the fascinating thing is that materials 'hidden' by a hydrophilic layer actually appear more repellent in terms of contact angle measurements than unhidden hydrophobic materials (i.e. Brown Surface Materials at 0cm depth). In all cases, repellency is more severe at depth, but even more so when found beneath hydrophilic materials.

Sieved vs. Unsieved – Sample TRAN (14) CM

As previously mentioned, if sample preparation destroyed or altered hydrophobic surfaces, heterogeneity between exposed hydrophilic surfaces and existing hydrophobic surfaces might be observed in the data as increased variability (King, 1981) (i.e. in standard deviations and ranges) or as lower contact angles. The more hydrophobic material data (i.e. 2cm depth for the entire data set), tend to report *smaller* standard deviations about mean values than hydrophilic materials. Since all materials underwent the same sieving preparation, it would appear as though these hydrophobic materials are less sensitive (if at all) to changes in contact angle caused by increased exposure of hydrophilic micro-surfaces, particularly in reference to wettable materials found at the site. This may indicate that these repellent materials are somewhat resistant to losing their repellency even during sample manipulation. However, the effect of lowered contact angles is difficult to isolate from the effects of surface roughness and/or chemical heterogeneity in measured contact angles, even between sieved and unsieved samples.

Table 2.2 shows reported contact angle statistics for paired sieved-unsieved measures on Char Surface materials. It should be pointed out that both samples, while showing near intermediate wettability in terms of mean values (i.e. 85° and 90°), also have maximum measures above the 90° threshold. These data show that the unsieved material has a lower standard deviation about the mean. The range also reports values that are over 8° higher when comparing minimum values: one place likely to show evidence of increased exposure of hydrophilic constituents in a hydrophobic sample. Since these samples show both wetting and non-wetting angles, the degree of this effect is not readily identifiable. Interestingly, there is very little difference in observed maximum values (approx. 4°). The mean values also reveal a comparably lower contact angles for the sieved sample. It seems in this case that sieving can result in lower average contact angles through increased exposure of hydrophilic

Table 2.2 Paired samples – ACAA's on sieved and unsieved materials

Location	Depth	# of measures	Mean	Standard Deviation	%Coefficient of Variance	Minimum	Maximum
TRAN (14a): Sieved	**0-2**	21	84.69	12.79	15.1	71.28	99.53
TRAN (14a): Unsieved	**0-2**	33	90.11	5.28	5.9	79.97	103.29

surfaces. However, the role of roughness in contact angle measurement cannot be discounted in this analysis. For contact angles greater than 90° (i.e. for hydrophobic materials), increased surface roughness is thought to increase CA's, while for hydrophilic materials, increased surface roughness is thought to lower contact angles (Dussan, 1979; McHale et al., 2004). While these two samples are close to 90°, both wetting and non-wetting contact angles were observed in each sample. Both increases and decreases in contact angle might therefore be affecting measurements in both samples. It follows that where heterogeneous surfaces exist (i.e. a Cassie condition), combined effects of both wetting and non-wetting materials may be influenced by the role of roughness more than initially considered. For a non-wettable region of the sample, large particles, that would, according to this line of reasoning contribute to increases in observed contact angles, may in fact be lowering local contact angles because of hydrophilic surface chemistries. If this were the case here, one could expect to see lower CA's for unsieved materials. The data here show otherwise; indicating that 3 things may be the case: 1) the fraction of materials removed during the sieving process are hydrophobic in nature 2) sieving contributes to increased exposure of hydrophilic surfaces and/or 3) unsieved sample drops are in a Cassie–Baxter state and do not sink into spaces between particles. The last condition (3) could appear in the standard deviation and mean values; Cassie-Baxter (eq. 2.4) predicts an increase in contact angle, but a reduction in the attenuation (range) of values between advance and retreat (Yeh et al., 2008). Whether this appears in advancing angle variation alone is unclear.

Our conceptual understanding of surface roughness in water repellent systems is one that is overly simplistic in terms of describing water repellency in

natural systems. This may be true in microscopic, homogeneous systems. However, in heterogeneous, macroscopic, water repellent systems, the opposite may also be true. While a rough, evenly coated hydrophobic particle may exhibit a contact angle greater than a smooth evenly coated hydrophobic particle, natural systems rarely have this type of homogeneity both in terms of surface chemistry and particle roughness. One might argue that what is more likely to occur is that combinations of both wettable and non-wettable particles coexist. For a wettable soil, increases in roughness should yield decreases in apparent contact angle. However, in non-wetting systems, increases in roughness could be contributed by wettable particles. Perhaps more relevant to the issue is the question of which has the stronger effect; the wettable materials or the microtopography. It seems that for non-wetting systems, water repellency has the greater effect, particularly if the non-wetting fraction is dominantly expressed.

It also appears that the source of repellency should be considered. If interstitial matter is the cause of repellency, then a coarser base material may lower the initial apparent contact angle as hydraulic (capillary) action will be inherently weaker for a porous media with larger pores than smaller ones. If the source of repellency is caused by hydrophobic coatings that are more ubiquitous, it may appear that coarser regions (of a particular material) display larger contact angles due to roughness. While Doerr et al. (2000) has noted that measures of repellence severity in fine textured soils are among the highest reported, insight into the net effect of these variables is certainly worthy of further investigation. Obviously this data is not exhaustive in scope, but it does bring to light considerations to be aware of when contact angle measurements are being made on organic soil materials.

2.5 Summary and Conclusions

In this investigation we used Axisymmetric Drop Shape Analysis to measure advancing contact angles on organic soil materials collected from a wildfire site approximately 1.5 years post fire. The data indicate that measures of contact angle made on sieved organic materials using ADSA are reasonable when placed in context with other studies that use alternative methods (e.g. Valat et al.,1991; Carillo et al., 1999). Further, these data indicate that both wetting *and* non-wetting contact angles can be observed within each of the materials (i.e. Char and Brown), regardless of the hydrophobicity expressed in WDPT tests. A number of statistics (e.g. mean, min, max, standard deviations) were reported upon and provided useful information in analysis. Advancing contact angles are a direct measure of the wettability of surfaces and we found that these organic materials exhibited fractional wettability as expressed through these statistics (in the observance of contact angles >90° and <90° within a single sample). Advancing contact angles as measured through ADSA exhibited characteristic behaviour in materials of similar burn condition and distinct behaviour between materials of different burn condition. We found that:

1. At-depth (2cm) vs. Surface (0cm) materials:
    a. At-depth materials all have mean contact angle measures >90° regardless of surface condition. Across both materials (i.e. Char and Brown), a greater fraction of non-wettable materials was found at depth.
    b. More consistently hydrophobic materials i.e. those with a smaller variance, were found at depth in most samples (i.e. 8 out of 9). Lower standard deviations and ranges in at-depth contact angles is an indication of more homogeneous composition of materials / wettability of materials / a strongly expressed non-wettable fraction.

2. Surface materials with hydrophilic mean contact angles (<90°) (Char):
    a. Materials with hydrophilic mean contact angles have the largest ranges and standard deviations of all materials investigated here. These statistics suggest that these materials exhibit the biggest range in wetting behaviour and are most sensitive to both wetting and non-wetting fractions of materials.
    b. Overlie hydrophobic materials that appear just as, or more hydrophobic than non-wetting Brown materials (at surface and at depth).
3. Surface materials with hydrophobic mean contact angles (>90°) (Brown):
    a. Have a level of consistency and similarity between surface and at-depth measures not observed in Char materials. Given the relatively high consistency of maximum contact angles between samples, this measure may be most indicative of the non-wetting fraction. The consistency supports Good's (1992) assessment that maximum advancing contact angles are most associated with the non-wetting fraction.
    b. Have maximum and minimum values that are within a narrow range (unlike Char Materials). These materials are easily characterized based on the statistical behaviour of contact angles apart from other materials found at the site.

From this assessment we conclude that distinct differences in contact angle measurements between apparently hydrophilic and hydrophobic materials are easily identified when a sufficiently large number of measures are taken. Further, we found that the variability in measures provide additional information and facilitated a fuller analysis of these materials with respect to fractionally wettable surfaces – information that is typically averaged out in other investigations. From

these statistically meaningful measures, it is clear that different wettability characteristics exist in these materials. These characteristics are likely to have profound effects on infiltration and moisture distribution processes.

Analytical methods for determining accurate contact angle measurements are still under evaluation if for no other reason than surface energies of solid surfaces are not directly measurable. In spite of all the complexities and variability between ideal, intrinsic contact angles and observed ones, there is hesitant acceptance that initial advancing contact angles are the most reliable measures of contact angle (Dussan, 1979) and are most related to Young contact angles (Kwok et al., 1997). Decker et al. (1999) have indicated that often we look to macroscopically averaged contact angles when hysteresis is present. Yeh et al. (2008) note that the maximum observed contact angle is the most relevant measure. These references all point to our lack of understanding regarding contact angle measures, their meaning, and the 'choice' that is made when analytical results are presented. It seems important then, when performing analysis and considering the statistical significance of contact angles, that multiple pieces of statistical information are included in analysis to facilitate better understanding of appropriate and meaningful measures on materials, particularly in cases where fractional wettability is suspected.

In regards to porous media, the value of contact angles is measured in terms of the ability to assist in the development of our understanding of wetting processes in bulk media. For materials with fractional wettability the view that receding angles are associated with the wetting fraction and that advancing angles are associated with the repellent fraction seems overly simplistic. While perhaps accurate, it is important to consider the possibility of a range of valid measures (e.g. max, min, mean) for chemically and structurally heterogeneous surfaces that exhibit more than 2 possible fractions of differently (non)wettable materials. If we consider that Good (1992) is correct in the assessment that advancing contact angles measure the highest contact angle in materials and

receding angles measure the lowest, it still tells us little about the relative contributions of each and the overall effect on wetting in porous media. To not consider the relative contributions of wettable and non-wettable micro-scale surfaces in natural media could lead to overestimations of the relative importance of roughness in CA measurements through this failure to more fully consider the consequences of heterogeneous surface chemistry on constitutive relationships.

2.6 Implications

Fractional wettability, until now, has not been directly assessed in terms of its contribution to infiltration processes in naturally hydrophobic porous media. We argue that insight into the fractional nature of naturally repellent materials can be discerned using ADSA when a large number of measures are taken. The extent to which wettable particles exist in a system determines how these systems respond to long duration rainfall events, as well as short duration, high intensity rainfall events. Many studies have sought to identify the hydrological effect of increased fractions of non-wettable particles within soil and for all cases, relatively small amounts of non-wettable materials induce observable repellency in samples (e.g. Bauters et al., 2003; Quyum et al., 2002; Bradford and Leij, 1996; Hwang et al., 2006). The notions of mixed (each pore has a particular CA) and fractional wettability (each pore wall may have a particular CA) have also been considered in numerous soil repellency investigations (e.g. Al-Futaisi and Patzek, 2004, Imeson et al., 1992; Diehl and Schaumann., 2007; Doerr et al., 2000; Goebel et al., 2007; Clothier et al., 2000; Bachmann et al., 2007; Franco et al., 1995). The effect of increased fractions of hydrophobic materials in otherwise wettable media has been shown to have far-reaching implications on capillary pressure-saturation relations (Bradford and Leij, 1995; Bradford and Leij, 1997). However, the noted investigations have not fully examined and assessed its possible influence on wetting in non-synthetic (i.e. natural) materials where temporal dependencies exist.

Infiltration into and through hydrophobic materials have traditionally been attributed to breaks, cracks or hydrophilic patches in otherwise water repellent layers (e.g. Shakesby et al., 2003; Doerr et al., 2000; Doerr et al., 2006). In the following chapters, we will evaluate the presence of a wettable fraction in bulk hydrophobic media (and vice-versa) in relation to time dependent changes in contact angles and infiltration processes. The presence of a wettable fraction within a hydrophobic system has the potential to serve as a significant source for fluid transport at the onset of rainfall events and facilitate more evenly distributed moisture than previously considered.

Chapter 3: The Role of Dynamic Contact Angles - Infiltration into Fractionally Wetting Media

3.1 Background

3.1.1 Time Dependence of Repellency

Hydrophobicity is often cited as a changing property with increased exposure to water (Letey, 2001; Doerr et al., 2000). Critical soil moisture thresholds are thought to describe or mark the minimum moisture content / transition zone (Dekker et al., 2001) where water repellent media become wettable / where repellency disappears (Doerr et al., 2000). This has been shown to be variable depending on the materials investigated (Doerr and Thomas, 2003). The causal relationship between moisture conditions and repellency expression is contingent upon hysteretic constitutive relationships (van Dam et al., 1996; Naasz et al., 2008; Bachmann et al., 2007), wetting history (Quyum et al. 2002), and the origin of hydrophobic substances (Doerr and Thomas, 2003). Further complicating the observance of a simplified relationship between moisture conditions and water repellency are unexpected moisture distributions in water repellent materials observed over time (Ritsema and Dekker, 1994).

In the preceding chapter, we saw that the wetting of surfaces is contingent upon the contact angle at which a fluid, gas and solid meet. While contact angle measures are a highly effective way to discern the instantaneous behaviour of fluids on surfaces, they are limited in terms of their capacity to provide longer term information on wetting in hydrophobic pore spaces.

The observance of a temporal component to water repellency expression is not unique to burned materials, and this temporal component is a primary assumption in one of the most widely used tests in water repellency investigations: the Water Drop Penetration Time (WDPT) test (Roy and McGill, 2002). The test involves monitoring the time required for a drop of water resting on the surface to enter the soil matrix; thereby estimating the persistence of repellency or the time required for the contact angle to change from a non-

wetting angle (>90°) to a wetting one (<90°) (Letey, 2001; Letey et al., 2003). Put another way, WDPT is intended to measure the dynamics of repellency.

In spite of the heavy reliance on the Water Drop Penetration Time (WDPT) method as a measure of hydrophobicity, problems are often cited. Weaknesses of the method are commonly associated with high variances and low reproducibility (Huffman et al., 2001; Scott, 2003; Verheijen and Cammeraat, 2007), sensitivities to temperature and relative humidity (Diehl and Schaumann, 2007) and low correlation to Molarity of Ethanol results in heterogeneous and more weakly hydrophobic media (Doerr, 1998; Verheijen and Cammeraat, 2007). Most notable in the list of complaints, is that the test is not a true indication of the hydrologic response of hydrophobic materials (Cerda and Doerr, 2007; Miyata et al., 2007). Regardless of the tests shortcomings, its frequent use implies there is widespread recognition that water repellency is a dynamic phenomenon governed by changing contact angles.

3.1.2 Infiltration Behaviour in Fractionally Wettable Capillaries

To better understand the nature of wetting in variable pore spaces where individual pores may express a range of repellence and where contact angles exhibit dynamic behaviour, it is essential that we explore the relationships that determine wetting in porous media at a larger scale than single drops on surfaces.

In any pore space, the tendency to wick a particular fluid (i.e. water or air) is determined by the pore water pressure. Where the wetting of *surfaces* was defined (ideally) by Young's (1805) equation, wetting in pores and the larger soil matrix is defined by the Young-Laplace equation for capillary pressure which is given by:

$$P_c = \sigma\left(\frac{1}{r_1}+\frac{1}{r_2}\right)=\frac{2\sigma\ \cos\theta}{r} \qquad \text{(eq. 3.1)}$$

where, σ is the air-water surface tension, r_1 and r_2 are the principle radii of curvature of the air-water interface, θ is the effective water-solid contact angle, and r is the effective radius of the pore at the location of the air-water interface (Bear, 1988). Alternatively, the capillary pressure can be expressed for capillary rise in water pressure head units with the water having negative pressures (below atmospheric) under wetting conditions using (Letey, 2001; Czachor, 2007):

$$h_p = \frac{-2\sigma\cos\theta}{r\rho g} \qquad \text{(eq. 3.2)}$$

Where h_p is the water pressure head in the pores and g is the gravitational constant. The water pressure head (h_p) is directly proportional to the surface tension (σ) and the cosine of the effective liquid-solid contact angle (θ) (as measured through the water phase), and inversely proportional to the effective pore radius (r), and water density (ρ). While it could be argued that this relationship is too simplistic, microscopic relationships provide a starting point from which larger scale observations can be assessed (Letey, 2001; Bachman et al., 2007).

According to equation 3.2, for systems where the wetting fluid experiences no changes in surface tension, water pressure head is determined by the radius of curvature between the wetting and non-wetting fluid and the contact angle between the porous media and two immiscible fluids (i.e. water and air). Relative to the discussion at hand, for homogenous, wettable media where contact angles are assumed to be < 90° (i.e. $\cos(\theta) > 0$), water pressures are negative. For these materials, the tendency will be to wick water into pore spaces; with smallest pores having the strongest suction and the largest pores having the weakest suction.

For homogeneous, *non-wettable* materials where contact angles are greater than 90° (i.e. $\cos(\theta) < 0$), the tendency will be to repel water by the same

magnitude. The smallest pores will have the strongest repellence to wetting and the largest pores will have the weakest repellence to wetting for a given set of static conditions (e.g. contact angle, surface tension of fluid, pore radius). Because of this, the tendency in water repellency literature has been to attribute the majority of flow in water repellent systems to the weakest capillaries: large pores (e.g. Bauters et al., 2000; Feng et al., 2001; Carillo et al., 2000a). While this may be true in certain scenarios, it is prudent to question the validity of this assumption in the presence of 1) dynamic contact angles (as measured in WDPT tests), and 2) fractionally wettable media.

3.2 Introduction

Infiltration-based experiments in water repellency investigations are intended to elucidate wetting behaviour in soil (e.g. Kobayashi and Shimizu, 2007), permit the quantification of controlling parameters on infiltration (e.g. soil moisture content), facilitate analysis of hydrological effects resulting from soil water repellency (e.g. Martin and Moody, 2001), and give insight into solute transport in hydrophobic soils (e.g. Clothier et al., 2003). There is no question that hydrological processes in water repellent media are highly complex and incompletely understood in an empirical context.

While it is commonly *reported* that water repellency contributes to irregular wetting, preferential flow, and reduced infiltration, thorough explanations and insights into governing controls are in short supply. In spite of the effort put forth by researchers, the conditions under which reduced infiltration occurs and unstable flow develops are yet to be systematically identified and investigated. It is apparent, however, that infiltration in hydrophobic soils is markedly different than that of consistently wettable soils. Unlike wettable soils, water repellent soils are often characterized as having increased infiltration rates with time (Wallach and Graber, 2007; Clothier et al., 2003; Letey, 2001; Wang et al., 2000).

In a review paper, Debano (1975) suggests two possible mechanisms for the observance of increased infiltration rates: 1) increased solubilising of

hydrophobic constituents and 2) adsorption of water onto breaks in hydrophobic coatings. Though it is not difficult to imagine that both of these mechanisms play a role in infiltration into hydrophobic media, the empirical detection and identification of controls on these mechanisms has proven more so.

The problem of properly identifying and understanding controls on infiltration in water repellent media has stemmed in part from the spatial and temporal scales at which these systems are often investigated. Drop tests, while providing small scale information, have numerous unknowns related to temporal and larger scale dependencies of water repellency in general (Orfanus et al., 2008), and infiltration processes in particular (Cerda and Doerr, 2007). Conversely, larger scale investigations often employ techniques that while highly useful for measuring and identifying certain processes, are limited in their capacity to describe fundamental wetting processes at smaller scales and for a range of wetting conditions. For example, *in situ* rainfall simulations are often employed to identify runoff and erosion processes (e.g. Imeson et al., 1992; Shakesby et al., 2003; Miyata et al., 2007; McNabb et al., 1989; Pierson et al., 2008). It is common that in these investigations hourly rainfall amounts mimic rainfall intensities observed in the wettest months of the year when repellency is often least expressed (e.g. Cerda and Doerr, 2007) or with long (>5 years) return intervals (e.g. Pierson et al., 2008). To help isolate infiltration from erosion and overland flow processes in water repellent soils, Leighton-Boyce et al. (2007) utilized surfactant-treated water to promote infiltration in water repellent soils. They note the uncertainty inherent in using reduced surface tension fluids to mimic wettable infiltration. Wallach and Graber (2007) used water and aqueous-ethanol mixtures in ponded infiltration tests and identified that using reduced surface tension fluids in water repellent systems did *not* mimic water infiltration into wettable media. They found that lower surface tension fluids (i.e. 20% ethanol by volume) were useful in changing the shape of cumulative infiltration plots from convex to concave, but did not elicit the unrestricted infiltration

response of wettable materials. Thus, finding a wettable-system analog to assist in the development of our understanding of water repellent soil systems has been difficult.

In response to the inherent complexity of these systems, some have attempted to simplify their investigations by using increased fractions of synthetically hydrophobized sands in ponded infiltration experiments (e.g. Bauters et al., 2000; Feng et al., 2001; Carillo et al., 2000a). While useful in providing information related to the effects of fractional wettability in systems with static contact angles, forced imbibition or infiltration under a positive hydrostatic head is largely controlled by the magnitude of hydrostatic force applied, and *not* by the system's changing properties (Feng et al., 2001). Forced imbibition relies on the assumption that water 'must' be forced into a water repellent pore (Feng et al., 2001; Bauters et al., 2000). While the assumption may be valid for a specific set of soil and moisture conditions (e.g. contact angle never changes, hydrophobic compounds are insoluble, porous media are completely dry), it certainly is not true for all cases; particularly for systems that show changes in contact angle with time or are fractionally wetting. Additionally, the method inherently assumes that macropore flow is a primary infiltration mechanism in water repellent materials. When water is forced into pores under a positive pressure head condition, the pores with the weakest capillary pressure will allow water entry first. Furthermore, testing under positive pressure heads is difficult to set up in non-wetting media (Wang et al., 2000). Because of the height of water, it is difficult to separate infiltration *through* the porous media and infiltration along the wall of the containing apparatus.

Alternatively, some investigations in water repellent media have made use of tension infiltration experiments. With an increasing awareness of the temporal nature of many water repellent materials, tension infiltrometers or disc permeameters are being more seriously considered as a means to observe hydraulic properties and time dependent changes in these systems (e.g. Lewis et

al., 2008; Clothier et al., 2003; Doerr and Thomas, 2003; Bens et al., 2007; Lichner et al., 2007; Hallet et al., 2004; Tillman et al., 1989). Tension infiltrometers have long been used in unsaturated flow investigations as a means to determine hydraulic properties and transport processes (Reynolds and Elrick, 1991; Logsdon, 1997; Clothier et al., 1996; Ankeny et al., 1991; Cook and Broeren, 1994; Clothier and White 1981; Reynolds, 2006). In contrast to ponded infiltration techniques, tension infiltrometers rely on the matric suction of porous media to wick water out of the instrument under a set tension head (Felton, 1992). For non-wetting systems, this type of instrument allows the investigator to look at system response using a method that is sensitive to changes in contact angle with increased exposure time to water.

3.3 Research Plan

In this chapter, we report upon the use of tension infiltrometers to measure and characterize infiltration behaviour in the fractionally wetting materials investigated in the previous chapter. We hypothesised that the instrument would be an instructive tool that would provide insight into the controls and processes governing infiltration behaviour in layered non-wetting systems where fractional wetting exists. For materials with an increased wettable fraction, we hypothesised that faster infiltration rates could be observed over the duration of 1D column experiments and that infiltration rates would be sensitive to fractional wetting in layered hydrophilic-hydrophobic systems.

Further, in concluding sections we examine the effect of changing contact angles in these materials. We expected to see distinct differences between the non-wetting materials investigated. We anticipated that the highest initial contact angles found beneath char materials (observed in the chapter 2) will have longer transitions between non-wetting and wetting angles than lower initial contact angle materials (i.e. Brown Materials). This was based on the assumption that the *rates* of contact angle change for all non-wetting materials investigated are similar.

Our analysis examines the effect of these fixed (fractional wettability) and temporal dependencies (dynamic contact angles) in relation to real time and post-infiltration moisture content information collected during experiments.

3.4 Materials and Methods

3.4.1 Testing Overview

Two phases of 1D infiltration tests were carried out on fire affected materials collected from Halfway Lake Provincial Park 1.5 - 2 years post-fire. All experiments as described in this chapter were designed to test a layered system of surface (organic) cap material overlying B (mineral) horizon material; this was the primary observed orientation at the field site. In material screening WDPT / MED tests (see section 4.2.3), organic materials exhibited a range of repellence from not repellent to severely water repellent based on the classification scheme of Dekker and Ritsema (1994). All mineral horizon material was hydrophilic in WDPT tests (<5s to drop disappearance).

3.4.2 Phase I Materials

Phase I collected materials were transported in plastic containers and stored in an outdoor shed from November, 2008 to March, 2009; after which samples were stored in a chest freezer at -4 °C until use. When required, samples were partially thawed and sub-samples were collected and placed in shallow aluminum pans to air-dry. Remaining materials were then put back in the freezer.

While the preparation for mineral (B) horizon materials was the same for all experiments, preparation of organic materials varied. As much as was possible, organic materials were sampled from undisturbed soil profiles / surface layers that had been sampled as larger block units. This was the preferred method because it preserved the natural cohesion and structure of organic materials.

For Brown Organic Materials (Brown OM), infiltration tests samples were collected from larger 'slabs' of material that had been collected in November. This material showed signs of some burning, however, evidence of charring at the surface did not exist (or had been naturally removed) 1.5 years post-fire. Once slabs were air dried, a stainless steel ring and small stainless steel spatula were used to cut out a puck of material such that it would fit the diameter of the infiltration column Fig 3.1. Significant undulations on the contact-side (bottom) of the puck were removed to ensure a good contact between organic and mineral materials in the 1D column.

Another organic material of interest was termed Mixed Organic Materials and was collected from a (largely) frozen soil block. This organic material was characterized as having visible signs of burning / charring in the top 1-2cm of the organic horizon. Organic materials lost a significant amount of cohesiveness when in a charred state, and so these materials were extracted from the top of the soil profile while still frozen, but malleable. After some thawing, a stainless steel ring was driven into the top 3-4cm of the frozen block. Light twisting action separated the partially thawed surface material from more frozen subsurface materials. These samples were then air dried.

A third organic material of interest was collected in the field from various areas within a single sample site at the centre of the burn area. Due to the lack of inherent cohesion of these materials, Char Organic Materials were scraped from multiple surfaces *in situ*. These materials required little thawing once removed from the chest freezer. To prepare these materials for use during infiltration tests, char material was scooped and packed to a maximum depth of 2cm into the same stainless steel ring as used for the other organic materials. The moisture in the thawed material helped serve as a glue so that when removed from the stainless steel ring, char materials would maintain their puck shape. These samples were then allowed to air dry.

(a)

(b)

(c)

Fig. 3.1 Showing a) slab material in aluminum pan b) material in stainless steel ring and c) material in infiltration column. Ring diameter in (b) = 4.6 cm.

Following air-drying of B Horizon materials, peds and small cohesive units were broken up by hand and hand-sieved through a 2mm mesh (U.S.A. Standard stainless steel test sieve, A.S.T.M. E-11 Specifications) to remove any gravel and cobbles. The < 2mm sieve fraction was then mixed and split using a soil splitter (Versa-Splitter, model no. SP-2.5, Gilson Co., Inc. Worthington, OH) to avoid particle / sample bias. Soils were then re-mixed, and a final split separated samples into adequate volumes required for column experiments. Textural properties of B horizon material were analysed using the mechanical sieving technique outlined in Carter (1993). All B Horizon materials were texturally Loam.

All soils (organic and mineral) used in column experiments were air-dried in the lab for a minimum of 7 days prior to each experiment. Five replicates of each of the material configurations (i.e. Mineral only, Char over mineral, Mixed over mineral, Brown over mineral) were conducted randomly during a 10 week period, over which time multiple sample preparations took place.

3.4.3 Phase I Apparatus

The apparatus used in the column experiments was constructed using 4.4 cm inside diameter acrylic tubing 40 cm in length (Fig. 3.2). A bottom-end support structure was attached to the tubing to reinforce and secure the inner stage. The inner stage served the purpose of supporting materials in the column. Holes were drilled into the stage to allow air flow; a fine mesh was placed on the stage to prevent material from falling through air ports. The inner stage was attached to an aluminum rod that extended from the bottom of the column. The rod was used to extrude materials from the apparatus post-infiltration. A clamp around the aluminum rod at the support structure plate could be adjusted to set the stage height within the column and prevent the stage / materials inside the column from moving. The apparatus was clamped to wall-mounted rods to maintain a vertical orientation in all tests.

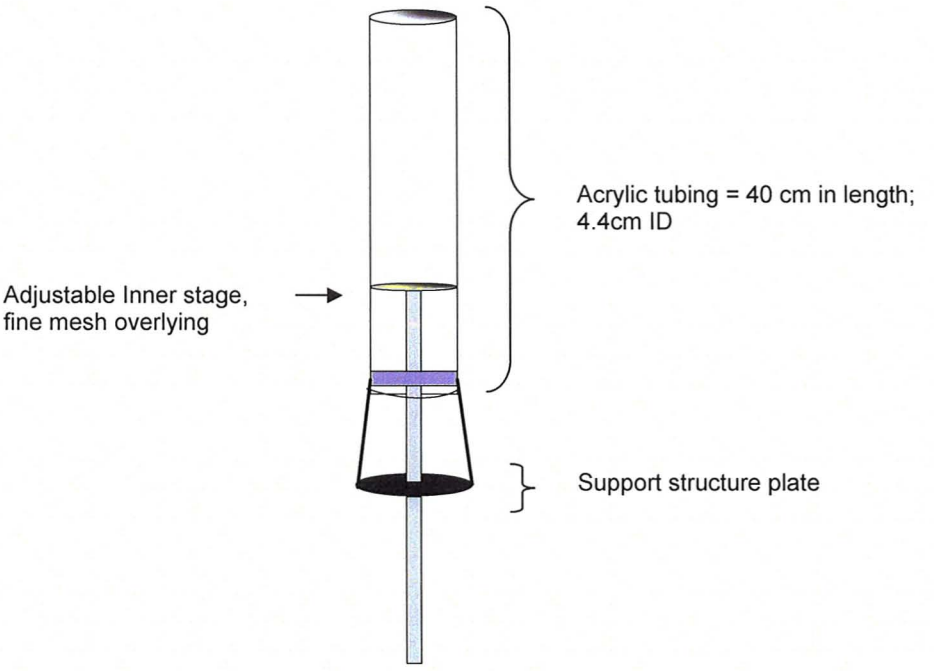

Fig. 3.2 Phase I Infiltration Apparatus

A Mini Disc Infiltrometer (Decagon Devices, Pullman, WA) was used in all Phase I experiments (Fig. 3.3). The infiltrometer is made of a single piece of polycarbonate tubing split into a bubble chamber and reservoir and a 4.4 cm diameter stainless steel porous plate. The diameter of the porous plate was ideal relative to the dimensions of the column diameter. Both the bubble chamber and reservoir are filled with water; the bubble chamber controls the applied suction / tension at the porous plate and the reservoir houses the water that will eventually be wicked into the material. The negative pressure head is set prior to test initiation by sliding the bubble chamber tube (that is open to the atmosphere) up or down depending on how much tension is required. The reservoir has graduated markings so that volume (ml) measurements can be read from the device during the course of the experiment. All Phase I experiments were conducted using a disc pressure head of minus 2cm.

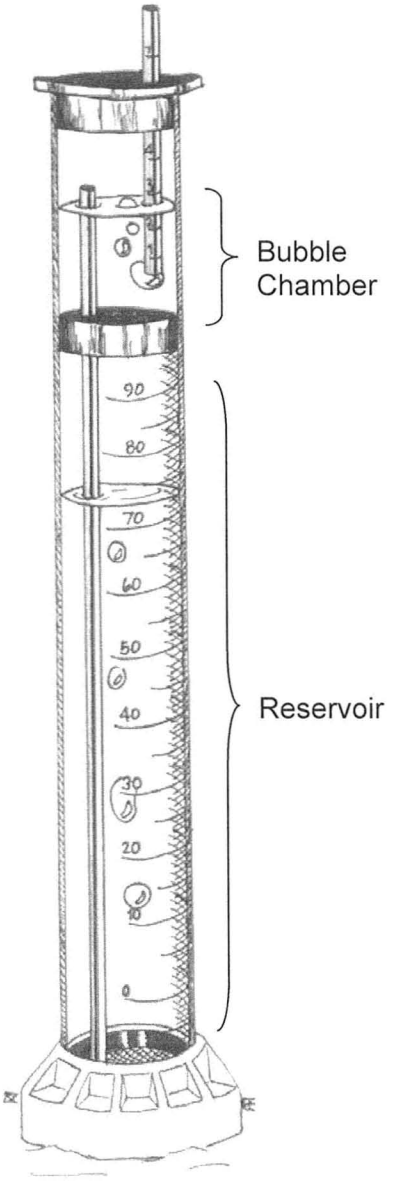

Fig. 3.3 Decagon Mini Disc Infiltrometer (Decagon Devices, 2009)

This tension infiltrometer has been used in other water repellency investigations albeit in a different capacity. Hallet et al., (2004) and Lichner et al., (2006) have used the apparatus to look at sorptivity of repellent materials using water and ethanol as infiltrating fluids. Lewis et al. (2006), Lewis et al. (2008), and Robichaud et al. (2008) have promoted the use of this instrument as a means to determine repellence severity through a time to first bubble term and

an initial infiltration rate (measured during the first minute). Both the plate and column had measured diameters of 4.4cm, equal to 15.2cm^2 surface areas.

3.4.4 Phase I Method

Columns were prepared according to the 4 material configurations of interest: Mineral only, Char over mineral, Mixed over mineral, Brown over mineral. In all tests, air-dried B Horizon materials were first weighed and then packed into the column using a constant pour method. Two people poured each column. To prevent microlayering, one person continuously poured material through a funnel while the other tamped the sides of the column using rubber handled pliers. The handles were used to tamp alternate sides of the column continually to increase bulk density in the column. Mineral materials using this method were filled beyond the height of the column. The resulting height of the column varied between experiments (i.e. 9.5 – 25cm). This largely depended on the material configuration (i.e. Char over miner vs. Brown OM over mineral); it was required in all cases that wetting fronts not reach the bottom of the column at any point during experiments.

Overflow material was captured and weighed. In the case of the layered column experiments, small amounts of mineral soil were removed from the top of the column with a small spatula to accommodate the thickness of the organic materials being used (Fig. 3.4). This removed material was also weighed so that estimates of bulk density could be made for the mineral layer. Mineral horizon materials were packed to 1.1g/cm^3 average bulk density (range: 1.0-1.2 g/cm^3). These values compare well to (oven) dry bulk densities of field samples (see section 4.3.1).

Organic materials were weighed prior to testing so that organic bulk density estimates could be made. They were then pressed into the mineral horizon using sufficient force to achieve good contact across the diameter of the mineral-organic material interface. For 'mineral only' experiments, soil at the top of the column was levelled approximately 1mm above the surface of the column.

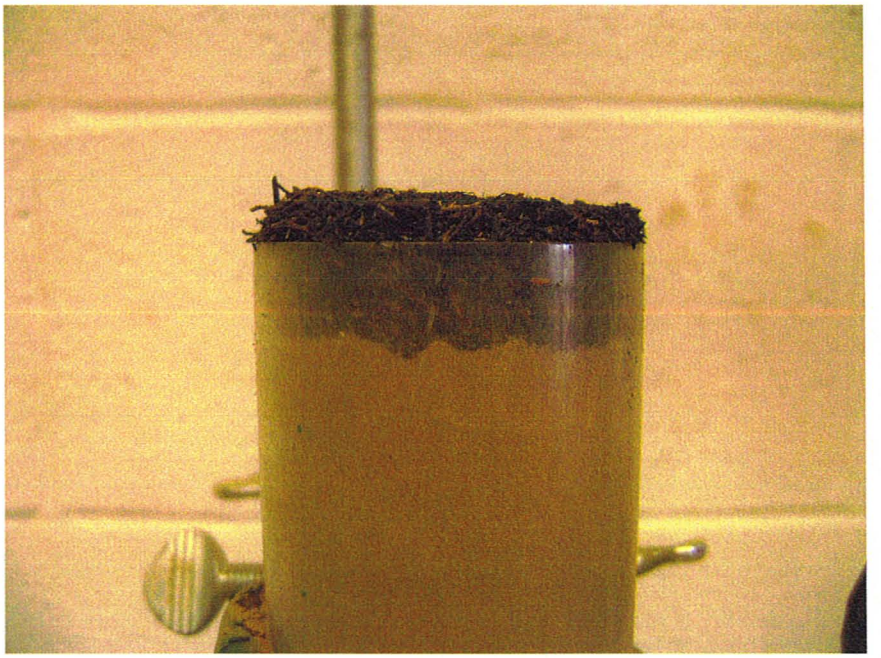

Fig. 3.4 Organic cap material overlying hydrophilic B Horizon Material in column. Column OD = 5cm

This was done to ensure contact of the infiltrometer disc to the surface of the mineral soil throughout the test in the event any particle settling occurred during the test.

All organic pucks were between 1.1 and 1.9 cm in height (inclusive). Variability in thickness was more noticeable between materials (opposed to within a specific organic material type). While this variation in height would affect the tension / boundary condition at the mineral-organic interface for each test differently, under the variation observed here (i.e. 0.8 cm), a negative pressure head condition existed at the (hydrophilic) boundary in all tests. Once set up, small adjustments were made to the column to ensure vertical orientation before test initiation.

A mounted digital still camera (model: Cannon Power Shot SX100IS) was used to capture sequential images of wetting front advance at regular intervals for the duration of tests. Software (Cannon: Remote Capture DC) was used to set timing preferences. All images were automatically saved to a hard drive. A

hand-held digital still camera (Sony: DSC-S650) was used to capture additional early time infiltration behaviour around the perimeter of the column.

Before each test, the bubble chamber of the infiltrometer was filled with water and set to a pressure head of minus 2cm. The infiltrometer reservoir was then filled to capacity with approximately 90ml of deionized water. During this time, the porous plate was wetted in a beaker of deionized water. While upside down, the porous plate was then pushed onto the bottom of the infiltrometer, after which it was turned right side up. This resulted in some water flowing out of the instrument, typically ~5 ml. The plate was then cleared of excess water using a paper towel and a bubble was established at the opening of the bubble chamber tube. This was done to set the initial condition for capture of 'time to first bubble' data / the time to infiltration initiation.

Time zero was defined as the time when the infiltrometer was placed on the material surface. The infiltrometer was placed with sufficient force to ensure good contact across the disc diameter. Materials compressed differently under this force depending on the bulk density / burn condition of samples. Compression of the organic surface was between 0.1 and 0.7cm for all tests. The infiltrometer was then clamped to the same support structure the packed column was clamped to. The vertical orientation of the infiltrometer was checked with a level and small adjustments were made (if required) without losing contact between the porous plate and material surface.

Tests were conducted until the entire infiltrometer was emptied. The duration of tests depended entirely on the wettability of packed column materials since the disc pressure head was set to minus 2cm in all tests. At the end of each test, a final measure was taken and the infiltrometer was lifted off the surface of the column. The column was then unclamped and turned horizontal to minimize infiltration due to gravity down the length of the column and the core was immediately sectioned and sampled. The adjustable stage was designed so that materials could be pushed out of the column in a matter of seconds.

However, it was quickly established through early testing that through the introduction of moisture into the column, mineral materials adhered to column walls and prevented this.

While the column was being held horizontally by one person, a second excavated materials using a stainless steel spatula. All materials were collected over 2cm intervals and put into sealable glass containers. For experiments where the top 2cm of the column consisted of both organic and mineral materials, wet organic materials were collected separately from mineral soil. The remaining material was then collected according to the 2cm interval markings on the outside of the column. Upon reaching the last ~4cm of wetted material, the stage often became free and was able to move in the intended way. These materials were extruded and sliced off into containers. Dry material at the bottom of each column was collected irrespective of the 2cm interval used for wet materials. The post-infiltration material collection process lasted between 3 and 5 minutes.

Following excavation / extrusion, the glass containers were then covered with a fitted lid to prevent evaporation. Samples were then weighed, uncovered and then dried to constant weight in a 40-60 °C oven. This temperature range was chosen to avoid any burning off of organic materials. All samples were cooled in a dessicator prior to weighing. These weights were used in conjunction with organic and mineral soil bulk densities to construct volumetric moisture content profiles for each test. In addition to post-infiltration samples, control samples for mineral and organic materials used in each experiment were also weighed and then dried to constant weight at 40-60 °C to obtain representative initial gravimetric moisture contents.

3.4.5 Phase II Materials

Materials used in Phase II experiments included organic materials collected in November, 2008 and May, 2009. Organic materials used in Experiment #1 were collected in November and stored according to the description in section 3.4.2 (Phase I). These materials were allowed to air dry for

2½ weeks prior to use. Organic materials used in Experiment #2 and mineral materials used in both tests were collected in May, 2009. These materials were stored in a 3 °C refrigerator for 10 days and then were allowed to air-dry for 3 weeks. The additional drying time (compared to Phase I experiments) was to ensure that organic slabs from which large caps (i.e. ~4cm depth) would be sampled had sufficient time to air dry such that weight only fluctuated according to changes in the lab's relative humidity (Roy and McGill, 2002).

Both tests used Mixed material pucks (similar to that of Phase I experiments), however, the amount of surface scorching on the materials used in experiment #1 was noticeably less that on materials used in experiment #2. Materials were sampled from larger slabs using a piece of clear tubing the same diameter as the infiltration column (i.e. 9.5 cm) in a similar manner as described in section 3.4.2. The tubing served as a stencil on the soil surface; a stainless steel knife and pair of scissors were used to cut around the perimeter of the tubing and through any roots or large fibres. The tube was then pushed down so that the material would be contained in the cylinder. This material was then weighed. Mineral materials were prepared in the same manner described in section 3.4.2.

3.4.6 Phase II Apparatus

The column used in Phase II experiments was made of 9.5 cm inner diameter clear Polyethylene tubing 20cm in length (Fig. 3.5). The bottom end of the cylinder was covered in fine nylon mesh and small gauge coarse screening to retain material while allowing air flow. A metal ring gear-clamp secured the mesh and coarse screening to the cylinder.

For these infiltration tests, moisture content information would be collected from soil capacitance probes (model: ECH_20 EC-5 Moisture Sensors, Decagon Devices, Pullman, WA) inserted into B horizon and Organic horizon materials. To accommodate the probes, sections of plastic were cut from the sides of the column to create access ports. These windows were taped over on

the inside wall of the column prior to packing to retain material. The column was then clamped to wall-secured rods using two adjustable ring clamps and levelled to vertical orientation.

As previously mentioned, soil capacitance probes were employed in these infiltration tests to measure changes in water content over the course of infiltration tests. The two-pronged probes are 5.5cm in length. Three probes were used in each of the experiments. The probes were set to collect data at one minute intervals over which time data was automatically averaged and stored in a battery-operated data logger (model: Em 5b, Decagon Devices, Pullman, WA).

The tension infiltrometer used in these experiments was a large capacity infiltrometer with an 8cm diameter porous disc. In contrast to the stainless steel disc of the Phase I infiltrometer, the porous disc used in Phase II experiments was made of thin nylon mesh. Although the construction of this larger infiltrometer is different, the infiltrometer functions the same as the Mini Disc Infiltrometer used in Phase I experiments.

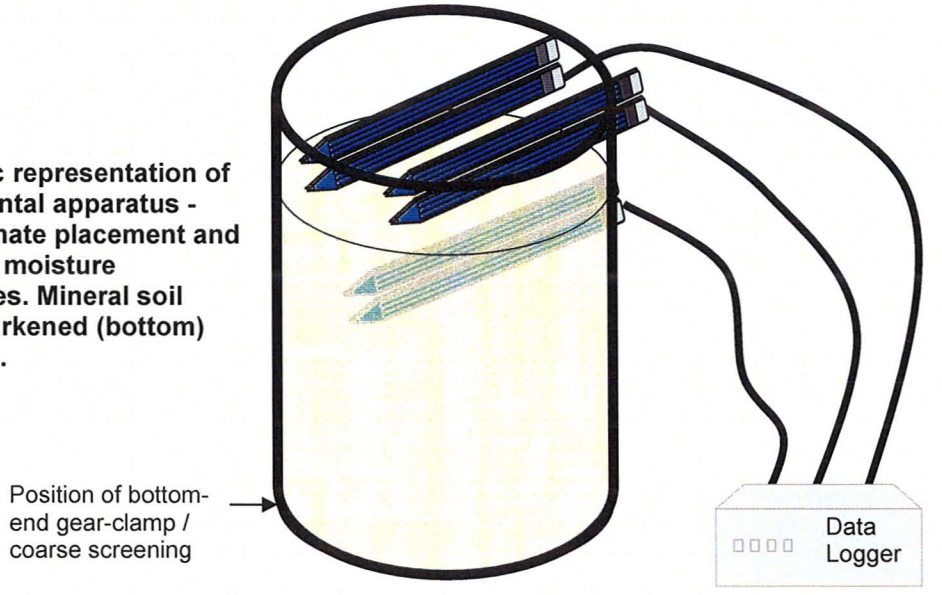

Fig. 3.5 Schematic representation of Phase II experimental apparatus - showing approximate placement and orientation of soil moisture capacitance probes. Mineral soil represented as darkened (bottom) portion of column.

3.4.7 Phase II Method

The two packed columns in this series of experiments were prepared somewhat differently than described in section 3.4.4. Because of the size of the column (9.5 cm diameter), the rate of *pour* of material had to be increased so that the rate of *fill* (in cm's) would be proportional to the rate of fill of the smaller diameter column. To this end, material was poured directly into the column without the assistance of a funnel. In addition, the rubber handled pliers used previously were too light to increase bulk density in the wider column, so two rubber mallets were used to tamp the sides of the column while material was being poured by the lab assistant. For these experiments, thicker organic pucks would be used; the additional clearance at the top of the column provided a buffer so that it was not necessary to fill beyond the height of the column. Any material that did not end up in the column during packing was collected and weighed. A small spatula was used to remove additional material from the top of the cylinder so that the position of the organic puck and mineral horizons would align with the access windows in the top portion of the column. The remaining material in the pour beaker was then weighed. Mineral horizons were packed to a bulk density of 1.05 g/cm^3 in these experiments and were assumed to be constant for the depth of the mineral layer.

Organic pucks used in these experiments were weighed so that bulk density estimates could be made. The cylinder that contained the organic material was then aligned with the mineral–packed column and organic materials were pushed onto the mineral horizon material. Additional gentle force was applied at the organic surface to ensure good contact at the organic-mineral interface. A dry height measurement of the organic material was recorded.

Once test materials were packed in the column, a large metal ring clamp was adjusted and positioned so that it would support an eventual layer of poured contact sand and rest securely such that it did not interfere with the position of the infiltrometer on the column. A double-layer of cheesecloth was then draped across the material surface / ring clamp support and positioned to match the

contours of the organic material surface. This also served to 'protect' surface materials while soil capacitance probes were being inserted. Three soil capacitance probes were used in each of the Phase II experiments to measure volumetric moisture content over the duration of tests.

Probes were inserted into materials through the access ports that had been taped over prior to packing (Fig. 3.6). Cuts were made in the tape with a knife so that probes could be inserted without obstruction. In each experiment one probe was inserted vertically into the B horizon material. The centre of the probe was positioned approximately 4cm from the top of the column. Two additional probes were inserted into the organic layer. For Experiment #1, one probe was positioned 1.7cm from the top of the column on an angle so that water would not pond on the probe blades. The third probe was positioned 2cm from the top of the column at a similar angle. The position of the mineral (B) horizon soil capacitance probe for the second experiment (#2) was the same as in

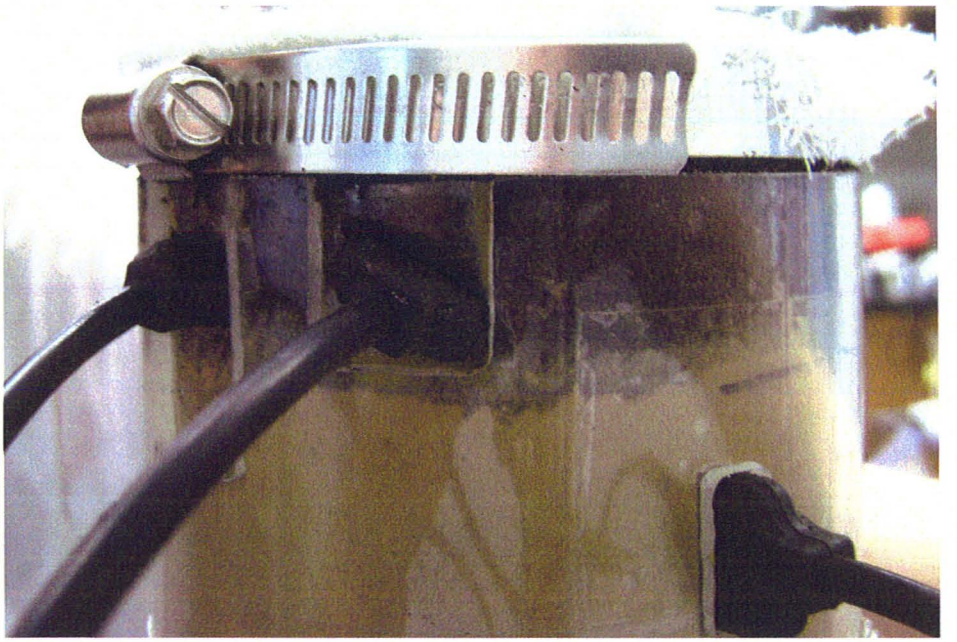

Fig. 3.6 Phase II experimental set up showing inserted soil moisture capacitance probes for Experiment #2

Experiment #1. Organic soil moisture capacitance probes differed for Experiment #2 in that both probes were positioned at the same height relative to the top of the column (1.3cm), angled and parallel to each other. This was done to determine if any differences in moisture content could be observed in the organic layer for the locations of the probes. In all cases, care was taken so that no probes touched.

Once soil capacitance probes were inserted into column materials, a layer of fine quartz silica sand (Ricci Brothers: 56-3-10) was poured slowly on the cheesecloth and levelled so that the cheesecloth would maintain contact with the organic surface in the presence of microtopographic undulations. The amount of water required to saturate the cheesecloth and contact sand was predetermined prior to experimentation. This procedure using cheese cloth and contact sand is an established method (Reynolds, 2006) recommended by the manufacturer of the infiltrometer to ensure good hydraulic connection between the infiltrometer disc and the surface (SMS, 2006).

The vertical offset caused by the contact sand layer (1.1-1.2cm) was added to the offset in pressure head required for the apparatus (5.0cm) so that a negative pressure head would be maintained throughout the organic layer. The pressure head was set in the same manner as for the Mini Disc Infiltrometer by sliding the bubble tower tube up or down. In both experiments (#1 and #2) the pressure head was set to minus 10.1cm. The average (dry) height of the organic layer was 3.5cm in Experiment #1 and 3.3cm for Experiment #2. These average values took into consideration small scale undulations across the organic surface. Effectively, this resulted in a minus 0.6cm pressure head at the organic-mineral interface for Experiment #1 and a minus 0.8cm pressure head at the interface for Experiment #2.

The same camera set up was used in Phase II experiments as described in section 3.4.4.

Before each of the two tests, the bubble chamber and reservoir were filled with deionized water according to the directions of the manufacturer (i.e. SMS, 2006). In contrast to the manner in which the Mini Disc Infiltrometer was filled, a hand vacuum pump was used to draw water into the bubble chamber and reservoir through the porous plate while the infiltrometer sat in a tub of water. The reservoir was filled to capacity in both experiments (approx. 300ml).

Time zero was defined as the time when the infiltrometer was placed on the contact sand layer. The amount of time required for the contact layer to fill was 20 seconds, and approximately 30ml of water infiltrated into this layer at the start of each test. Time to first bubble was not recorded in these experiments. The size of the porous disc (8cm diameter) relative to the size of the column (9.5cm diameter) was such that divergent flow was expected to occur at the beginning of the test. However, since the sand contact was fitted to the diameter of the column and not to the size of the porous disc, divergent flow would only occur in the contact layer and was limited to the time required for the sand contact layer to fill with water (approximately 20 seconds).

The infiltrometer was gently placed on the surface with sufficient force to ensure contact between the infiltrometer and the contact sand and the organic surface for the entirety of the test. Because of the nature of the organic materials used, this material compressed under the weight of the infiltrometer and force applied. It was also observed during testing that organic layers compressed as the test progressed to an extent, which was different between the two tests. The largest increase was observed in Experiment #1 with a 1cm difference between dry (starting) height and wet (2 hours in) height.

Approximately 300 ml of water (the capacity of the infiltrometer) was used in each test. At the end of these tests, the column was unclamped and turned horizontal. Because the support structure at the bottom of the column was fixed to the column, all materials were scooped out of the top of the column. Materials were collected in 2cm intervals and put in large glass containers which were

immediately covered with a fitted lid. Post-infiltration sample collection lasted approximately 10 minutes. These samples were then weighed and dried to constant weight in a 60 °C oven to determine moisture content profiles. Control samples were also dried to obtain initial gravimetric moisture contents of tested materials.

3.5. Results and Discussion

3.5.1 Phase I – Infiltration

Cumulative Infiltration vs. Time for *Mineral Only (MO)* B Horizon materials is presented in Fig. 3.7 and corresponding Infiltration Rate vs. Time data are presented in Fig. 3.8. The infiltration data follow curves commonly observed in hydrophilic. Higher initial infiltration rates that decrease near exponentially over time and approach an eventual rate of sustained flow at late time are typical of 1D vertical infiltration. The drop in infiltration rate is due to the decreasing contribution of the capillary (or pressure head) driven component of the hydraulic gradient that develops as the wetting front moves further away from surface where the porous disc tension equals -2cm. At late time the infiltration rate approaches a value equal to the hydraulic conductivity since the capillary (pressure head) component of the hydraulic gradient approaches zero and the gravity driven component of the hydraulic gradient (dz/dz=1) becomes the remaining driving force (Hillel, 1982). This set of data shows that approximately 80 ml of water infiltrated in 17-24 minutes for the 5 replicates. This set of Mineral Only experiments serves as a valuable reference case for direct comparison to the behaviour of the later experiments which include hydrophobic materials. It should be noted that in all the 1D experiments presented herein, the mineral material below the surface layers is this same Mineral Only material.

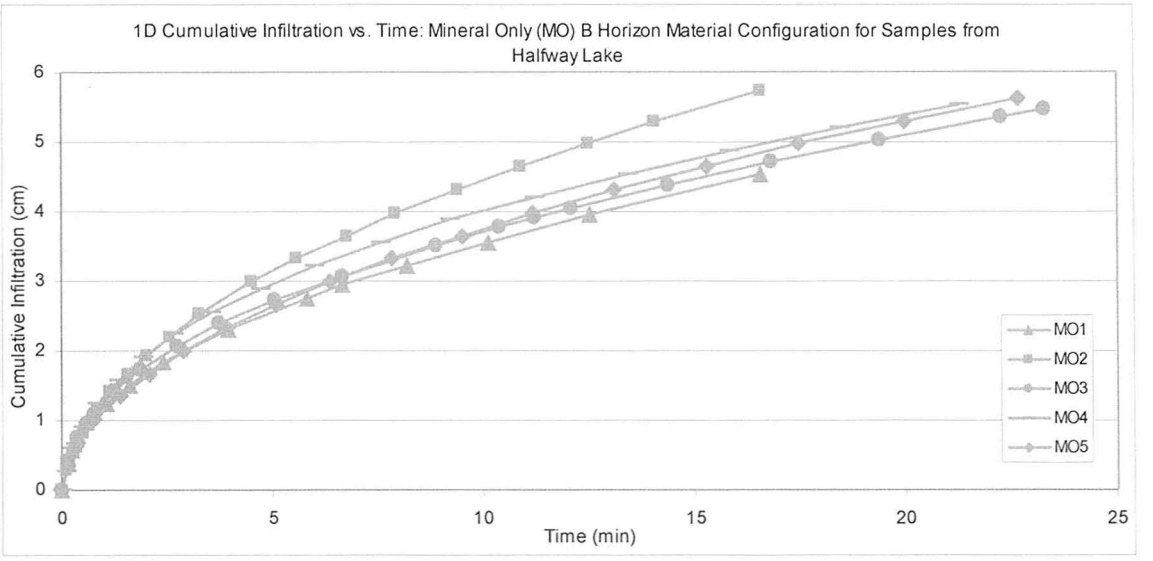

Fig. 3.7 Phase I - Cumulative Infiltration vs. Time plot for Mineral Only (MO) B Horizon material configuration test replicates

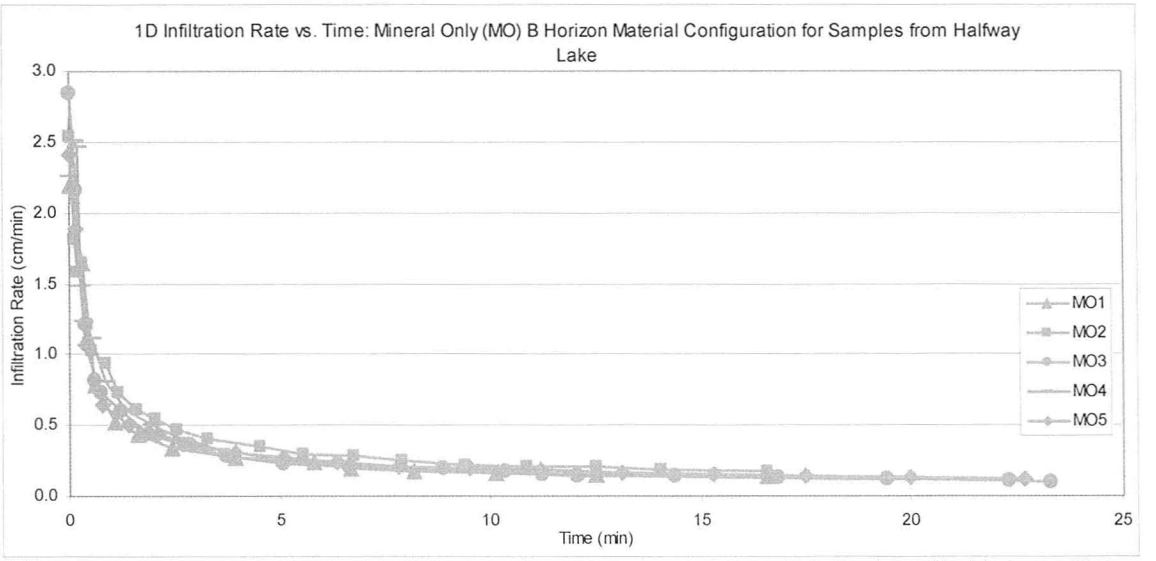

Fig. 3.8 Phase I - Infiltration Rate vs. Time plot for Mineral Only (MO) B Horizon material configuration test replicates

Cumulative Infiltration vs. Time for *Char over Mineral (COM)* B Horizon materials are presented in Fig. 3.9 along with the Mineral Only (MO) data from Figure 3.7. The corresponding Infiltration Rate vs. Time for Char over Mineral are presented in Fig. 3.10. The COM material configuration behaves similar to the Mineral Only (MO) infiltration data, with tests lasting 19 to 23 minutes and exhibiting minor (secondary) differences. Early time data show that infiltration into Char over Mineral (COM) columns was marginally slower than in MO columns in the first minute of infiltration. This small difference is likely attributable to a slightly weaker initial capillary component of the hydraulic gradient within the coarser Char material. Late time data (i.e. >1 minute) for COM columns indicate a slight increase in overall infiltration such that test tend to reach 5cm of cumulative infiltration a few minutes before the majority of Mineral Only columns, however these differences are relatively small. This data indicates that the Char material is behaving as a hydrophilic material with indiscernible changes in contact angles (wettability) over the duration of the test. This is consistent with the mean contact angle determination for Char materials reported in table 2.1 (i.e. 72 -90°).

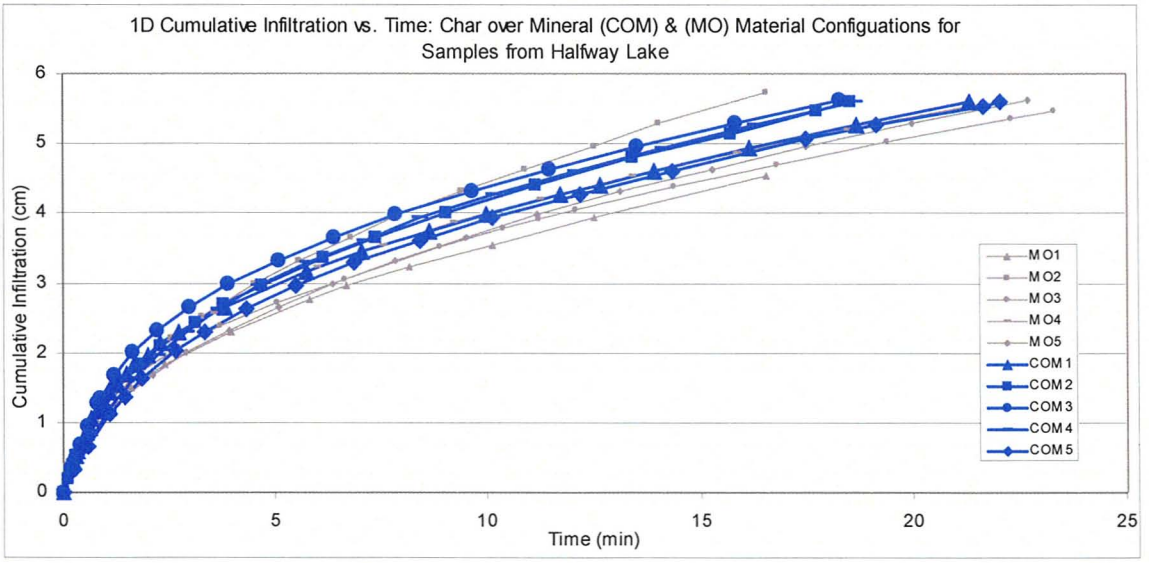

Fig. 3.9 Phase I – Cumulative Infiltration vs. Time plot for Char over Mineral (COM) and (MO) material configuration test replicates

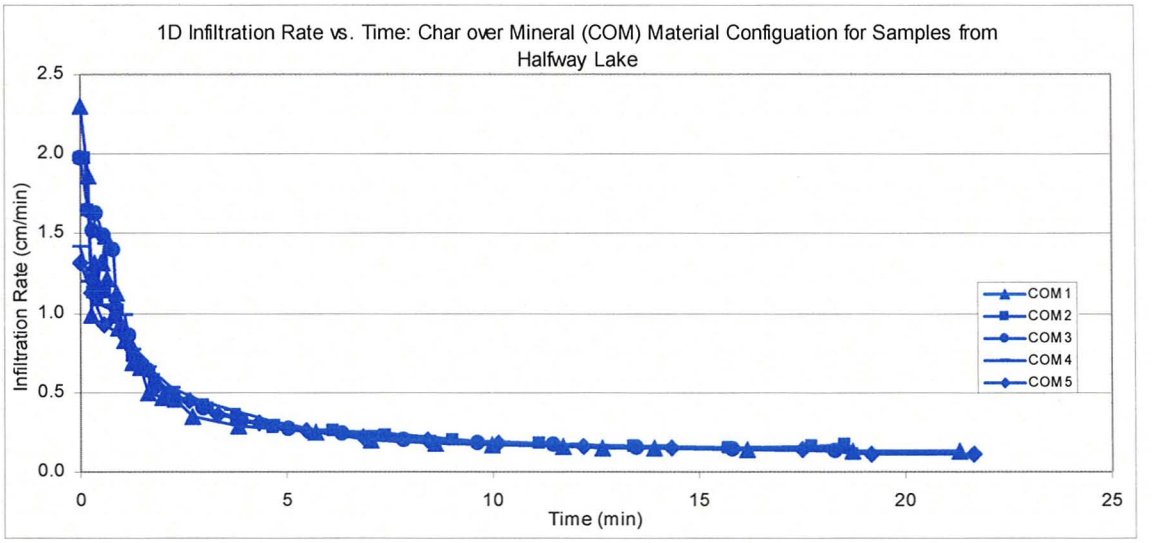

Fig. 3.10 Phase I - Infiltration Rate vs. Time plot for Char over Mineral (COM) and (MO) material configuration test replicates

Mixed over Mineral (MOM) plots for Cumulative Infiltration vs. Time are plotted with Mineral Only and Char over Mineral data in Fig. 3.11 and Infiltration Rate vs. Time for MOM tests appear in Fig. 3.12. These experiments show highly distinct infiltration behaviour which differs significantly and substantially from infiltration into hydrophilic porous media. The cumulative infiltration vs. time data exhibits a general concave shape, i.e. a trend to increasing slope with time. This (increasing slope with time) behaviour under a negative applied constant head (tension) at the surface is not observed in layered hydrophilic materials. It is indicative of dynamic wettability (contact angles) within this initially hydrophobic material. The infiltration data also shows a higher variability between tests than observed in Char over Mineral or Mineral Only tests. We attribute this to the differing dynamic rates of change of the wetting of the Mixed Material and varied proportions of initially wettable surfaces (i.e. initial differences in fractional wettability).

Highly complex changes in infiltration rates over time are in direct contrast to the typical hydrophilic behaviour observed in the previous material

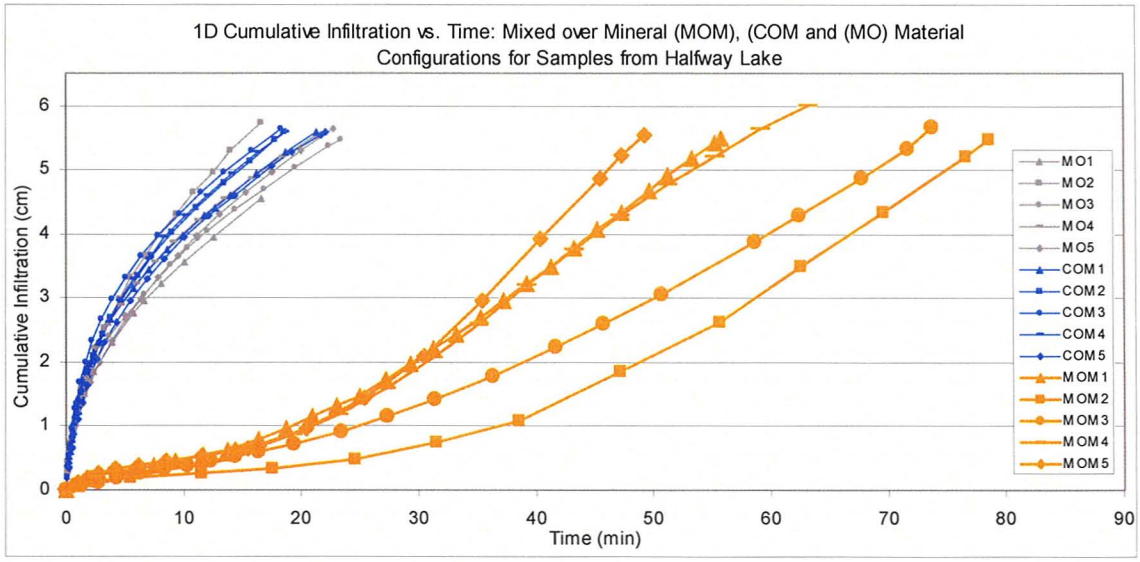

Fig. 3.11 Phase I – Cumulative Infiltration vs. Time plot for Mixed over Mineral (MOM), (COM) and (MO) material configuration test replicates

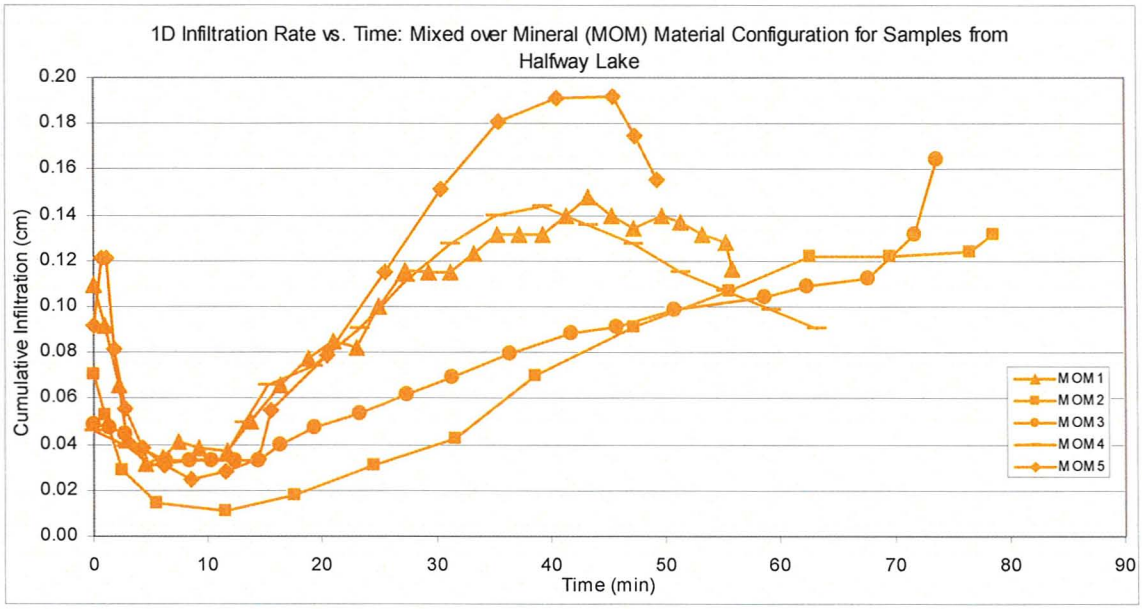

Fig. 3.12 Phase I – Infiltration Rate vs. Time plot for Mixed over Mineral (MOM), (COM) and (MO) material configuration test replicates

configuration cases (Fig 3.12). At early times (up to 10 minutes across the 5 replicates) the Mixed Material infiltration shows decreasing infiltration rates similar to typical hydrophilic systems. The behaviour can be attributed to a largely wettable fraction of surface (0cm) materials (identified in chapter 2). However, thereafter the infiltration rates tend to increase substantially with time. Where highest infiltration rates for MO and COM tests occur at the beginning of tests, the highest infiltration rates for MOM tests are observed at late time (i.e. >37 minutes). In three of the five replicates, infiltration rates reach a maximum infiltration rate between minutes 37 and 47, after which time infiltration rates decrease for the remainder of the test. This may indicate the transition point between hydrophobic and hydrophilic states. If water repellent media are largely identified as having increasing infiltration rates and hydrophilic are characterized by monotonically decreasing infiltration rates, then it would appear as though these materials started to become hydrophilic (i.e. bulk media contact angle change elicited a negative pore water pressure head) during the course of testing. What is unique about these data is the observance of decreasing rates at multiple time points, indicating that the behaviour is not random. However, we cannot be certain that the material was completely hydrophilic since end-of-test rates are not comparable to the end-of-test infiltration rates of hydrophilic cap material tests (i.e. Mineral Only and Char over Mineral) and the capacity of the reservoir limited the duration of testing. Even still, because of the nature of infiltration using the tension infiltrometer (i.e. with the tension infiltrometer the system must 'switch' to a negative pore water pressure before infiltration occurs), a possible time stamp for when dynamically changing contact angles approach 90° may now be more systematically identifiable.

The other (2) replicates have increasing infiltration rates from ~10 minutes onward. It is noteworthy that at the end of the tests, which are about three times longer than the hydrophilic systems discussed earlier, the final infiltration rates are close to those of the hydrophilic systems. That is, the typically hydrophilic

tests exhibited monotonically decreasing infiltration rates approaching a constant at late time, while these hydrophobic materials exhibit lower and more variable rates that at late time approach values similar to gravity driven infiltration through the Mineral Only and Char over Mineral tests. These data indicate that these hydrophobic materials (as expressed through increasing infiltration rates over time) are 1) experiencing changes in contact angle (i.e. becoming more wettable) and 2) reaching sustained rates of flow comparable to wettable materials within an hour. The apparent critical level of hydrophobicity reached in 3 of the 5 replicates (where infiltration rates begin to decrease at later time) could be better evaluated with a larger capacity infiltrometer.

Cumulative Infiltration vs. Time data for Brown over Mineral tests are shown along with the other material configurations in Fig. 3.13. These data have significant and long delays in infiltration not observed in any of the other tests. Further, the nature of infiltration into these materials is much more variable between replicates in spite of these materials being visually similar. Two of the five replicates reached 4cm of cumulative infiltration *before* 140 minutes, while the three other replicates did not reach 4cm until *after* 380 minutes. Like the Mixed materials, the Brown material exhibits convex cumulative infiltration (vs. time) in this plot, which is interpreted here as indicative of hydrophobic material with dynamic wettability (contact angle).

Corresponding *Brown over Mineral (BOM)* Infiltration Rate vs. Time data are presented in Fig. 3.14. Similar to Mixed over Mineral tests, BOM tests exhibit decreasing infiltration rates at early time (i.e. <100 minutes vs. 10 minutes in MOM) and increasing infiltration rates over the longer term. In contrast to MOM test, infiltration rates start at much lower values (i.e. <0.02cm/min) and decreases are proportionally less than observed for Mixed over Mineral tests. Differences between minimum and maximum infiltration rates between the two material configurations are proportionally similar (i.e. MOM factor of 4.5-13; BOM factor of 4.6-14.5), however there is an order of magnitude difference between average

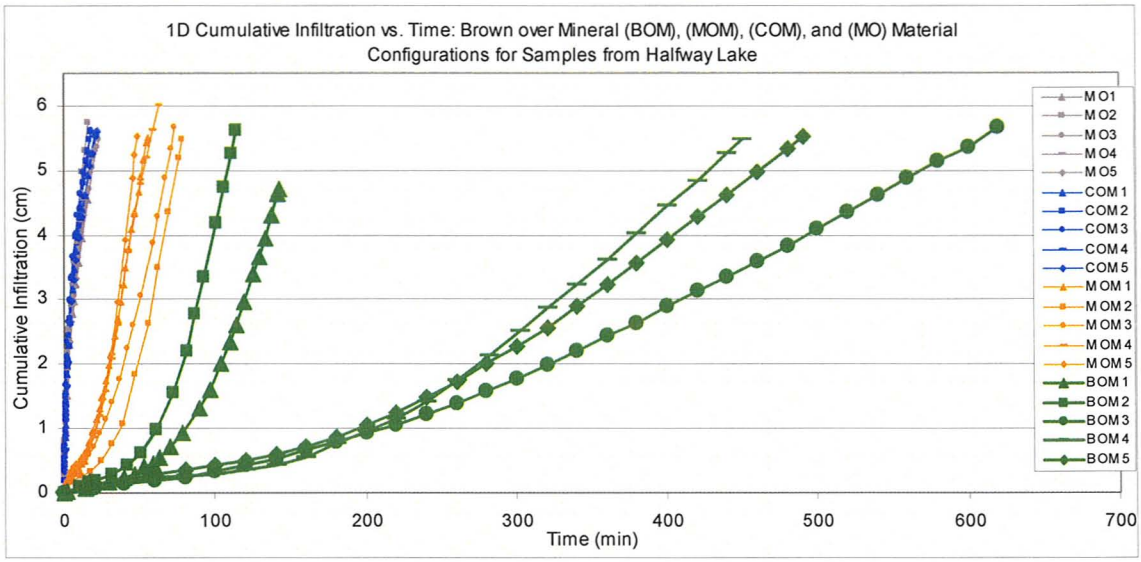

Fig. 3.13 Phase I – Cumulative Infiltration vs. Time plot for Brown over Mineral (BOM), (Mixed over Mineral), (Char over Mineral) and (Mineral Only) material configuration test replicates

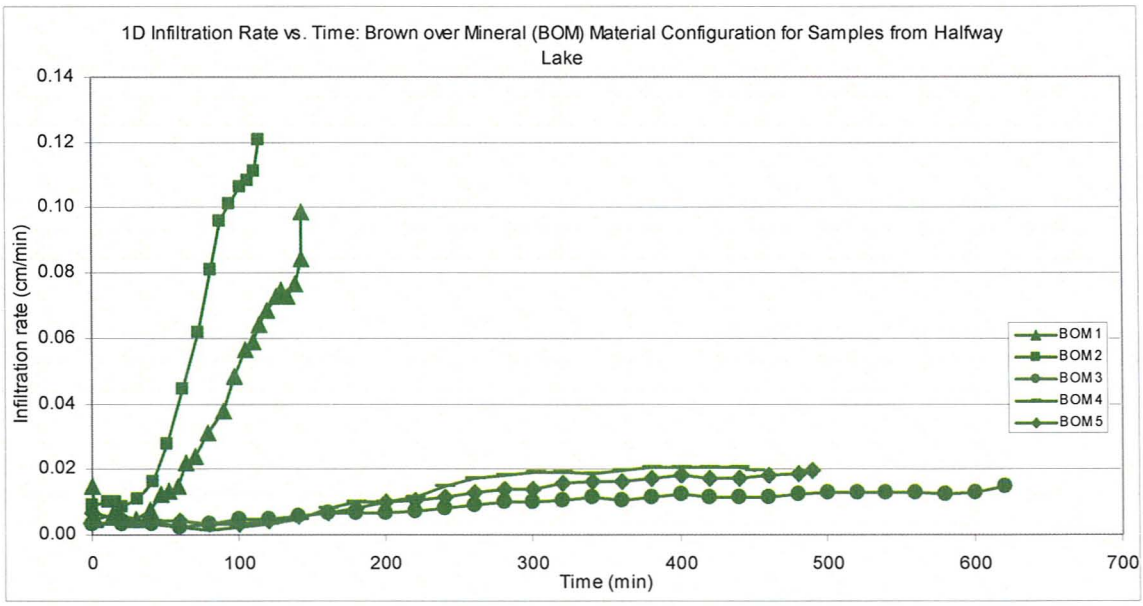

Fig. 3.14 Phase I – Infiltration Rate vs. Time plot for Brown over Mineral (BOM), (Mixed over Mineral), (Char over Mineral) and (Mineral Only) material configuration test replicates

minimum infiltration rates (of MOM vs. BOM). Additionally, 2 of the 5 replicates behave much more similarly in terms of cumulative infiltration response to Mixed over Mineral tests. What these data indicate is that even in identifiably similar materials, large differences in fractional wettability and contact angle dynamics can exist.

As a group, these data indicate that significant differences between varying degrees hydrophobicity are readily identifiable in 1D tension infiltration tests. Most significant are the differences between wetting and non-wetting infiltration rates. Wettable materials have decreasing infiltration rates with time; non-wettable materials exhibit completely opposite behaviour with large increases in infiltration rates over time. This is also apparent in the shape of the cumulative infiltration vs. time plots with the Hydrophilic materials exhibiting distinctly concave plots in contrast to the *convex* plots of hydrophilic materials. Hydrophilic materials also exhibit infiltration rates orders of magnitude greater than hydrophobic counterparts.

These data clearly demonstrate that visual and quantifiable differences in tension infiltration tests capture unique characteristic hydraulic behaviours that provide added insight into system dynamics beyond other tests. When comparing Mixed to Char over Mineral tests, it could be inferred from these data that a deeper hydrophobic fraction slows overall infiltration rates in wettable surface materials at early time. However, when comparing Mixed to Brown over mineral tests, it seems that a wettable fraction not only increases overall infiltration rates initially and at later time, but speeds up contact angle dynamics within hydrophobic materials.

3.5.2 Phase I – Post-Infiltration Moisture Content Profiles

Initial moisture contents for air dry B Horizon materials were between 0.01 and 0.04 m^3/m^3 for all tests. Moisture profiles for Char over Mineral (COM), Mixed over Mineral (MOM), and Brown over Mineral (BOM) are presented along with Mineral Only (MO) moisture profile data which provide a reference for profile

comparisons (Fig. 3.15). With the exclusion of organic cap materials and mineral materials within in the top 2cm interval, moisture contents were sampled in 2cm intervals along the lengths of columns. Data points represent the centre depth at each interval (i.e. 2-4cm interval assigned 3cm). Organic cap points and immediately adjacent mineral materials fall at the centre depth relative to each material height since there was some variability in the heights of cap materials between tests (in the 0-2cm interval at the top of the column).

Char over Mineral moisture profiles (Fig. 3.15a) indicate that moisture contents in surface Char materials are higher (0.60-0.72 m^3/m^3) than underlying B Horizon materials (0.50-0.60 m^3/m^3) as well as surface (i.e. 1cm depth) moisture contents in Mineral Only (MO) tests (i.e. 0.56-0.62 m^3/m^3). Moisture contents between 3 and 14cm are similar between the two material configurations.

Mixed over mineral (MOM) profiles (Fig. 3.15b) exhibit different behaviour compared to Char materials. Moisture contents in Mixed material caps are, on average, *lower* than subsurface B Horizon materials and Mineral Only surface moisture contents. Deviations from this average behaviour (i.e. more similar to hydrophilic tests) occur in MOM tests lasting less than 1 hour. Also, the range of moisture contents found in Mixed material caps (0.46-0.65 m^3/m^3) is larger than found in Char cap materials (0.62-0.72 m^3/m^3). Moisture contents between 3 and 14cm are similar between the two material configurations.

Surface moisture contents observed in the Brown OM cap materials (Fig. 3.15c) are within a more narrow range of values (0.43-0.54 m^3/m^3) than Mixed cap materials. Similar to Mixed cap materials, Brown OM cap materials have lower moisture contents than subsurface materials, only more consistently so. Further, moisture contents tend to be lower in comparison to Mineral Only test, particularly for depths shallower than 8cm. With respect to mineral materials found directly below organic caps, moisture contents were also within a narrow

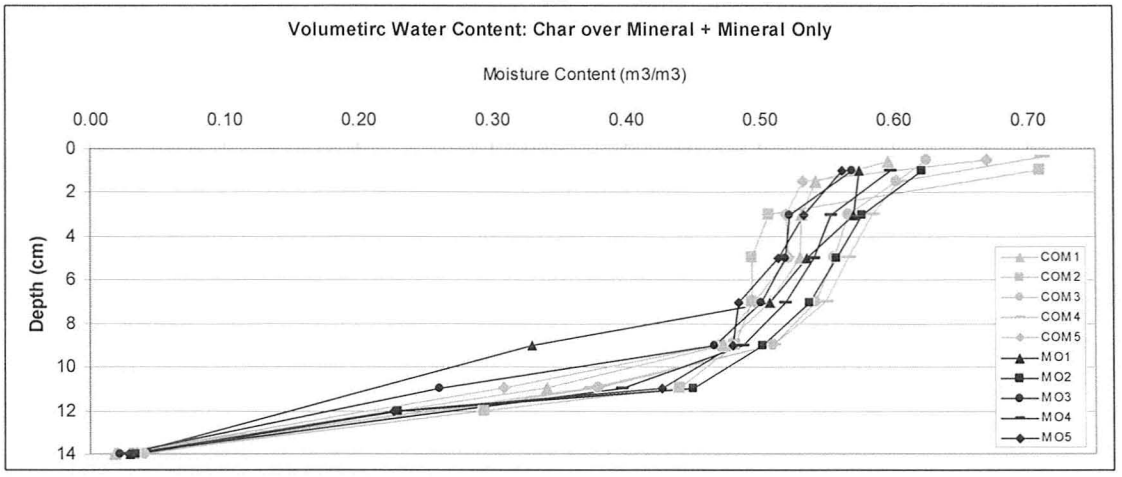

(a)

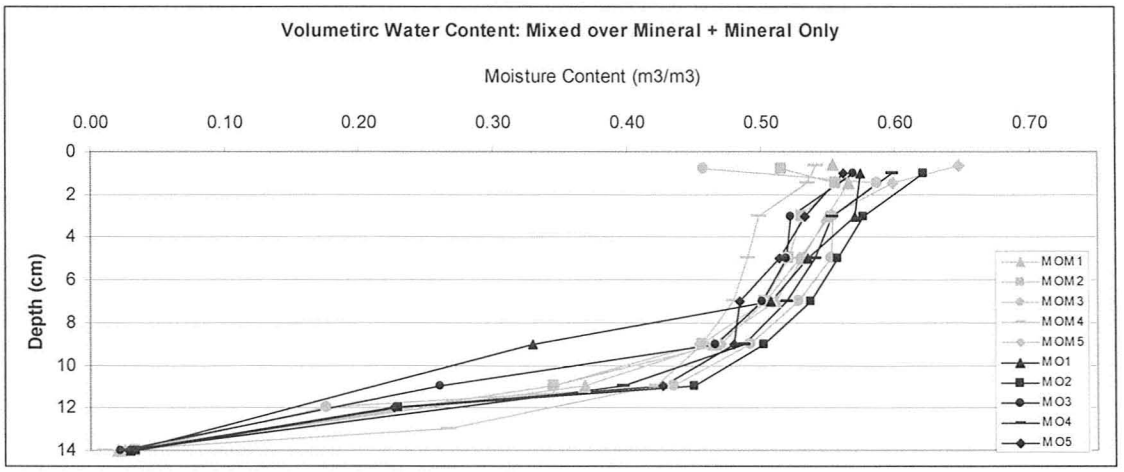

(b)

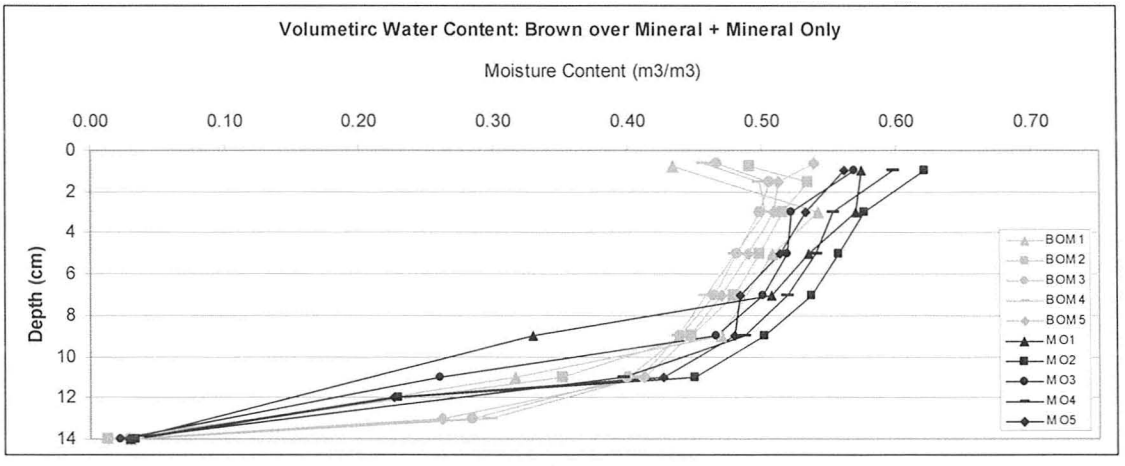

(c)

Fig. 3.15 Phase I Post Infiltration Volumetric Water Content profiles for 1D column experiments

range and lower than observed in the other tests (i.e. 0.50-0.54 m^3/m^3). This is consistent with the lower infiltration rates (Fig 3.14) measured for these Brown materials which indicate that the organic layer in the BOM tests was supplying a lower flux to the underlying mineral layer relative to the other Char or Mixed configurations.

The depth of the wetting front for all tests is similar between tests, however the most hydrophobic materials (Brown caps) exhibit lower moisture contents overall and marginally deeper profile wetting compared to other materials. However, this is expected since similar volumes were applied in all cases and time differed between materials. These data inform that surface water repellency does affect subsurface moisture distribution noticeably in layered systems and particularly in surface materials. Cap material moisture contents tend to exhibit an indirect, but variable relationship with water repellency i.e. as repellency increases moisture content in organic media tends to decrease. Char caps have high moisture contents relative to subsurface materials, whereas Mixed caps tended to have lower moisture contents relative to subsurface materials. Deviations in Mixed cap moisture contents relative to subsurface materials related well to the duration of tests (i.e. <1 hour testing resulting in higher relative moisture contents in cap materials) supporting the concept of dynamic wetting. Brown cap materials have lower moisture contents than subsurface materials in 4 of the 5 replicates. In contrast to mixed materials, the duration of testing does not explain this variation in behaviour.

3.5.3 Phase II – Infiltration Data

Infiltration into contact sand is not shown in the infiltration plots for Phase II experiments. Regarding the compression noted in section 3.4.7, the contact layer and infiltrometer behaved as expected for both tests and sunk in correspondence to the compression that occurred in organic materials. Infiltration Rate vs. Time data for Phase II experiments agree well with expectation that increased surface burning would result in higher infiltration rates

at early time (Fig. 3.16). However, Experiment #2 infiltration rates are higher than Experiment #1 infiltration rates for the durations of these tests. While the difference in early time infiltration rates can be explained by an increased wettable fraction (charring) at the surface (i.e. 0cm) in Experiment #2, it is interesting that the entire test appears to be affected by the increased fraction of wettable materials at the surface.

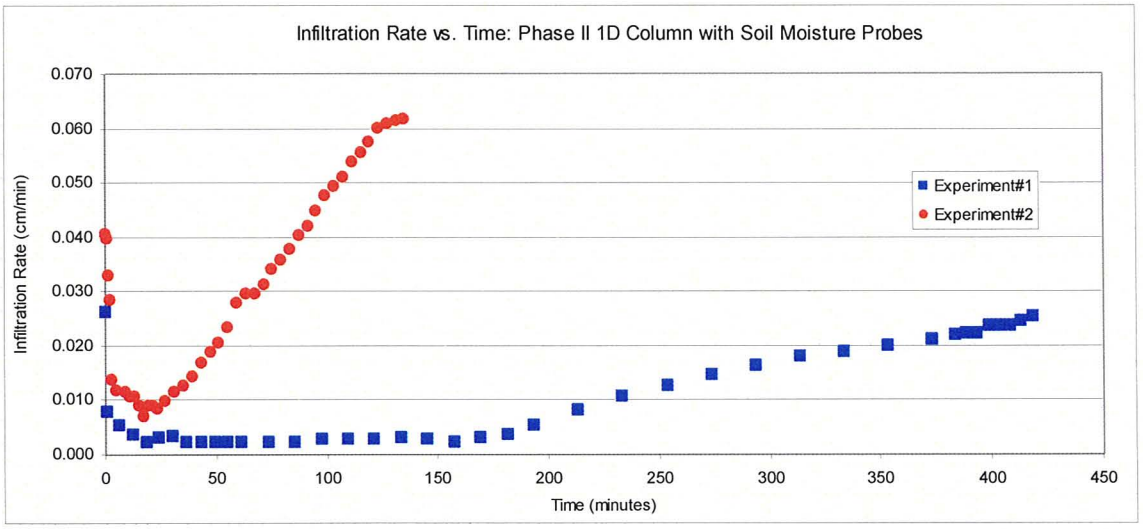

Fig. 3.16 Phase II Infiltration Rate vs. Time for Experiments #1 and #2

Similar to Phase I experiments, these test show decreasing infiltration rates at early time and increasing rates at later time. What is most notable in these data, however, is that for less burned materials (Experiment #1), the infiltration rate decreases and remains low for an additional 100 minutes before gradual and consistent increases in infiltration rate are observed, whereas Experiment #2 test shows a sharp rebound effect in infiltration rate. This is significant considering that the first 3 hours of infiltration rate data (for #1) follows that of a low permeability wettable material, which this clearly is not. Clothier et al. (2000) saw similar behaviour to Experiment #2 on undisturbed cores of hydrophobic silt loam (i.e. quick rebound with near-linear increases in infiltration rate for 600 minutes using a pressure head of minus 4cm).

In more heavily burned materials (Experiment #2), increases in infiltration rate appear highly linear for a period close to 90 minutes (up to 130 minutes of infiltration time) at which point increases in infiltration rate appear to begin to taper off. It might be discerned from these data that an increased fraction of wettable (combusted) materials at the surface of an overall non-wetting material can contribute to more consistent increases in infiltration rate. In contrast, the infiltration rate of Experiment #1 materials (i.e. less surface scorching) remains essentially constant between minutes 35 and 175, after which time more gradual increases occur.

Similar to Phase I experiments on hydrophobic materials, the hydrophobic materials exhibit the same kind of concave infiltration behaviour in the Cumulative Infiltration vs. Time plot (Fig. 3.17). The major difference between the two tests is that Experiment #1 data are near-linear up to 180 minutes and Experiment #2 data is linear only for the first ~40 minutes of testing.

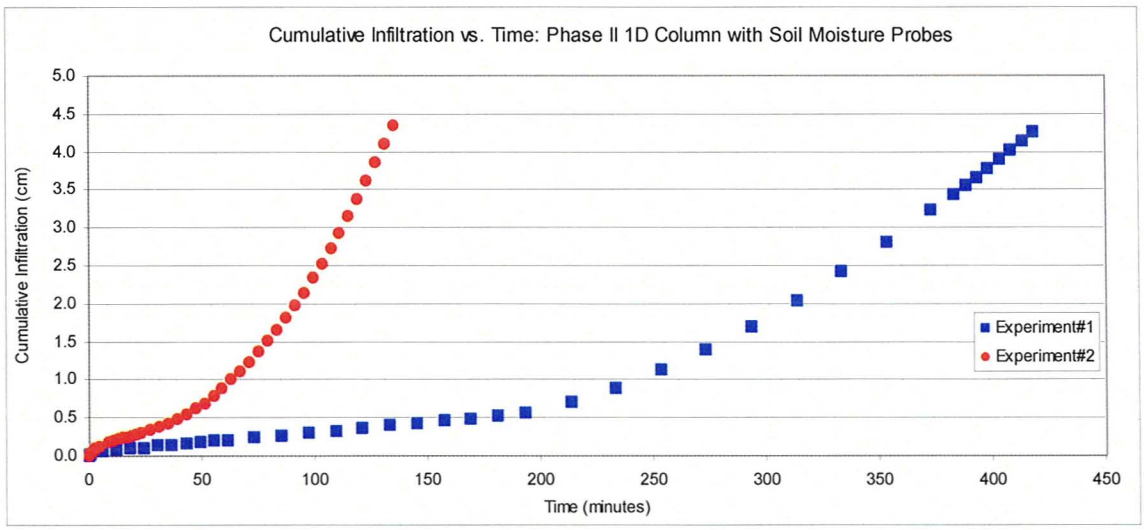

Fig. 3.17 Phase II Cumulative Infiltration vs. Time for Experiments #1 and #2

5.3.4 Phase II – Post-Infiltration Moisture Content Profiles

Volumetric moisture content profiles for Experiments #1 and #2 display centered (i.e. 0-2cm interval assigned to 1 cm) moisture content values in Fig. 3.18. Similar to the Brown OM cap material cases, these profiles show that surface organic caps have lower moisture contents than subsurface materials. In spite of apparently significant differences in infiltration rate behaviour, moisture profiles between the two tests are remarkably similar. Also similar to Phase I experiments is that even with vastly different test durations, the application of a similar total volume of water results in similar wetting depth into the column profile i.e. not significantly greater in the more hydrophobic case.

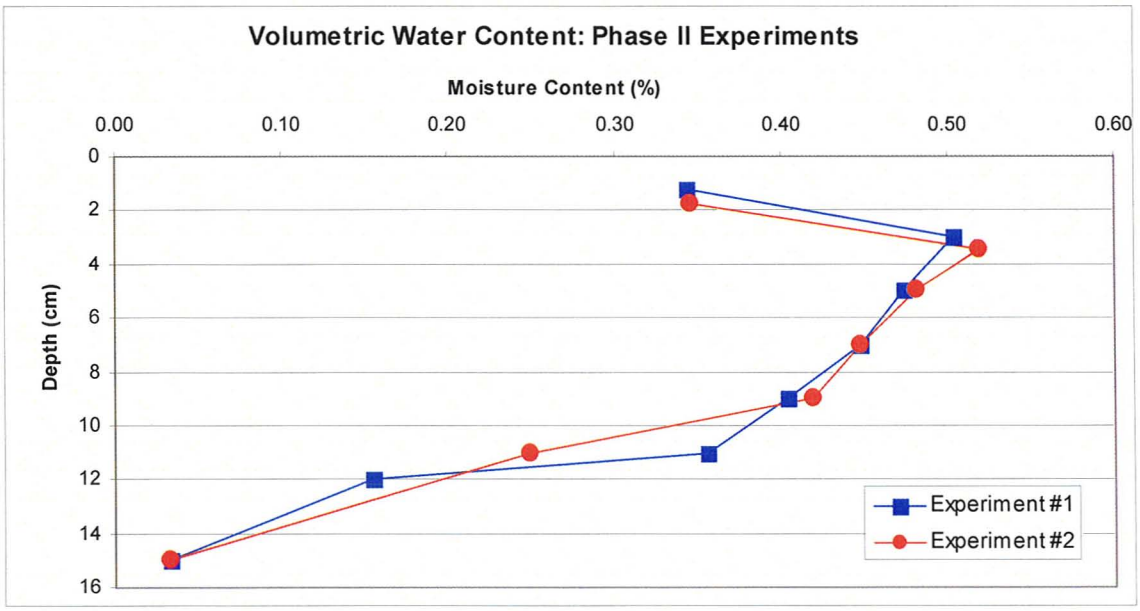

Fig. 3.18 Phase II Volumetric Moisture Content Profiles for Experiments #1 and #2

3.5.5 Phase II – Infiltration and Real Time Moisture Content

All moisture content data collected from moisture capacitance sensors were linearly calibrated to measured initial and post-infiltration volumetric moisture contents consistent with recommendations of the manufacturer (Cobos, 2009). Infiltration rate data for Experiment #1 are presented with corresponding real time volumetric moisture content data collected and logged with in situ moisture probes (Fig. 3.19). From early time, small and consistent increases in moisture content are observed in the shallowest probe (i.e. 1.7 cm from top of column), OM-17. It is likely that these small and consistent increases in deeper (2cm depth) organic materials are related to the wetting up of scorched surface materials (0cm) in the organic layer. At 50 minutes, however, a steepening in moisture content occurs; this also corresponds with increased moisture contents being detected in OM-20. Infiltration rates do not change over this interval. If wetting at both depths within organic materials was the same, it might be

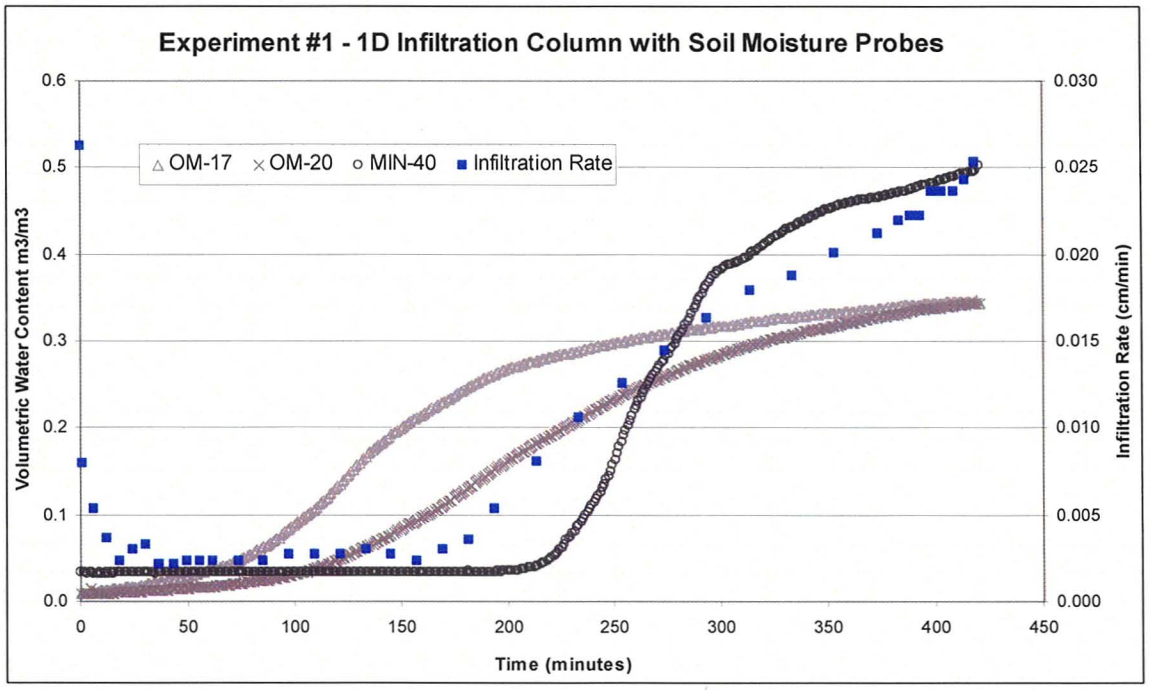

Fig. 3.19 Phase II Real Time Moisture Content and Infiltration Rate Plot for Experiment #1

expected that moisture content curves follow similar rate behaviour. In this test, OM-20 exhibits a distinctively muted (more gradual) response to the advancing front relative to OM-17 (the shallower of the two by 0.3cm). However, the shape of both dispersed fronts indicate that wetting in these materials is not akin to the sharp wetting fronts often identified in hydrophilic materials.

Steeper increases in infiltration rates appear to coincide with breakthrough / infiltration into the underlying hydrophilic layer. A small increase in infiltration rate occurs between 140 and170 minutes, but significant increases in infiltration rate correspond to the time breakthrough was visually observed in B Horizon materials (i.e. 190 minutes). While breakthrough was observed visually at 190 minutes, 'MIN-40' (B Horizon material) did not detect increases in moisture content until 195 minutes due to its position 0.5cm below the organic-mineral interface. This is likely due to the positioning of the moisture sensor blades in relation to the interface. Also of importance is the lack of a sharp (steep slope) wetting front in the hydrophilic B Horizon material. While it is much sharper than observed in OM-20 and OM-17, the shape of the front indicates that the rate of supply to this layer is largely controlled by the overlying hydrophobic materials.

It is interesting that no significant increases in infiltration rate were observed before breakthrough into B Horizon materials given that moisture contents increased substantially in organic cap materials. This indicates that even relatively large moisture contents (i.e. up to 0.24 m^3/m^3) do not necessarily contribute to substantially increased infiltration rates during early time; even for these apparently relatively highly dispersed fronts. This means that water was infiltrating and being stored in hydrophobic organic layers for nearly 3 hours before breakthrough into B Horizon materials / significant increases in infiltration rate occurred. The majority of increases in moisture content of shallow organic materials (OM-17) occurred in the period before breakthrough. Deeper organic materials (OM-20) saw the majority of increases in moisture content following breakthrough.

Subsurface hydrophilic layers may limit the amount of moisture that persists in overlying hydrophobic materials. Where slopes of moisture content curves for OM-17 and OM-20 (hydrophobic media) begin to dampen, moisture contents in hydrophilic media (MIN-40) still appear to be climbing, albeit at a lesser rate than observed earlier in the test. While not examined fully here, hydrophilic materials at a hydrophobic–hydrophilic interface may actually wick water away such that interface moisture contents (of hydrophobic media) remain lower than near-surface moisture contents, and particularly so where flux rates are significantly less than the infiltrability of materials.

Increases in infiltration rate are observed even after the wetting front is evenly distributed around the circumference of the column (i.e. at 370 minutes). These increases are also well correlated to the shallower moisture content slope in hydrophobic organic materials. While the capacity of the infiltrometer (i.e. 300ml) limits the extent to which changes in moisture contents and infiltration rates can be observed beyond 370 minutes, we can see that infiltration rates and moisture contents in these layered systems exhibiting hydrophobicity do not behave like hydrophilic systems do. Relative to breakthrough, significant increases in infiltration rate were observed in this layered system. It is likely that the effective infiltration rate (i.e. the one measured via the infiltrometer) is a combination of the infiltration rate of the sub-layer hydrophilic media and overlying hydrophobic media (whose conductivity is changing with time). In contrast to normally wetting systems, however, where lower conductivity subsurface materials can dominate eventual infiltration rates (Hillel, 1982), for these systems, it appears that hydrophobic media dominate infiltration processes and subsurface media influence the observed changes. So, while it appears that subsurface B Horizon materials can contribute significantly to increasing rates following breakthrough in these types of systems, late time and overall changes in infiltration rate are tempered / enhanced most substantially depending on the changing and/or static properties of overlying hydrophobic materials.

Infiltration rate data for Experiment #2 are presented with corresponding real time volumetric moisture content data in Fig. 3.20. Moisture content behaviour for OM-P4 over the course of the test can be characterized by small and gradual increases up to 25 minutes, where a sharp increase in moisture content appears. For the remainder of the test, the curve follows a convex curvilinear trend with a gradually decreasing slope to the end of the test. Probe 3 (OM-P3) exhibits similar behaviour, although, a delay in this rise extends to 40 minutes before moisture contents increase substantially. MIN-40, which is embedded in B Horizon material, does not show any noticeable change in moisture content until 85 minutes. Similar to the previous case, B horizon material exhibits the greatest amount of change over the duration of the test. However, in relation to the prior case, moisture contents in B Horizon materials in Experiment #2 show a much steeper increase in moisture content. This steepening is directly related to the supply of water being made available to hydrophilic B material by the overlying

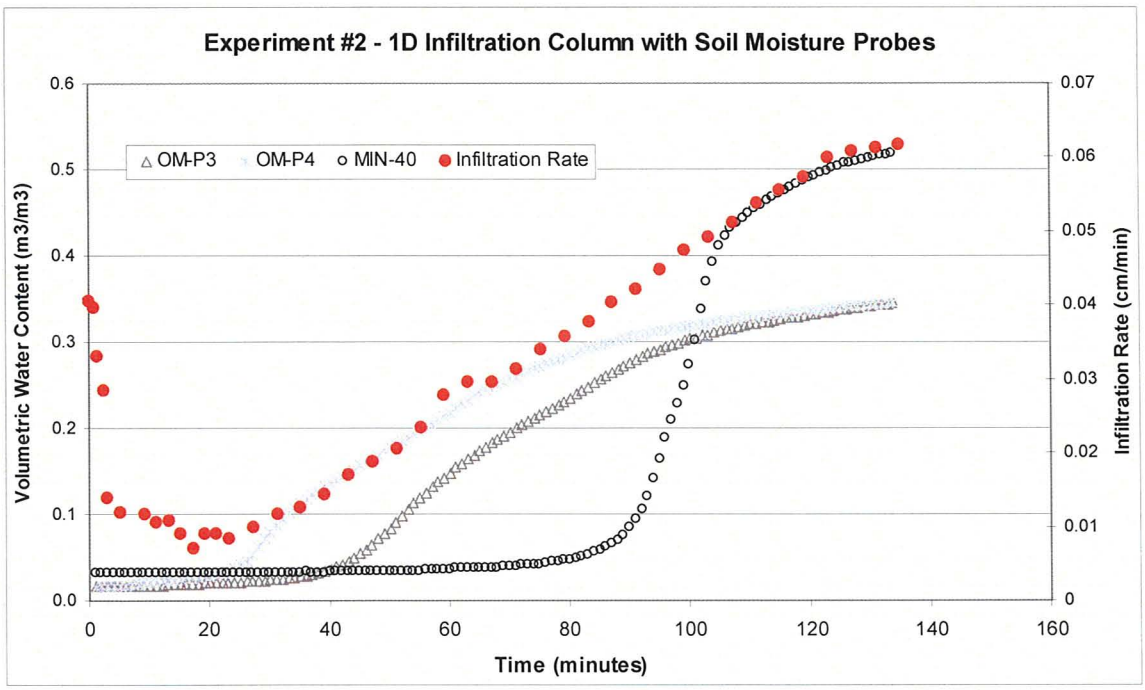

Fig. 3.20 Phase II Real Time Moisture Content and Infiltration Rate Plot for Experiment #2

hydrophobic organic materials. If supply was not impeded at all, one would expect to see a steeper moisture profile (in MIN-40). This is not the case in either test; changes in moisture content in hydrophilic materials are gradual in both instances, Experiment #1 being more so.

Similar to the Experiment #1, Experiment #2 breakthrough into hydrophilic B horizon materials relates well with increases in infiltration rates. Small bulbous localised access areas were identified from 30 to 48 minutes. It is evident that infiltration into sublayer B Horizon materials contributed to a near linear increasing infiltration rate with time as the wetting front grew to encompass the area of the column. What is less obvious is that infiltration rates continued to increase even after the wetting front was level in the column at 110 minutes. It is also at this time that moisture contents in the organic materials became the same; this suggests that the entire volume of organic material was evenly wetted at this point in the test.

Both tests exhibit the same relative behaviour between moisture contents and increases in infiltration rates. Initial infiltration behaviour in both tests is marked by decreasing infiltration rates quickly followed by a minimum. In the longer of the two tests, infiltration rates persist at this relative minimum during which time moisture contents increase substantially; whereas infiltration rates quickly rebound in the shorter duration test with no significant increases in moisture content. Where increases occur, breakthough into B Horizon materials was observed at or near to the time of observed increases in infiltration rates. When moisture contents in organic materials align (i.e. OM-17 and OM-20 in #1 vs. OM-P3 and OM-P4 in #2), the wetting front developed to the point where wetting is even all the way around the column. At this point, infiltration rates continued to increase, although at a seemingly slower rate than prior. What is different between the two tests is that at the end of Experiment #1, increases in infiltration rate are still occurring, whereas in Experiment #2, an apparent gradual tapering in infiltration rate is starting near 125 minutes.

3.6 Summary and Conclusions

In layered water repellent systems, the complex interplay between fractionally wettable surfaces and dynamically changing contact angles play a significant role in determining both initial *and* long term infiltration behaviour in hydrophobic materials. This is in direct contrast to established theory explaining infiltration into layered water wettable (hydrophilic) systems (Hillel, 1982).

For hydrophobic systems, initial infiltration rates are heavily influenced by the fraction of wettable surfaces present in near-surface materials. Char over Mineral column tests showed only mild resistence to wetting (in reduced initial infiltration rates) compared to Mineral Only columns; both material configurations exhibited hydrophilic infiltration behaviour. In contrast, cap materials with hydrophobicity at depth and significant charring at the surface (Mixed Materials) had high initial infiltration rates that quickly decreased in the first 5 minutes of testing. These initial rates were an order of magnitude lower than rates observed in (Char Material) hydrophilic materials of the same origin. Comparatively, much smaller initial infiltration rates were observed in the most hydrophobic material (Brown Organic Materials) (i.e. an order of magnitude lower than MOM tests). These materials were much more variable in terms of the direction of the change (i.e. up or down) of initial infiltration rates. Decreasing initial infiltration rates lasted up to 100 minutes in Brown Organic Materials before increases in infiltration rates were observed. This is a significant period of time relative to low magnitude, high frequency precipitation events, but field tests in hydrophobic systems are seldom carried out over periods as long.

Subsequent infiltration rate behaviour (following initial infiltration rates) is also largely related to the wettable fraction-dynamic contact angle relationship found in bulk hydrophobic materials. Between the hydrophobic materials investigated here (i.e. Mixed Materials and Brown Organic Materials), the quickest infiltration rate rebound was found in materials with a greater proportion of charring (wettable material) at the surface. Infiltration rates rebounded at

earlier time and increased faster in Mixed materials than in Brown Organic Materials, indicating a faster rate of contact angle change in Mixed Material tests. Further, the presence of an increased wettable fraction at the surface of hydrophobic materials contributed to overall infiltration rates an order of magnitude larger than hydrophobic materials with a smaller wettable (charred) fraction at the surface. However, over the cumulative infiltration of approximately 80ml in each of the tests, increases in infiltration rate were proportional to more hydrophobic (Brown) materials. In Phase I experiments, the faster increase in infiltration rate appears to have contributed to a hydrophobic-hydrophilic 'switch' in organic materials at the ends of 3 of the 5 replicate Phase I tests (i.e. contact angles changed from >90° to <90°). These results indicate that the tension infiltrometer is sensitive to changes in the contact angles of hydrophobic materials and differences in fractional wettability. Increasing infiltration rates over time are indicative of dynamic hydrophobicity and while further work is needed to better quantify the system, it appears that both the trend and rate of change of infiltration rates over time provide direct information about the rate of change of contact angles and fractionally wettable portions within the hydrophobic layers.

In addition to retarding infiltration in surface materials, water repellent materials deliver water to subsurface media at reduced rates. Because of this, subsurface materials with strong matric potentials are likely to exhibit infiltration and moisture redistribution behaviour simultaneously, particularly during breakthrough into subsurface materials at early time and at the hydrophilic-hydrophobic material boundary for the duration of infiltration. It is probable that this combined behaviour is highly dependent on the dynamics of the system, and more pronounced in systems with extremely long delays to infiltration, more persistent water repellency, and a smaller initially wettable fraction.

An indirect relationship exists between post-infiltration moisture content and the magnitude of hydrophobicity for these materials (i.e. as water repellency increases, post infiltration moisture content tends to decrease). Kobayashi and

Shimizu (2007) found the opposite to be true in forest materials. In the layered hydrophobic systems investigated here, moisture contents were on average lower in surface materials that exhibited water repellency (i.e. compared to hydrophilic organic and mineral materials). In materials displaying the most hydrophobicity, surface material moisture contents were the lowest in the entire series of experiments and were lower along the entire depth of soil profiles than all other material configurations. Given that bulk densities were similar across organic materials, these moisture profile differences indicate that storage is affected by water repellency and supply into subsurface hydrophilic layers is largely governed by the persistence of hydrophobicity in these materials.

Water repellency is often reported as a spatially discontinuous phenomenon (e.g. Lieghton-Boyce et al., 2007; Carillo et al., 2000b; Ritsema and Dekker, 1994; Dekker and Ritsema, 1996). Leighton-Boyce et al. (2007) also identified a discontinuous wetting front in litter materials, noting the patchy breakdown of repellency or flow through macropores as possible mechanisms. Images collected during testing (see Fig. 5.2- Fig. 5.4) show that wetting fronts that develop in hydrophobic material are highly discontinuous and largely dependent upon the fractionally wettable component in particular pore spaces. If water repellency is itself spatially discontinuous, one might expect that post infiltration wetting also be spatially discontinuous and highly contingent upon the heterogeneous composition of water repellent and wettable surfaces in bulk media. At larger scales, this type of wetting behaviour has been identified as preferential flow. While visual inspection of (field test) infiltration areas may show discontinuities in moisture conditions following infiltration events, this in no way guarantees that macropore related preferential flow mechanisms contributed to the identified moisture condition. In ponded infiltration experiments, infiltration caused by a wettable fraction cannot be distinguished from flow caused by flow through macropores due to non-uniqueness. However, in using the tension disc infiltrometer, we have isolated the effect of variable wetting due to infiltration

along fractionally wettable and dynamically changing surfaces from macropore flow. Had infiltration *been* ponded, this type of infiltration behaviour (e.g. isolated breakthrough points, patchy pore network development) might wrongly have been attributed to another preferential flow mechanism. So, while preferential flow may often be associated with wetting in water repellent media (Letey, 2001), the term itself is not necessarily indicative of the contributing controls or forming mechanism.

These data support the suggestion of Wallach and Graber (2007) that these water repellent materials did not behave as zero contact angle surfaces would in a completely wetting system. While these data cannot exclude that water repellency has not broken down in these materials – they give no indication under the time scales observed here, that water repellent materials behave similarly to wettable materials of the same origin after achieving some critical moisture content; quite the opposite. Here, we show evidence to support the conclusions of Bayer and Schaumann (2007) that these materials may become more wettable (i.e. less repellent), but by no means has repellency 'disappeared'. If it had, one might expect this system to behave as a normally wetting two-layer system where the subsurface material (with a smaller mean pore diameter and lower conductivity) would over the long term dictate infiltration behaviour. In none of these tests was this observed with exception. It can be concluded that for even relatively high moisture contents, the effects of dynamic repellency can still be observed in hydrophobic materials (i.e. through increasing infiltration rates), particularly when there is a smaller initial wettable fraction of materials at the surface.

Chapter 4: Halfway Lake Provincial Park Post-Fire Field Study

4.1 Field Investigations in Water Repellent Media

Water repellency is a spatially variable phenomenon often investigated under field conditions. The role of water repellency on infiltration and redistribution under field conditions has been investigated extensively using semi-quantitative methods (e.g. Water Drop Penetration Time) and infiltration experiments. Ponded infiltration (e.g. Scott, 2003; King, 1981) and rainfall simulation techniques (e.g. Rosso et al., 2007; McNabb et al., 1989; Robichaud, 2003; Martin and Moody, 2001; Imeson et al., 1992; Cerda and Doerr, 2007; Robichaud et al., 2003; Leighton-Boyce et al., 2007; Shakesby et al., 2003) have been the preferred methods for some time, but this is changing. There is an increasing awareness that controls on natural hydrologic processes are not well represented in these traditional measures.

Many attempts have been made to 1) reconcile observed infiltration behaviour with existing theory and 2) make sense of a highly non-linear relationship between hydrophobic and hydrophilic behaviour under changing moisture conditions with variable success (e.g. Rodriguez-Alleres et al., 2007; Verheijen and Cammeraat, 2007; Keizer et al., 2007; Cerda and Doerr, 2007; MacDonald and Huffman, 2004; Doerr and Thomas, 2003). As we have observed in the preceding chapters, infiltration into water repellent soils is a complex phenomenon that is controlled by fractional wettability (i.e. decreased resistance to wetting via a particular soil fraction) and system dynamics (i.e. wetting of the overall medium as time of contact with water increases / changes in contact angle). Regardless of the conditions under which water repellency develops, it is these two variable controls that ultimately determine how water repellent soils will wet and the conditions required to do so.

Investigations on fire-affected water repellent media are often associated with the erosional impact due to the removal of vegetation and existence of

repellency. It is commonly reported that fire can lead to increased surface runoff and overland flow due to the presence of a hydrophobic layer (Huffman et al., 2001), however it has been difficult to isolate this effect from degradation processes related to vegetation removal (Doerr et al., 2000). While there is a significant body of literature that addresses the possible erosional effects of fire-affected materials (e.g. Robichaud, 2003; Shakesby et al., 2003; Ferreira et al., 2003; Dekker and Ritsema, 2003; Leighton-Boyce et al., 2007; McNabb et al., 1989; Pierson et al., 2008), these studies have neglected to investigate more thoroughly the critical role of infiltration processes using techniques that are representative of a range of infiltration scenarios. This limited treatment inherently discounts the function of low magnitude, high frequency rainfall events in these (erosive) processes and fails to inform us about infiltration processes that are largely governed by the concerted controls of fractional wettability and contact angle dynamics.

4.2 Research Plan

In this chapter, we outline and report upon a series of *in situ* experiments conducted on fire-affected porous media using tension disc infiltrometers, soil moisture measurements, and Water Drop Penetration Time / Volumetric Ethanol Percentage tests. In these tests, we scale up from 1D experiments documented in chapter 3 to investigate 3D infiltration processes and controls in water repellent media.

We sought to examine the functional relationship between field moisture conditions and early / longer term infiltration behaviour in fire-affected materials exhibiting both fractional wettability (chapter 2) and dynamic contact angles (chapter 3). Three materials of similar origin but variable repellency were tested at Halfway Lake Provincial Park, Ontario, Canada approximately 1.5 years post-fire. We use 3D data collected from tension infiltrometers to assess the temporal dependence of hydrologic processes in water repellent media under field moisture conditions. While many field investigations of soil water repellency

utilize forced wetting techniques through ponded infiltration and rainfall simulations (see section 4.1), forcing water into hydrophobic soil under positive pressures is a fundamentally different flow mechanism than capillarity driven infiltration. That means positive pressure infiltration tests generate results that combine two differing flow mechanisms (i.e. macropore flow and contact angle dynamics) without a means to de-convolute the data. We hypothesised that superior insight could be gleaned from tension disc infiltrometer data.

4.3 Location

In the past 7 years, Halfway Lake Provincial Park has undergone two major disturbances. In 2002, a short duration, high intensity storm event (i.e. microburst) resulted in the development of a 700 ha windthrow area in the northern portion of the park (Ryan Gardner, personal communication, September 29, 2008). In May of 2007, the park experienced (based on visual inspection of the site approximately 1.5 years post-fire) a high fireline intensity and low to moderate severity forest fire which burned approximately 525 ha of parkland to the south of the windthrow area. Fireline intensity is a term related to fire behaviour from the surface up; and burn severity describes duff and litter consumption and subsurface heating (NWCG, 2001). The human-caused fire began on an island in the south western portion of the park and moved across the park in a Southwest-Northeast direction (Fig. 4.1) (Gardner, personal communication, September 29, 2008). Above seasonal temperatures contributed to the fire's propagation and a fire warning had been in place. Discussion with park staff revealed that no fire suppressants were used to combat the fire and water bombing targeted specific sections of the northern portion of the burn perimeter to prevent propagation into the windthrow area. The fire crossed a two-lane highway (Highway 144) that runs in a north-south direction through the park.

Halfway Lake Provincial Park is located approximately 90 km northwest of Sudbury, Ontario Canada (N 46° 52.789; W 081° 37.947). Average annual

temperature for Sudbury (N 46° 37.800, W 80° 48.000; elev: 347.5m) is 3.7 °C and average annual precipitation is 899.3 mm, which includes 656.6 mm of rainfall (Environment Canada, 2009). The park is classified as part of the Southern Boreal forest ecosystem and is 4,730 ha in size. Tree species at the site include Jack Pine, White Birch, Poplar, White Spruce, Black Spruce, White Pine; stand composition is variable throughout the site. Tree stand composition of the area under direct observation consisted of 60% Jack Pine, 20% Black Spruce, 10% White Birch, and 10% Poplar. The working group species (i.e. Jack Pine) was approximately 24 years old at the time of the fire, had an average height of 19 m, 80% crown closure and was of moderate productivity (OMNR, 2008). Ground cover consisted of mosses (ubiquitous), small shrubs and lichens.

No soil maps are available for the area. A single large soil pit dug at Fire Site High and a number of shallower soil profiles observed throughout the area of study showed a ubiquitous LH horizon 3-7cm in thickness, a discontinuous Ae Horizon 1-4cm in thickness, and a Bf horizon 10cm-65cm in depth. The configuration is indicative of a Humo-Ferric Podzol. Bedrock outcrops occur frequently, particularly in upland elevations.

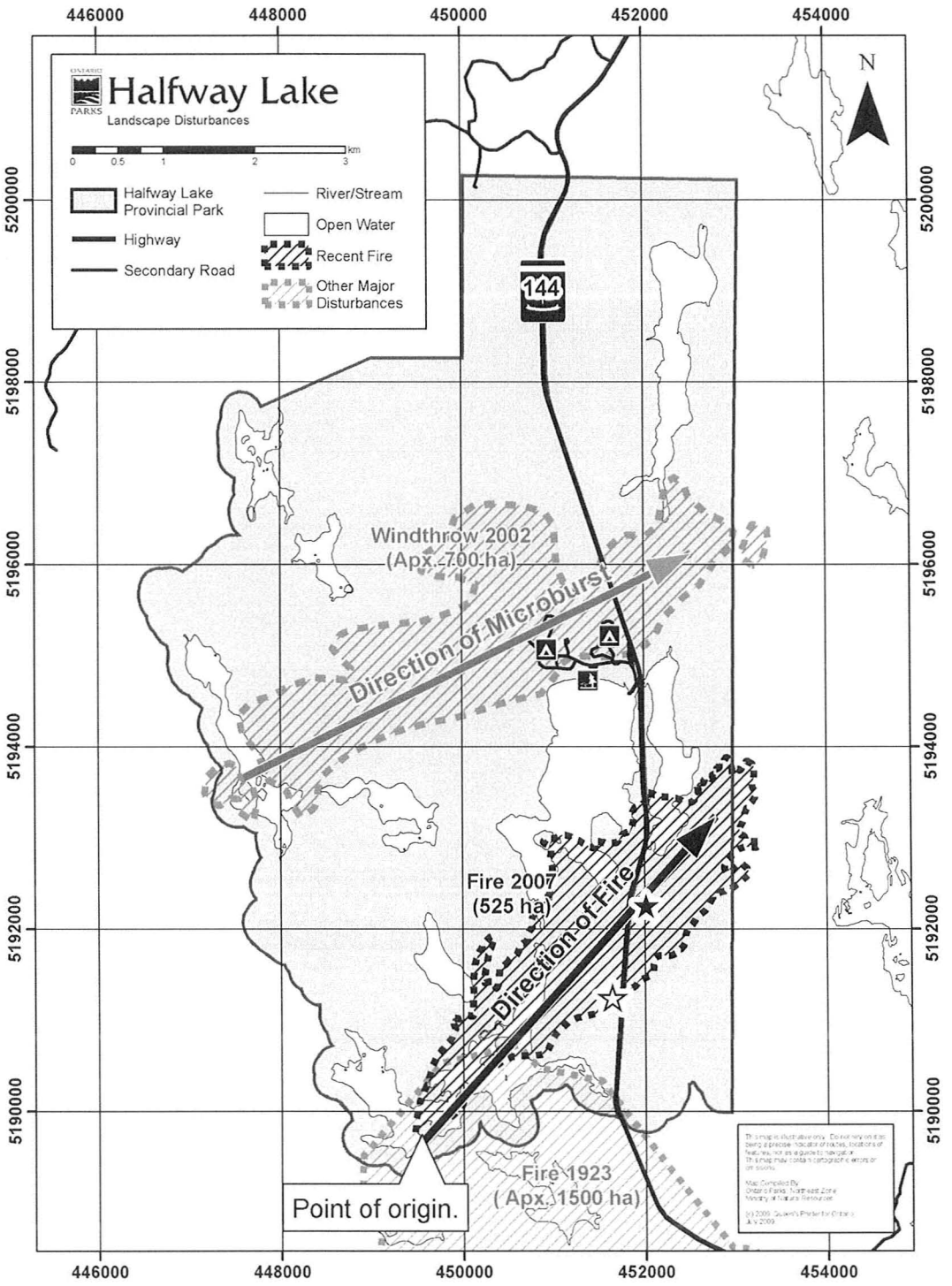

Fig 4.1 Halfway Lake Landscape Disturbances: showing park boundary, fire perimeter, and approximate locations of sample grids established at Fire Site High and Fire Site Low (black star), and Transition (white star) (OMNR, 2009; courtesy of Ed Morris)

4.4 Methods

4.4.1 Site Selection

In September 2008, a preliminary site evaluation trip utilised Water Drop Penetration Time (WDPT) tests using the method described by Bisdom et al. (1993) to evaluate the presence of water repellency in fire affected materials at Halfway Lake Provincial Park. Water Drop Penetration Time tests involve placing 10 drops of deionized water on a soil surface and measuring the time to drop disappearance by infiltration. A quick yet effective approach was used whereby materials were considered hydrophilic if drops infiltrated within 5 seconds and hydrophobic for times greater than 5 seconds. For the hydrophobic materials that were identified, it was often observed that WDPT tests exceeded 60 seconds; however, these tests were used only as a means to identify materials for more thorough investigation at later dates. Following the acquisition of research permits, sample / test grids were set up based on various criteria (e.g. ease of access, proximity to the fire perimeter, slope, elevation, tree cover, size and distribution of boulders and bedrock outcrops, and research goals).

In total, three grids were set up within the fire perimeter in October, 2008. Two grids were established in the centre of the burn perimeter (i.e. Fire Site Low, Fire Site High) on the east side of Highway 144 (Fig. 4.1). Fire Site High was located at an upland elevation (elev: 426m) approximately 30m west of Fire Site Low (elev: 422m). The third grid (Transition) was established on the west side of Highway 144, approximately 40m north of the southern fire perimeter (i.e. transition between burned and unburned ground material) (elev: 421m). The perimeter itself at this particular location was situated along a north-facing slope (the slope ran ~20m bottom to top). The grid was located on level ground approximately 20m from the base of the slope, being as close as possible to the burn perimeter without obstruction from fallen trees. In each case, grids were

established on relatively even terrain with soil horizons thick enough to accommodate research objectives.

Sample grids were set up to facilitate organization and record keeping efforts and were not intended to provide spatial statistics for comparison of sites or site characterization purposes. Specific test sites within the sample grids were chosen by a combination of both random and targeted selection. The selection process (i.e. random and/or targeted) was based on what type of test was being conducted (e.g. TDR tests were carried out randomly within sample grids and also targeted infiltration tests areas specifically; bulk density samples were always collected from pits dug for soil identification purposes).

4.4.2 Soil Properties: Soil Moisture and Bulk Density

Volumetric water content (VMC) measurements to a depth of 20cm were made in the field using a Moisture Point (Model: MP-917) Time Domain Reflectometry (TDR) system. The system proved to be additionally useful in that underlying bedrock material could be easily identified apart from cobbles or large roots. When the moisture probes could not be completely inserted at a location, probes were re-inserted at an adjacent area (<30cm away). For TDR measures taken near infiltration tests, care was taken so as not to disturb the infiltrometer or infiltration area with the rods of the TDR system.

Gravimetric moisture content samples were also collected during field work (in October only). Grab samples were collected 1-3cm from the surface and placed into glass jars with lined Teflon caps. Teflon tape was wrapped around the outer cap to seal samples and reduce evaporation. Upon return to the lab, samples were collected from jars, weighed, and then dried in a 105 °C oven for 24 hours. Samples were then placed in a dessicator and allowed to cool to room temperature before a final dry weight measurement was taken.

Bulk Density and volumetric water content samples were taken using $55cm^3$ stainless steel insertion rings to collect samples from soil profiles. Rings were inserted into the face of soil profiles and then excavated and trimmed using

a spatula. Samples were then triple bagged with Ziploc bags to minimize any evaporation that could occur between sample collection and processing in the lab. Once in the lab, samples were weighed and then oven dried in a 105 °C oven to constant weight. Samples were cooled to room temperature in a dessicator and then re-weighed.

4.4.3 Materials Selection for Water Repellence Testing

During early site evaluation work (i.e. in October), three materials of interest were identified via Water Drop Penetration Time (WDPT) / Volumetric Ethanol Percentage (VEP) tests (Bisdom et al., 1993; Dekker and Ritsema, 1994) and volumetric moisture content measurements. These three materials or cover types were uniquely and apparently similar in terms of composition, yet visually distinct from one another (Fig. 4.2 and Fig. 4.3). They also appeared often and in multiple locations within sample grids. Most importantly, each showed distinct differences in repellence via WDPT / VEP tests (Fig 4.4). If drops of water (WDPT) did not infiltrate within 5 seconds, the Volumetric Ethanol Percentage (VEP) test was employed. VEP tests involved dispensing drops of increasing ethanol concentration from a 5ml syringe on undisturbed surface material until each of 10 drops using a particular concentration disappeared in under 5 seconds (Dekker and Ritsema, 1994). Ethanol mixtures (1, 3, 5, 7, 10, 13, 15, 17, 20, 25, and 30% ethanol by volume) were prepared in the lab using 95% technical grade denatured ethanol. Bottles containing ethanol mixtures were sealed with Teflon-lined caps and wrapped with Teflon tape for transport into the field.

Fig. 4.2 Example of Brown Material (BRM) left of the dashed line, and adjacent Mixed Material (MM) to the right

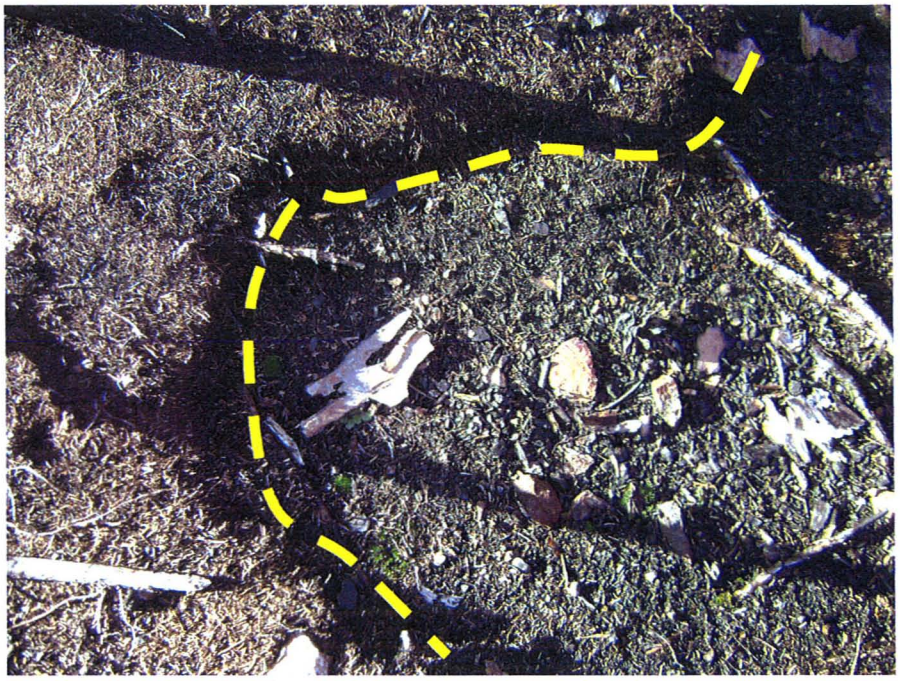

Fig. 4.3 Example of Char Material (CM) in depressed area to the right of the dashed line and BRM and MM materials to the left

Fig. 4.4 Drop of water on hydrophobic materials; drop size shown is ~5 times the volume of drops used in WDPT tests

By increasing ethanol concentration, the surface tension of the applied drops decreases to a point where (for hydrophobic materials) wetting is induced. This is known as the '90° surface tension' i.e. the surface tension required for drops to spontaneously wet surfaces hydrophobic surfaces at a theoretical contact angle ≤90° (Letey, 2001). The particular ethanol concentration that induced wetting (up to 30% ethanol) was recorded for each of the materials of interest. Although Water Drop Penetration Time tests are used to measure hydrophobic *persistence* (i.e. time required for infiltration) and Volumetric Ethanol Percentage tests measure hydrophobic *severity* (i.e. initial contact angle), the time limit (5s) with which the WDPT test was applied here renders it a 0% ethanol concentration VEP test. Leighton-Boyce et al. (2007) expressed that materials requiring a mixture of 36% ethanol to induce wetting are considered extremely hydrophobic. However, Dekker and Ritsema (1994) set the threshold for extreme hydrophobicity at a 20% aqueous-ethanol mixture. Here we only report measures quantitatively since it was not our intent to assign a qualitative classification, but rather to determine coarse quantitative differences in hydrophobicity between the three materials.

One material of interest was a brown, cohesive, organic material. At times, this material was somewhat darker or lighter, but overtly distinguishable from the other materials in that it showed little to no evidence of charring. Drop tests (WDPT and VEP) indicated that this material was repellent (i.e. WDPT ≥5s; 30≥VEP>15), and a VMC measure indicated that this material had the lowest moisture content of the three materials (22.9%). These materials were termed Brown Materials (BRM) (e.g. Fig. 4.2 and Fig. 4.4).

A second material was a char material (e.g. Fig. 4.3). This material showed signs of significant burning and tended to exist in low lying areas (relative to Brown organic materials). Though thoroughly combusted, these unconsolidated materials were still identifiably of similar origin to brown organic materials. This material showed the highest VMC of the materials (38.0%) and no signs of repellency in WDPT tests (i.e. WDPT = 0s; VEP not done). These materials were termed Char Materials (CM).

A third and final selected material of interest was more complex in that it appeared as a combination of materials. These materials showed evidence of charring at the surface, but topographically speaking, were at the same level as the brown materials (BRM). These were termed Mixed Materials (MM). Shallow excavations revealed that the subsurface materials were visually comparable in color and identifiably similar in composition to material found beneath the Brown organic (surface) materials (BRM). An intermediate VMC was present in this material (31.4%) and WDPT times were similar to brown organic materials, except that drops only partially infiltrated during the testing time frame (i.e. WDPT = 5s; VEP not done).

In the assessment outlined above, all materials were found within a $1m^2$ area. It was hypothesised that a relationship may exist between the amount of char present and the degree of repellency observed (i.e. degree of charring was directly related to moisture content and indirectly to water repellence); so these materials were specifically targeted for infiltration testing.

4.4.4 Water Repellence Testing Using the Tension Disc Infiltrometer

Having identified three different materials or (perhaps more appropriately) burn conditions on which this research would focus, repellence testing via tension disc infiltration experiments was carried out on materials at all sites (i.e. Fire Site High, Fire Site Low, Transition) according to the observed surface condition / classification of materials (i.e. Brown Material (BRM), Char Material (CM), or Mixed Material (MM)). To minimize heterogeneity as much as possible and isolate the effect of burn condition on soil water repellency for all test locations, beyond burn condition, test location decisions were based on proximity to other infiltration tests; visual inspection of small scale topography; and proximity to debris, tree roots, and rocks. Subsurface conditions were not always apparent based on visual inspection of surfaces.

Infiltration tests conducted at Halfway Lake Provincial Park took place during two separate field trips; on one day in October (the 30th) and on one day in November (the 6th). October temperatures taken from an alcohol thermometer during testing ranged from 3 °C (11 am) to 8 °C (2 pm). October tests began later in the day (11:30 am), as it was evident upon arrival to the site that although the fire had removed the canopy, aspect and topographical shading coupled with overnight freezing temperatures created a ubiquitous frozen soil crust ~2-3cm in thickness. Tests were carried out preferentially in grids that thawed quickest (i.e. Fire Site High). November infiltration tests did not have the same logistical requirement as ambient air temperatures ranged from 18 °C (12:30 am) to 8 °C (5 pm).

All infiltration tests conducted in this series of tests used the Mini Disc (tension) Infiltrometer (Decagon Devices, Pullman, WA). Using this infiltrometer was advantageous for three reasons. First, its small and rugged construction makes it a field-friendly instrument: its reservoir and bubbling chamber are constructed of a single 13 inch polycarbonate tube and has few other components (Fig. 3.3). Second, the porous disc is small (i.e. diameter of 4.4cm).

This allows the user to conduct the infiltration tests without having to pour a layer of contact sand. Although this is a common practice (Reynolds, 2006), it introduces foreign materials to the site and an additional component to set up. Third and lastly, the infiltrometer is designed to permit measurement of infiltration rates under a constant negative pressure (tension) head. Typically, in water repellency investigations, positive pressure tests are employed (e.g. Feng et al., 2001; Wang et al., 2000; Bauters et al., 2003; Scott, 2003). Ponding water on the soil surface changes the nature of flow into porous media such that the largest pores become the main conduits of infiltration and flow in these systems (Hallett et al., 2004; Felton, 1992). Since smaller pores in (hydrophilic) unsaturated media preferentially fill first as they are under higher negative pressure head than large pores, this type of information is limited in terms of its capacity to convey hydrophobic system behaviour over a range of infiltration scenarios and for dynamically wetting materials with changing hydraulic properties (with increased exposure to water).

For all tests, the infiltrometer was filled with approximately 90 ml of deionized water and set to a tension head of minus 2cm. Upon initiation, the starting volume was noted and the infiltrometer was placed onto the surface with enough force to ensure good contact between the disc and the soil surface. All tested surface materials were organic in composition and compressed 1-5mm under the applied force. The infiltrometers were held securely in position using clamps and retort stands (Fig. 4.5).

For October tests, we were most interested in determining whether infiltration behaviour would differ substantially in the three materials. However, after having preliminarily analyzed the data collected in October infiltration tests, we became interested in, and decided to further investigate the time to infiltration initiation, or the time between placing the porous disc on the surface and the first bubble observed in the infiltrometer tube (i.e. time to first bubble). It has been argued that time to first bubble provides a correlated, but more meaningful

Fig. 4.5 In-progress infiltration tests on Mixed Materials (MM) – left and Char Materials (CM) – right. Blue rectangle = TDR measurement probes.

measure of hydrophobic persistence when compared to Water Drop Penetration Time (WDPT) tests (i.e. Spearman r=0.59 for p<0.0001) (Lewis et al., 2006). Because of differences in WDPT drop absorption behaviour and self organization of particles on drop surfaces due to evaporation (McHale et al., 2007), time to first bubble of a tension disc infiltrometer is also regarded as a less subjective measure of hydrophobicity (Lewis et al., 2006).

October tests also revealed that very little further change occurred in late time data (i.e. > 45minutes). In response to these observations (i.e. time to first bubble and test duration), November data also included the notation of time to first bubble and tests were limited to 40 minutes or 40ml.

In all tests, the initial condition of the apparatus was standardized at the start of these tests by using a piece of paper towel to initiate a bubble in the bubble chamber of the infiltrometer (prior to placing the infiltrometer on the

selected surface). Throughout all infiltration tests, volume and time data were recorded.

Upon completion of tests, a final volume and time measurement were recorded and the wetted area was observed after removal of the infiltrometer from the surface (Fig 4.6, Fig 4.7). This was done to determine if any areas of the porous disc did not contribute to infiltration; observations indicated complete contact of the disc to material surfaces for all tests. Infiltration areas were then excavated carefully by cutting the wetted diameter in half to observe subsurface materials and the wetted bulb volume and geometry. Materials from within wetted regions were then collected and stored for transport.

4.5 Results and Discussion

4.5.1 Soil Properties: Bulk Density and Volumetric Moisture Content

Dry bulk densities of Ae and B Horizon materials are shown in Table 4.1. These data were collected at Fire Site High (FSH) and Transition (TRAN) sites. Based on visual inspection of shallow soil profiles during post infiltration test excavations at Fire Site Low (FSL), B Horizon and Ae Horizon bulk densities are expected to be similar to those of FSH. Corresponding photographs of soil profiles at Pits 1, 2, and 3 are shown in Fig 4.8 Fig. 4.9 and Fig. 4.10.

Table 4.1 Dry Bulk Densities and Volumetric Moisture Content for Halfway Lake Provincial Park at Fire Site High (FSH) and Transition (TRAN) sites

Site ID	Soil Description, Horizon, Colour	Location	Depth	ρ_b(g/cm^3)	VMC (m^3/m^3)
FSH	Mineral, Bf Horizon, Dark Ochre	Pit 1 (Shallow)	15 cm	0.83	0.12
FSH	Mineral, B Horizon, Ochre	Pit 2 (Deep)	15 cm	1.22	0.47
FSH	Mineral, B Horizon, Ochre	Pit 2 (Deep)	16 cm	1.06	0.42
FSH	Mineral, B Horizon, Dark Ochre	Pit 2 (Deep)	40 cm	1.01	0.48
TRAN	Mineral, B Horizon, Dark Ochre	Pit 3 (Deep)	15 cm	0.93	0.29
TRAN	Mineral, B Horizon, Dark Ochre	Pit 3 (Deep)	30 cm	1.17	0.34
FSH	Mineral, Ae Horizon, Grey	Pit 4 (Shallow)	8 cm	1.19	0.48

Fig. 4.6 Post infiltration wetted diameter for Brown Materials (BRM), showing no wetting around periphery of disc.

Fig. 4.7 Post infiltration wetted diameter on Char materials (CM). Pen pointing to wet region around periphery of disc area, indicating distribution flow.

Fig. 4.8 Fire Site High (FSH) Soil Profile: Pit 1 (shallow)

Fig. 4.9 Fire Site High (FSH) Soil Profile: Pit 2 (deep)

Fig. 4.10 Transition Site (TRAN) Soil Profile: Pit 3 (deep)

4.5.2 Soil Properties: October Moisture Contents

Average volumetric moisture content (VMC) data collected using TDR for October tests are reported in Table 4.2. Volumetric moisture content measurements were taken randomly within each 100m^2 area at the three sites. The data indicate some difference between sites, with the most significant difference between Fire Site High (31.1 %) and Fire Site Low (20.7%). Because of the probe length used (20cm), averages reported here represent moisture sampling that covered Organic (LH) and Mineral (Ae, B) horizons.

Table 4.2 Average Volumetric Moisture Content (VMC) sampled in October

Site ID	Location	Position (m)	Date	Temp °C	n	Average Reading %	Range %
FSH	Fire Site High	0,0 to 10,10	28-Oct	-2	7	31.1	24.3-35.5
FSL	Fire Site Low	0,0 to 10,10	28-Oct	-2	8	20.7	7.2-30.2
TRAN	Transition	0,0 to 10,10	29-Oct	-2	4	24.6	20.5-27.5

Table 4.3 shows gravimetric moisture content (GMC) data from small grab samples taken pre- and post-infiltration for tests conducted in October. These data indicate that increases in moisture content were observed between pre- and post-infiltration tests in all cases; the magnitude of changes in GMC, however, was not consistent across tests. For example, Test ID TFN34 has the lowest moisture content at the start of the test, and also at the end of the test (0.26 vs. 0.31g/g). One could expect a more substantial change in water content between pre- and post- infiltration conditions for this initially drier material. The UPLMM test also shows a small relative change (0.74 vs. 0.78g/g) between measures; however, given the higher initial moisture content, the (lack of) difference is not nearly as significant as these materials may be approaching field moisture capacity (i.e. saturation). In all other cases, larger changes between pre- and post-infiltration conditions can be observed (i.e. TFN16; TFN19; UPLBRM).

Table 4.3 Average Gravimetric Moisture Content (GMC) sampled in October

Site ID	Test ID	Soil Description, Horizon, Surface	Sample Type	GMC (g/g)
FSH	TFN16	Organic, LH Horizon, Char	Pre-Infiltration	0.64
FSH	TFN16	Organic, LH Horizon, Char	Post-Infiltration	0.76
FSH	TFN34	Organic, LH Horizon, Brown	Pre-Infiltration	0.26
FSH	TFN34	Organic, LH Horizon, Brown	Post-Infiltration	0.31
FSH	UPLBRM	Organic, LH Horizon, Brown	Pre-Infiltration	0.33
FSH	UPLBRM	Organic, LH Horizon, Brown	Post-Infiltration	0.55
FSH	UPLMM	Organic, LH Horizon, Mixed	Pre-Infiltration	0.74
FSH	UPLMM	Organic, LH Horizon, Mixed	Post-Infiltration	0.78
FSH	TFN19	Organic, LH Horizon, Mixed	Pre-Infiltration	0.50
FSH	TFN19	Organic, LH Horizon, Mixed	Post-Infiltration	0.75

4.5.3 Water Repellency Testing: October Infiltration Tests

The data for infiltration tests conducted in October are shown in Table 4.4. A plot of Cumulative Infiltration vs. Time for all tests is shown in Fig. 4.11 and Infiltration Rate vs. Time is presented in Fig. 4.12. Infiltration rates were calculated using a two point central difference method which is second order correct (Gerald and Wheatley, 1984).The table shows additional information not presented in the figures. In the cumulative infiltration vs. time plot, some differences between wetting behaviour can be observed in the slopes of lines. Mixed Materials (MM) and Char Materials (CM) have comparatively high infiltration rates (i.e. steep slopes) over the entire duration of tests relative to the Brown (BRM) materials.

In all cases, materials behave similarly in that infiltration rates start high and end low. This behaviour is what one would expect in wettable materials. It is interesting, however, that both MM and CM infiltration behaviour (as shown in

Table 4.4 List of infiltration tests conducted in October

Site ID	Test ID	Cover Type	Temp °C	Test Duration	Volume Infiltrated (ml)
FSH	TFN16	Char Material	8	45:51	81.0
FSH	TFN34	Brown Material	7	1:29:09	68.0
FSH	UPLBRM	Brown Material	5	1:09:13	18.5
FSH	UPLBTM	Mixed Material	5	58:59	83.0
FSH	TFN19	Mixed Material	4	35:17	67.0

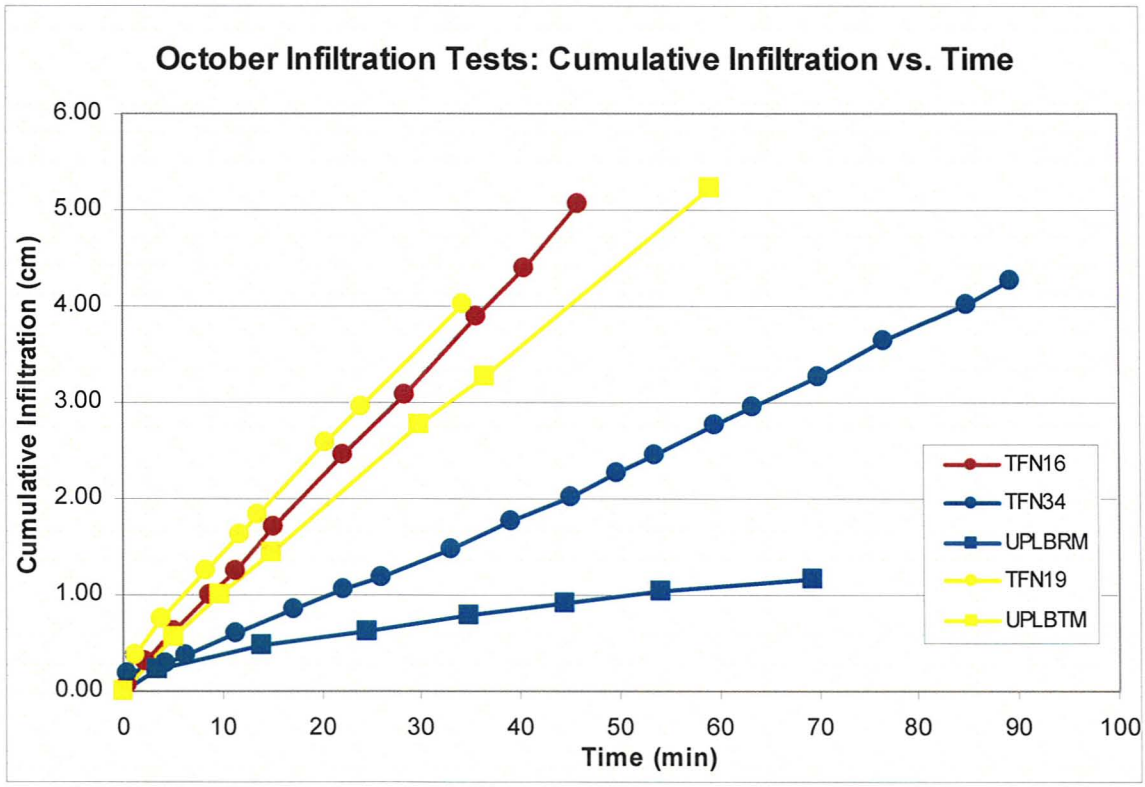

Fig. 4.11 Cumulative Infiltration (cm) vs. Time (min) for October infiltration tests. Gold indicates Char Material (CM) surface, Teal indicates Mixed Material (MM) surface, and Red indicates Brown Material (BRM) surface. Additional symbology: squares (UPL) and circles (TFN) to distinguish between Test ID Prefixes.

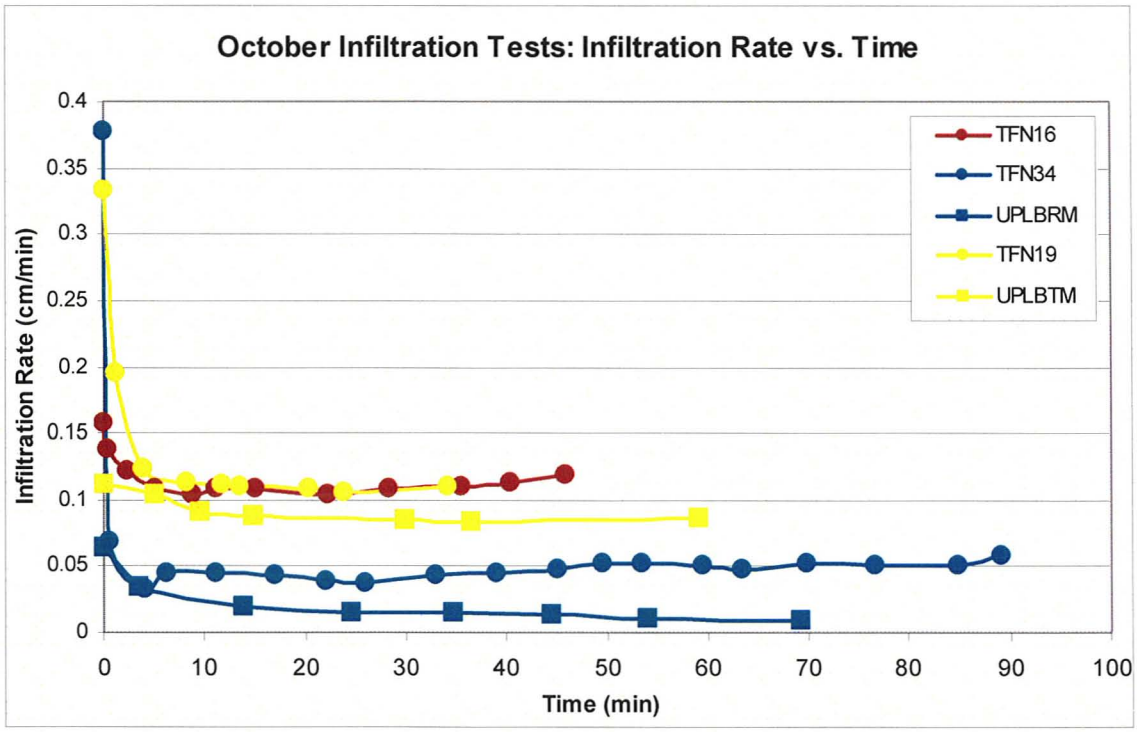

Fig. 4.12 Infiltration Rate (cm/ min) vs. Time (min) for October infiltration tests. Gold indicates Char Material (CM) surface, Teal indicates Mixed Material (MM) surface, and Red indicates Brown Material (BRM) surface.

Fig. 4.11 and Fig 4.12) are so similar given the apparent difference in burn condition of those materials. In observing the gravimetric moisture content data (Table 4.3) for these three tests, all three tests end at similar GMC's (i.e. 0.75, 0.76, and 0.78g/g). Further, the slowest initial infiltration rate (0.11cm/min) is associated with the highest initial moisture content (0.74g/g) and the fastest (0.33cm/min) initial infiltration rate is associated with the smallest initial moisture content (0.50g/g). In accordance with these data, the middle initial infiltration rate (0.16 cm/min) started with the intermediate moisture content (0.64g/g). This behaviour is easily explained by traditional infiltration theory into hydrophilic materials near field moisture capacity. If the relationship observed here holds true, then it appears that these visually distinct surface materials (CM and MM) actually behave much more similarly under wet field conditions than originally expected (see Fig. 4.13, 4.14 and 4.15).

Fig. 4.13 Post infiltration excavation at TFN16 (Char Materials)

Fig. 4.14 Post infiltration excavation at UPLBTM (Mixed Materials)

Fig. 4.15 Post infiltration excavation at TFN19 (Mixed Materials)

At early time (i.e. 0-1 minute), TFN34 (BRM) materials have the steepest slope / infiltration rate which quickly drops off to rates lower than MM and CM materials (Fig. 4.12). This may indicate that while BRM materials show relatively high rates of infiltration at the onset of infiltration events, infiltration rates in Brown Materials may not be sustained as the wetting front advances into new material over the long term.

Recalling from chapter 3 that one of the most identifiable characteristics of hydrophobic materials are increasing infiltration rates with time (Debano, 1975), small, yet consistent increases in infiltration rate can be observed at later times in both the Char Materials (20 minutes to 45) and Brown Materials (from 25 minutes to 90). While rate behaviour may differ substantially throughout the duration of these two tests, the other infiltration tests do not exhibit these kinds of sustained increases in infiltration rate with time. These data suggest that the effects repellency can still be observed in samples with gravimetric moisture contents as high as 0.76g/g (as was the case for TFN16) and that layered differences in wettability are not always apparent at the beginnings of tests.

It is noteworthy that one of the longer duration tests (i.e. >1hour) happens to have the smallest infiltration rate of the materials tested and had one of the lower pre- and post-infiltration moisture contents (i.e. pre: 0.33g/g and post: 0.55g/g). During the time of infiltration into this material, only 18.5 ml of water infiltrated. This is substantially low, especially considering that volumes infiltrated in other tests were nearly 3 times as much. While it may not always be possible to capture long term data as required, the apparently hydrophobic materials (i.e. materials that show increasing infiltration rate with time) reveal that differences in repellency may only become apparent at later time (when horizontal gradients become very small and infiltration primarily occurs downward into new organic layers). While initial infiltration behaviour and / or infiltration rates may behave similarly at the outset of infiltration tests for different surface materials, it appears that only sufficiently long tests can detect hydrophobicity in subsurface layers,

particularly under wetter field conditions. Post infiltration excavation further supports that water is not infiltrating as readily into subsurface layers found under Brown Materials (Fig. 4.16, Fig. 4.17).

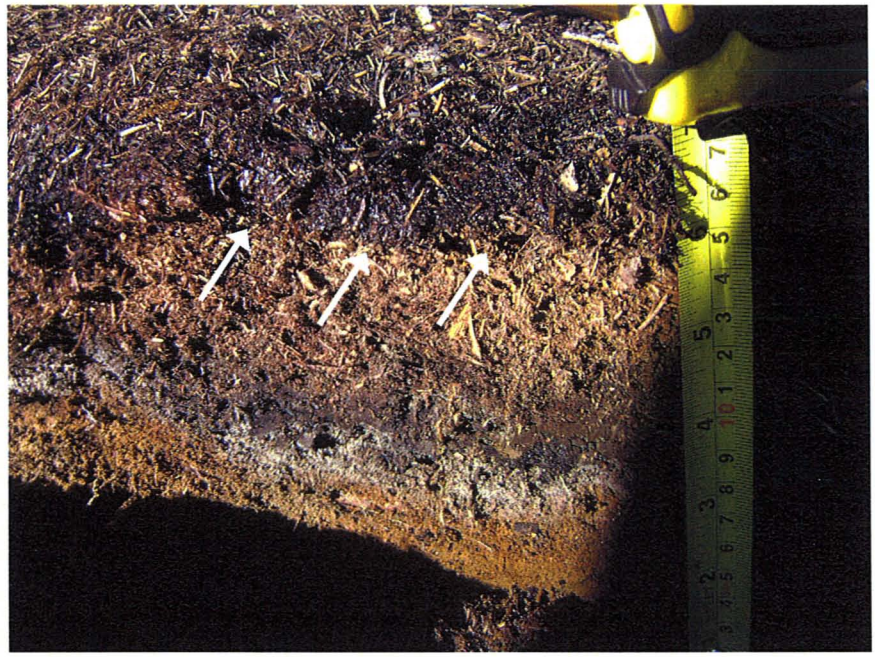

Fig. 4.16 Post infiltration excavation at TFN34 (Brown Materials) - Showing surface wetting (dark region) only and no wetting in subsurface organic materials after 89 minutes of testing

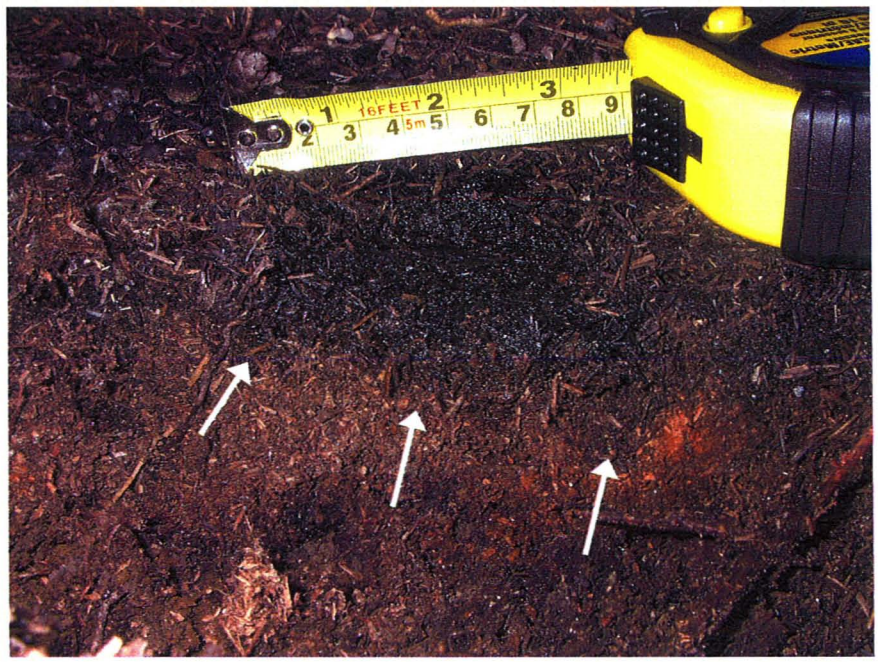

Fig. 4.17 Post infiltration excavation at UPLBRM (Brown Materials) - Showing darkened (wet) area where disc contacted surface, and irregular wetting into subsurface organic materials (arrows) after 69 minutes of testing

4.5.4 Soil Properties: November Moisture Contents

November Volumetric Moisture Content (VMC) data collected using TDR are presented in Table 4.5. These data represent average VMC's for November infiltration test locations (opposed to Site averages displayed in Table 4.2).

Materials tested at the Transition site have the highest water contents (36.6 - 31.1%). Fire Site Low has the lowest average moisture contents overall (15.7 - 24.0%), and Fire Site High moisture contents are found in-between (28.7 - 32.1%).

Site average moisture contents (VMC's) collected in October show little difference relative to November moisture contents at Fire Site High. Fire Site Low however, has higher average moisture content in November than October. Average moisture content at Transition indicates a significant increase in moisture content in November.

Table 4.5 Average Volumetric Moisture Content (VMC) for November infiltration tests

Site ID	Materials	Test # (Test ID)	Temp °C	n	Average Reading %	Range %
FSL	Char	#1 (MFN121)	17	4	23.5	18.3-27.5
FSH	Char	#2 (TFACM)	18-16	3	31.1	29.7-32.3
TRAN	Char	#3 (TRCM)	14-8	3	31.1	28.8-35.6
FSL	Brown	#4 (MFN78)	17	8	15.7	9.0-20.4
FSL	Brown	#5 (MFN132)	17	3	24.9	20.5-30.2
FSH	Brown	#6 (TFABRM)	18-16	3	28.7	26.1-29.7
TRAN	Brown	#7 (TRBRM)	14-8	5	36.6	28.8-39.4
FSL	Mixed	#8 (MFN133)	17	1	21.1	21.1
FSH	Mixed	#9 (TFAMM)	18-16	3	32.1	26.9-33.1
TRAN	Mixed	#10 (TRMM)	14-8	3	33.3	30.0-35.8

4.5.5 Water Repellency Testing: November Infiltration Tests – Overview I

Infiltration data collected during the November field trip are presented in the following sections. Part of the investigation presented in the following pages will cover time to first bubble data. It should be noted, however, that all infiltration rates and cumulative infiltration data are plotted according to an absolute time 0 (the time the infiltrometer was placed on the test surface) and not from time to first bubble / infiltration initiation.

Although 'time to first bubble' was regarded here as a measure of hydrophobic persistence, there are significant differences between the application of drops, as is the case in Water Drop Penetration Time (WDPT) tests and the measure of time to first bubble using the Mini Disc Infiltrometer (MDI). First, the WDPT test uses drops that exert a (small) positive pressure to the soil surface; the tension infiltrometer supplies water to the surface under a negative pressure (Felton, 1992). Second, the spatial scale of the two tests is significantly different. Drops sizes in the WDPT test are on the order of mm's (Hallet et al., 2004; Orfanus et al., 2008), whereas the wetted disc of the infiltrometer samples an area ~15cm^2. Although multiple drops are applied to a soil surface in the WDPT test, small scale variability and surface heterogeneity of hydrophobic surfaces contribute to substantial variation in data over relatively small spatial scales (Orfanus et al., 2008). While WDPT tests provide highly localized, but variable data, the MDI provides a measure averaged across the area of the disc. Here we support the idea that time to first bubble is a more representative measure of initial system response over scales relevant to infiltration events.

The following sections present data collected in November; these data are grouped by material type / burn condition. A comprehensive analysis for all materials is presented in section 4.5.9.

4.5.6 November Infiltration Tests: Char Materials

Infiltration rates for two of the three Char Material (CM) tests exhibit infiltration behaviour similar to that of hydrophilic materials (Fig. 4.18). That is, infiltration tests #2 (TFACM) and #3 (TRCM) have infiltration rates that start relatively high and decrease exponentially during early time. Within 10 minutes, tests #2 and #3 approach infiltration rates that continue to decrease with time, albeit at a much slower rate of change. This behaviour can be explained by decreasing moisture potentials due to the expansion of the wetting bulb. The effect is the result of a decreasing gradient caused by an increasing distance between the pressure potential at the disc (i.e. minus 2cm) and the pressure condition at the wetting front. In contrast, test #1 (MFN121) shows near linear increases in infiltration rate throughout the entire test, which ultimately results in a 70% increase in rate. This increase in infiltration rate cannot be explained by

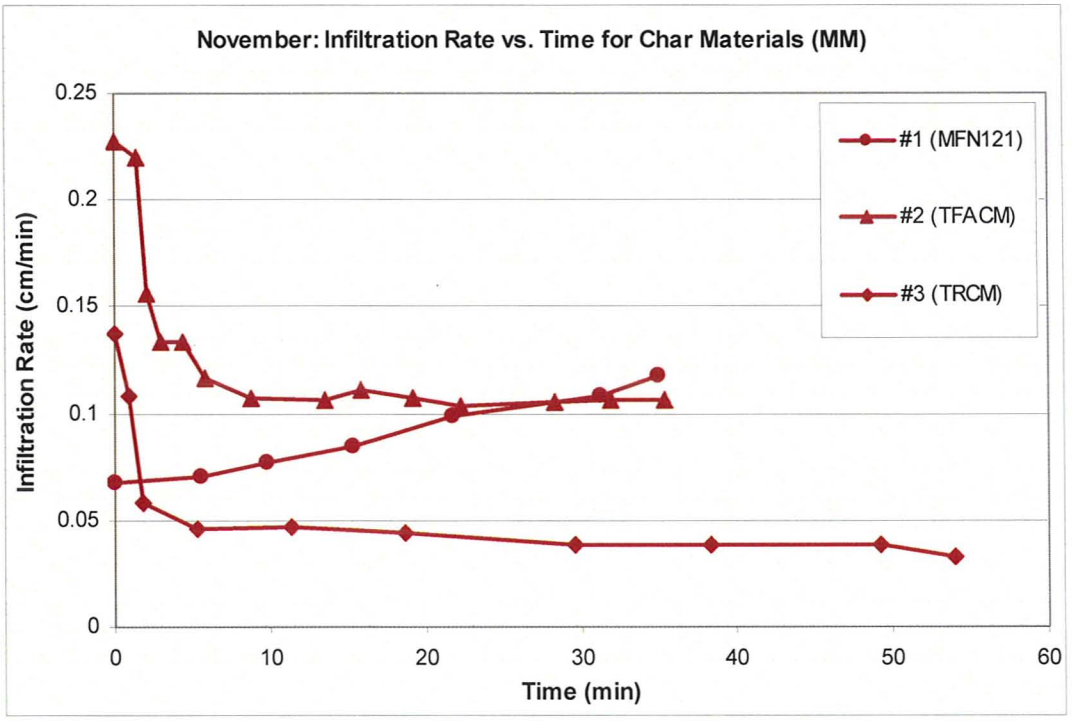

Fig. 4.18 Char Material (CM) - Infiltration Rate (cm/min) vs. Time (min) for November

theory describing infiltration behaviour in hydrophilic media (e.g. Hillel, 1982) and can only logically be explained as a direct expression of the dynamic hydraulic behaviour of this hydrophobic material.

From the time to first bubble data presented in Fig. 4.19, it is evident that test #2 and test #3 materials showed no resistance to wetting upon test initiation (0 and 1s). In contrast, test # 1 had a significant delay in infiltration initiation (21s). This delay is longer than two Mixed Material tests (# 8 (MFN133) and #10 (TRMM)) and one Brown material test (#7 (TRBRM)). Moisture content data for tests #1, #2, and #3, reveal that test #1 had significantly lower moisture content (i.e. 23.5 m^3/m^3 in test #1 vs. 31.1 m^3/m^3 in tests #2 and #3). Considering all other variables equal (i.e. material chemistry and soil properties), this could explain the difference in time to first bubble and infiltration rate behaviour. For similar subsurface materials, this suggests that there could be a relatively strong moisture content dependency on repellency expression in these (Char) materials.

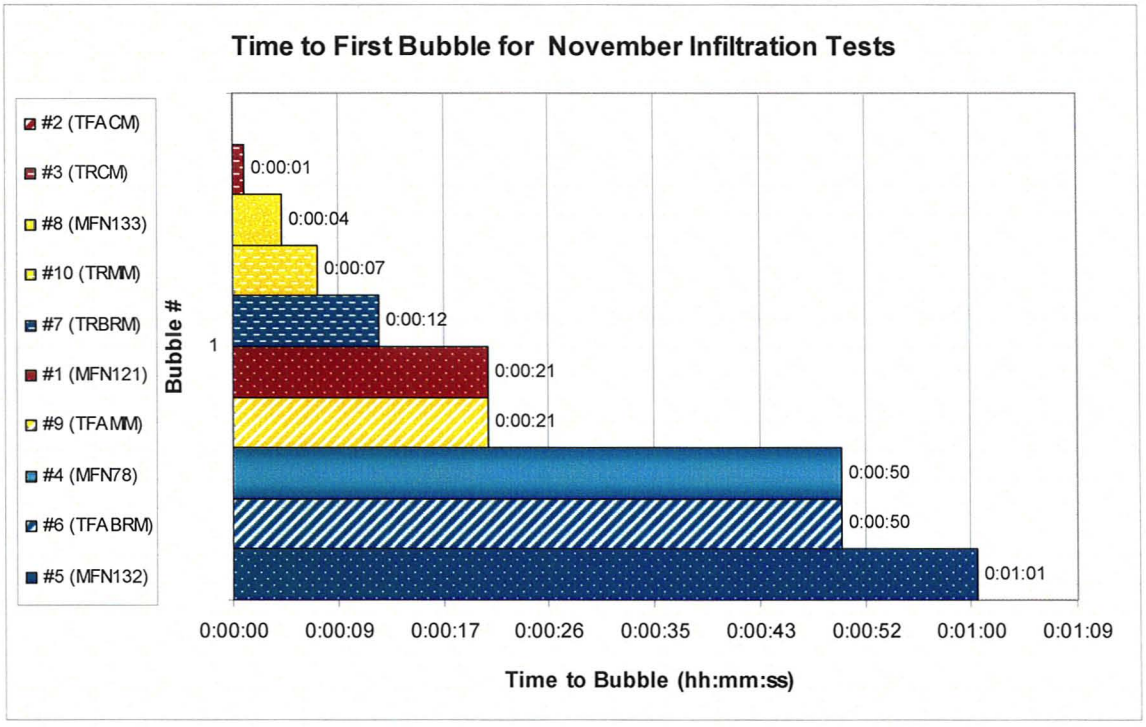

Fig. 4.19 Time to First Bubble – All Materials

Near surface material profiles as depicted in Fig. 4.20, Fig 4.21 and Fig. 4.22 vary somewhat in composition, with mineral Ae materials found in test #2 and organic materials found subsurface in tests #1 and #3. Water Drop Penetration Time (WDPT) tests on mineral Ae Horizon material indicated no repellency. The observational differences in subsurface material may help to further explain the difference in infiltration rates between tests #2 and #3 since average moisture content for the two tests was the same (i.e. 31.1 m^3/m^3). While visual observations of materials cannot exclude the possibility that materials tested in #1 and #2 are substantially different in composition, structure, texture, and chemistry, differences in initial moisture content between the two tests (i.e. 23.5 m^3/m^3 for #1 and 31.1 m^3/m^3 for #2) may alone sufficiently explain the differences observed in infiltration rate behaviour.

Fig. 4.20 Test #1 (MFN121), post infiltration excavation – Showing char surface material overlying brown organic material

Fig. 4.21 Test #2 (TFACM), post infiltration excavation – Showing char surface material overlying mineral Ae Horizon / intermixed B Horizon material. Dark red material =

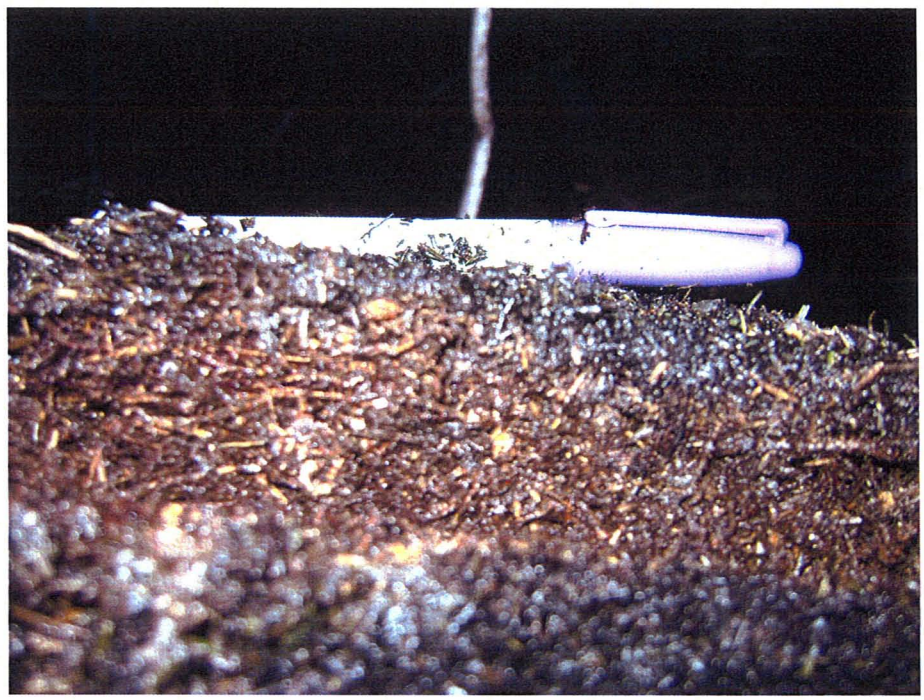

Fig. 4.22 Test #3 (TRCM) post infiltration excavation – Showing char surface material overlying brown organic material, thorough wetting in brown organic layer

4.5.7 November Infiltration Tests: Brown Materials

Infiltration Rate vs. Time data are presented for Brown Materials in Fig. 4.23. All tests express repellency through increasing infiltration rates at some point during the course of each test. Test #4 (MFN78), #5 (MFN132), exhibit similar behaviour at early time; infiltration rates double between 0 minutes and approximately 3 minutes, followed by a steeper increase to 5 minutes. Within the first 5 minutes of testing, #4 and #5 experience increases in infiltration rate by a factor of 5 and 7 (respectively). The infiltration rate of Test #6 (TFABRM) follows a similar pattern, although more subdued. Test #7 starts at the highest infiltration rate of the group, and after a small increase in infiltration rate, begins to decline variably with time. Infiltration rates in Brown surface material tests are within a narrow range of values (0.00-0.08cm/min) and are variable with time. Notable in the Brown materials is the prevalence of increasing infiltration rates, and abrupt

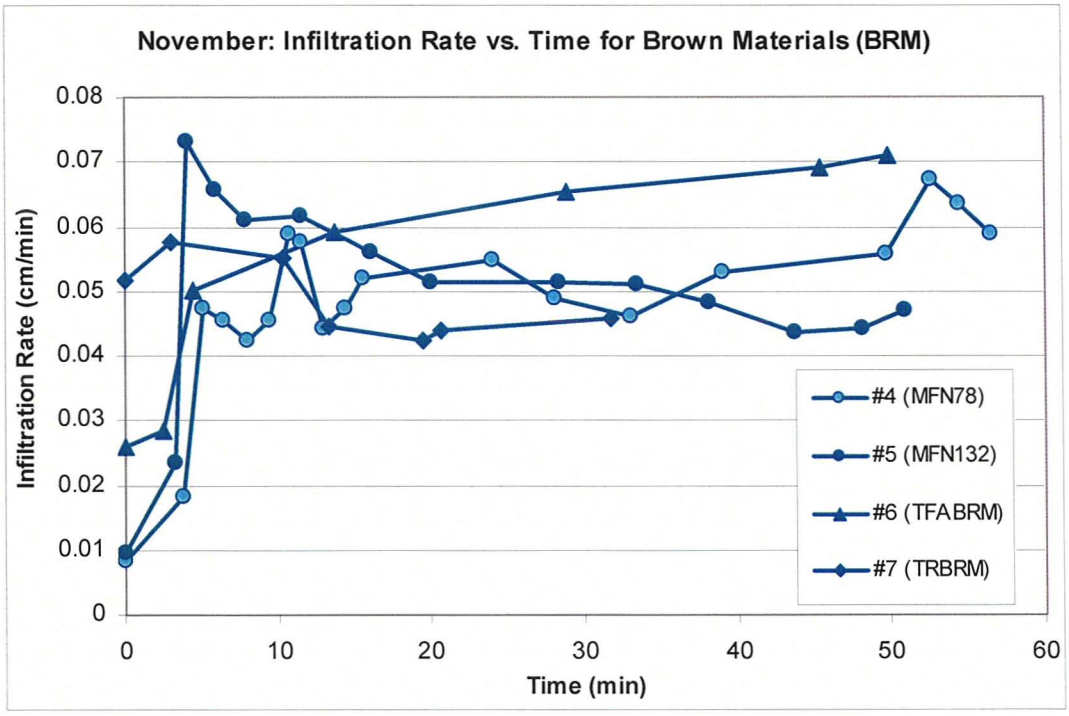

Fig. 4.23 Brown Material (BRM) - Infiltration Rate (cm/min) vs. Time (min) for November

variations between increasing and/or decreasing infiltration rates. These data indicate that both hydrophilic (i.e. decreasing rates with time) and hydrophobic (i.e. increasing rates with time) behaviours can occur within a single test. Further, it can be implied that in addition to dynamic changes in wettability of hydrophobic materials, fractionally wetting materials are affecting rate behaviour by providing pathways and/or restricting flow into subsurface materials at the wetting front. Where rates decrease with time, it could be said that wettable materials are being accessed by the wetting front and are moving farther away from the porous disc *or* that flow is being actively restricted by the hydrophobic fraction. Conversely, increasing rates with time can indicate a change in the restriction of flow via wettable fractions, or the dynamic change of contact angles in the hydrophobic fraction of the soil matrix. That the behaviour is so variable indicates distances between wettable and non-wettable fractions in Brown Materials are small (<cm's). This scale is in agreement with other investigations (e.g. Orfanus et al., 2008; Hallet et al., 2004). This also highlights potential non-uniqueness found in 3D field results.

Beyond 5 minutes, infiltration behaviour in all tests deviate from each other with the exception of tests #4 (MFN78) and #5 (MFN132). In #4 and #5, infiltration rates begin to decrease in a similar way. While #5 has a decreasing infiltration rate until 45 minutes, at 15 minutes the infiltration rate begins to increase again in #4. For the remainder of #4 test the infiltration rate is highly variable, yet overall, slowly increases with time. Small, yet consistent increases in infiltration rate exist beyond 45 min in test #5. Where infiltration rates are non-linear in these tests, after 5 min in Test #6 (TFABRM), regular increases in infiltration rate occur for the remainder of the test. For test #7, infiltration rate decreases between 5 and 20 minutes, at which time the rate begins to increase until the end of the test. These data, while highly variable, are more similar in overall infiltration rate than observed for Char Materials at the site.

Regarding the time to first bubble data collected for these materials (Fig. 4.19), there is general agreement between infiltration rate behaviour and infiltration initiation. Still, the data does highlight, that time to first bubble is not necessarily a strong predictor of early time (i.e. <3 minutes) infiltration rate. Lewis et al. (2006) found a good correlation between initial rate (i.e. <1 minute) and time to first bubble, however, for our data 1 minute was an insufficient time frame to observe infiltration at scales provided by the instrument (i.e. ml). In the case of #4 and #6, the same time to first bubble was observed, however the infiltration rate of #6 is 2½ times that of test #4. Additionally, #5 exhibits the strongest repellency in terms of time to first bubble; however, in terms of early time infiltration rate (i.e. <3 min), it is actually between #4 and #6. It may be the case that time to first bubble is not a strong indicator of early time infiltration rate because of contact angle variation between surface and subsurface materials (as observed in chapter 2) or possibly because it (TTFB) is a measure of hydrophobic persistence over relatively small temporal and spatial scales in surface materials only. In these data we find that time to first bubble share the shortcoming often experienced with WDPT tests; that longer term response to infiltration events cannot be predicted from this measurement alone.

According to the initial rate data and the time to first bubble data, #5 appears to be hydrophobic *only* at the beginning of the test, as rates decline for a significant portion of the test (between 5 and 45 minutes). Increasing rates observed at the end of the test may indicate that increases were occurring throughout the test, but were small relative to significant decreases in moisture potentials caused by the spreading of the wetting bulb through wettable media. Only once gradients were equal to or less than the effect of repellency would repellency appear in the data as increased infiltration rates. This highlights a potential shortcoming of 3D infiltration using the tension infiltrometer.

Near surface material profiles for tests #4 - #7 are presented in Fig. 4.24 – Fig. 4.27. All of the subsurface materials are organic in composition; three of the

four tests (i.e. #4 - #6) are comprised of materials similar to those found at the surface while subsurface materials tested in #7 (TRBRM) appear to be partially decomposed (hydrophilic) wood. This subsurface material composition may explain the decreasing infiltration rates observed after 5 minutes for this test.

Moisture contents for these tests imply that there is a direct relationship between moisture content and initial infiltration rate into water repellent materials i.e. higher moisture contents are well related to higher infiltration rates. This is in stark contrast to tests on wettable Char materials in November and Char and Mixed materials in October tests; where high antecedent moisture contents resulted in *lower* relative (initial) infiltration rates as is the case for classical infiltration into water wet hydrophilic soils.

Fig. 4.24 Test #4 (MFN78), post infiltration excavation – Showing wet (dark) surface wetting and wetting into subsurface brown organic matter (approx scale 1cm:1.25cm)

Fig. 4.25 Test #5 (MFN132), post infiltration excavation – Showing wet (dark) surface wetting and wetting into subsurface brown organic matter (approx scale 1cm:1.25cm)

Fig. 4.26 Test #6 (TFABRM), post infiltration excavation – Showing wet (dark) surface wetting and wetting into subsurface brown organic matter

Fig. 4.27 Test #7 (TRBRM), post infiltration excavation – Showing wet (dark) surface wetting and wetting into subsurface wood material

4.5.8 November Infiltration Tests: Mixed Materials

Similar to Brown Materials (BRM) discussed in Section 4.5.7, Mixed Material infiltration tests have a combination of both increasing and decreasing infiltration rates (Fig. 4.28). However, the initial infiltration rate of #8 (MFN133) is consistent with Char Material tests *before* 5 minutes while tests #9 (TFAMM) and #10 (TRMM) are more consistent with Char Material tests *after* 5 minutes. While different than all other tests, #8 exhibits infiltration behaviour similar to that found by Imeson et al. (1992) in rainfall simulations in Spain (i.e. application rate of 45-57mm/hour for 1½ hours). Under the constant low negative pressure head condition of tests conducted here, application rates were lower and therefore the behaviour was less pronounced than observed by Imeson et al. (1992).

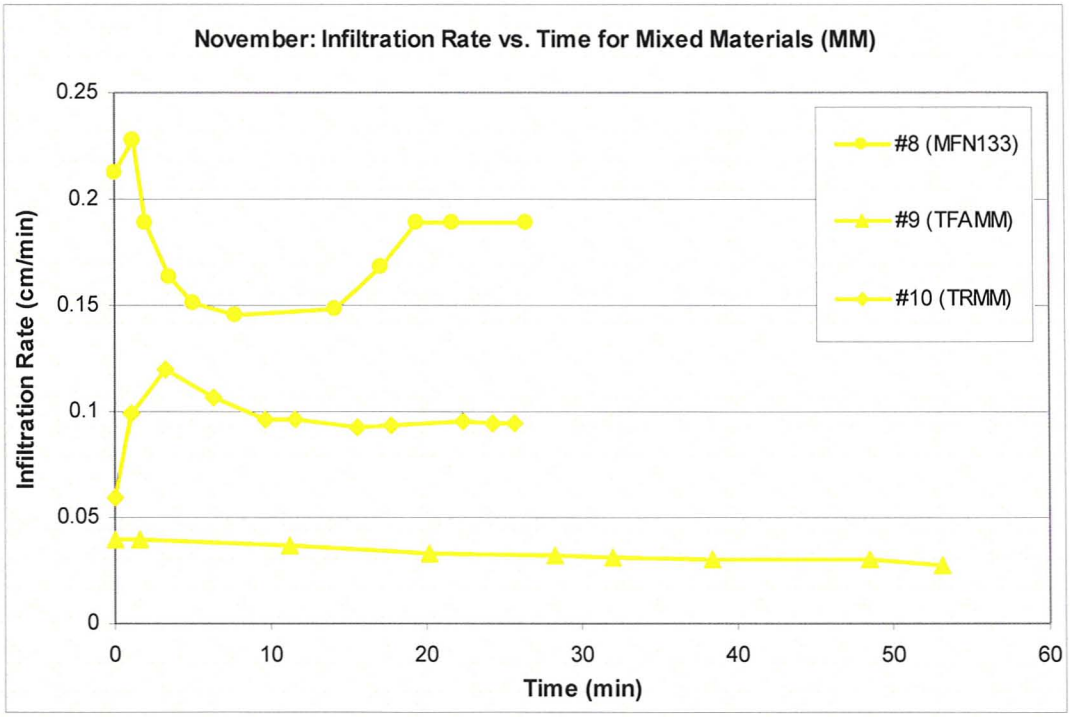

Fig. 4.28 Brown Material (BRM) - Infiltration Rate (cm/min) vs. Time (min) for November

Test #10 mimics that of the BRM material test conducted at the same site (i.e. #7 (TRBRM)), albeit at higher infiltration rates throughout the (MM) test. Test #9 is unique from all other tests conducted in that consistent decreases in infiltration rate are observed for the duration of the test.

Delays in time to first bubble data (Fig. 4.19) relate well to initial infiltration rates for Mixed Materials (i.e. increased time to first bubbles are associated with lower initial infiltration rates). Based on the (initial) infiltration rate data, however, one might suspect that time to first bubble for test #10 be closer to that of #9. By rough calculation, the initial infiltration rate of test #8 is larger than #10 by a factor of (approximately) 3 and the initial infiltration rate of #10 is larger than #9 by a factor of 0.5. The time to first bubble data give no indication of this approximate relationship. Since the tension disc equipment design is such that time to first

bubble should be an indicator of initial infiltration rate (as bubble rate relates directly to flow rate), it is unexpected that a more complimentary relationship does not exist between these two measures. In accordance with the observations discussed in section 4.5.7 for Brown Materials, this suggest that fractional wetting and/or rapid changes in material properties are occurring over early time periods or that the initial condition of the apparatus is highly variable regardless of standardization efforts.

Another issue that is most apparent in these data is that according to Water Drop Penetration Time standards, these three MM tests would be categorized as 5-60 s or 'slightly water repellent' (Dekker and Ritsema, 2003). While this may be an informative measure to some, it becomes quite apparent that significant differences in infiltration are observed between tests within this range.

Significantly noteworthy is that these materials do not exhibit the relationship to moisture content observed in the other two cases. Where Char Materials had lower infiltration rates with increased water content, and Brown materials had higher infiltration rates with increased water content, these materials display a strikingly different kind of relationship. Test #8 has the lowest moisture content of the group, but has the highest infiltration rate of the group, even while exhibiting water repellent behaviour (in the increasing infiltration rate). Test #9 exhibits the next highest water content, but has the lowest infiltration rate of the group, and because of longer term decreases in infiltration rate, does not appear to be hydrophobic at any point during the course of the infiltration test. Test #10, has the highest moisture content of the group, but exhibits hydrophobic infiltration behaviour. What is most interesting about this group is that there are increases in infiltration rate with both lower moisture contents and higher ones meaning that fractional wetting and dynamics of repellency is highly complex for these materials and are not always related singularly to surface material or moisture content.

Near surface material profiles are shown in Fig. 4.29-4.31. What is evident from these pictures is that subsurface materials in the 'Mixed Material' tests are not visually distinct from each other, or from other tests conducted at Halfway Lake Provincial Park (e.g. tests #1 and #3). For test #10 where long term infiltration rates decreased (and where infiltration rate behaviour mimicked that of test #7 (TRBRM)), it is interesting to see that subsurface materials in #10 are similar in nature to subsurface (hydrophobic) materials in BRM tests. Test #7 had woody (hydrophilic) subsurface materials and had decreasing infiltration rates after 5 minutes. From this, it might be discerned from the decreasing infiltration rates observed after 5 minutes in test #10 that these subsurface materials behave hydrophilically at moisture contents near to those observed in test #10 (VMC of 33.3m^3/m^3).

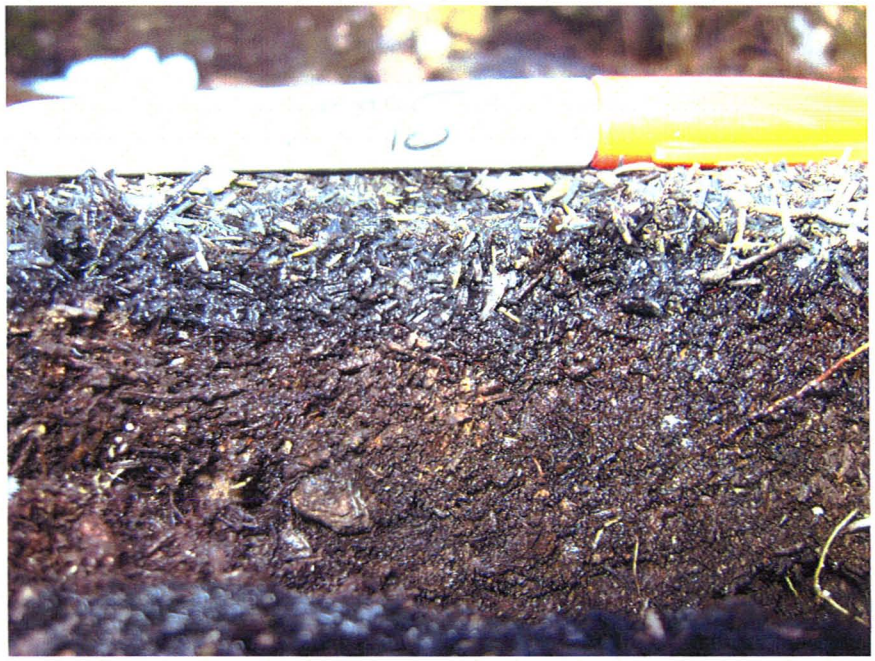

Fig. 4.29 Test #8 (MFN133), post infiltration excavation – Material surface and Brown OM subsurface material

Fig. 4.30 Test #9 (TFAMM), post infiltration excavation – Material surface and brown OM subsurface material

Fig. 4.31 Test #10 (TRMM), post infiltration excavation – Material surface and dark brown OM subsurface material

4.5.9 November Infiltration Tests: Overview II

All infiltration tests conducted in November are shown in Table 4.6.

Table 4.6 List of infiltration tests conducted in November

Site ID	Test # (Test ID)	Materials	VMC %	Average Infiltration Rate (cm/min)	Time to First Bubble	Volume Infiltrated (ml)
FSL	#1 (MFN121)	Char Material	23.5	0.089	0:00:21	50.0
FSH	#2 (TFACM)	Char Material	31.1	0.131	0:00:00	65.0
TRAN	#3 (TRCM)	Char Material	31.1	0.059	0:00:01	37.5
FSL	#4 (MFN78)	Brown Material	15.7	0.048	0:00:50	44.5
FSL	#5 (MFN132)	Brown Material	24.9	0.049	0:01:01	40.5
FSH	#6 (TFABRM)	Brown Material	28.7	0.053	0:01:10	48.0
TRAN	#7 (TRBRM)	Brown Material	36.6	0.049	0:00:12	24.5
FSL	#8 (MFN133)	Mixed Material	21.1	0.179	0:00:04	71.0
FSH	#9 (TFAMM)	Mixed Material	32.1	0.033	0:00:42	40.0
TRAN	#10 (TRMM)	Mixed Material	33.3	0.095	0:00:07	40.0

The Cumulative Infiltration vs. Time data indicate some differences between the three materials of interest, albeit not as clearly as in October (Fig. 4.32). Four of the 6 Char (CM) / Mixed (MM) tests have steeper slopes (higher infiltration rates) than Brown (BRM) materials over the lengths of the tests. This is expected as infiltration rates for Char and Mixed materials in October tests were also high compared to BRM materials. However, test #2 (TFACM) and #8 (MFN133) infiltration rates are more similar to BRM materials over their entire duration. The early time data (Fig. 4.33) reveals that infiltration rates for these two tests are actually higher until 5 minutes, and that only one Brown test has a higher infiltration rate at early time (i.e. #6 (TFABRM)). This may indicate that early time behaviour is best explained by (related to) surface material / burn condition, while later time data may be more sensitive to subsurface materials.

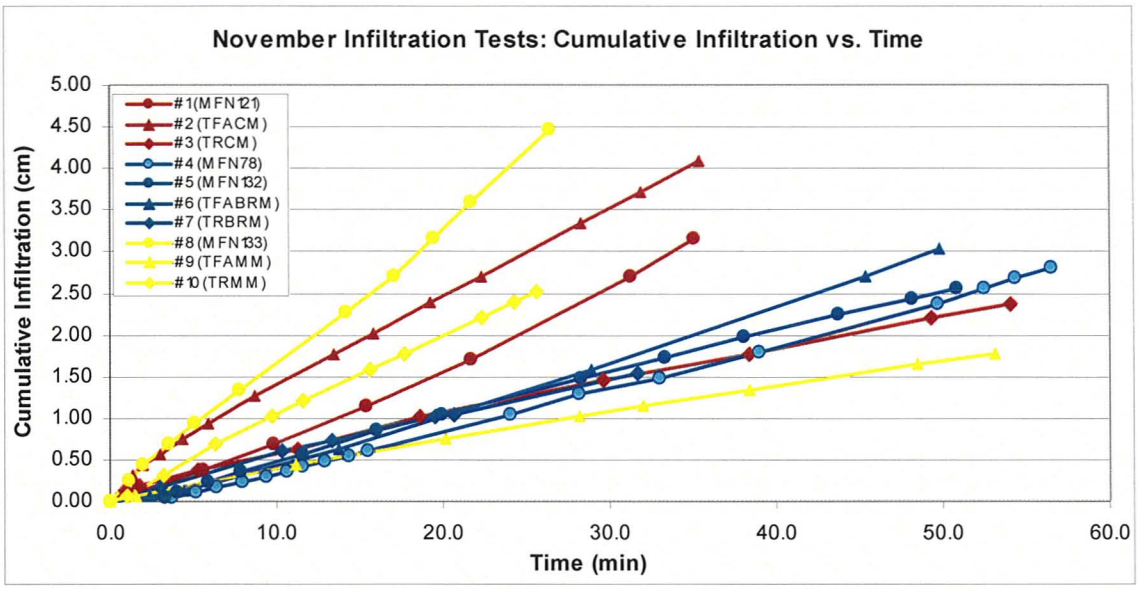

Fig. 4.32 Cumulative Infiltration (cm) vs. Time (min) for November infiltration tests. Blue indicates Char Material (CM) surface, Orange indicates Mixed Material (MM) surface, and Green indicates Brown Material (BRM) surface. Additional symbology: Circle data = Fire Site Low; Triangle data = Fire Site High; Hash Mark data = Transition

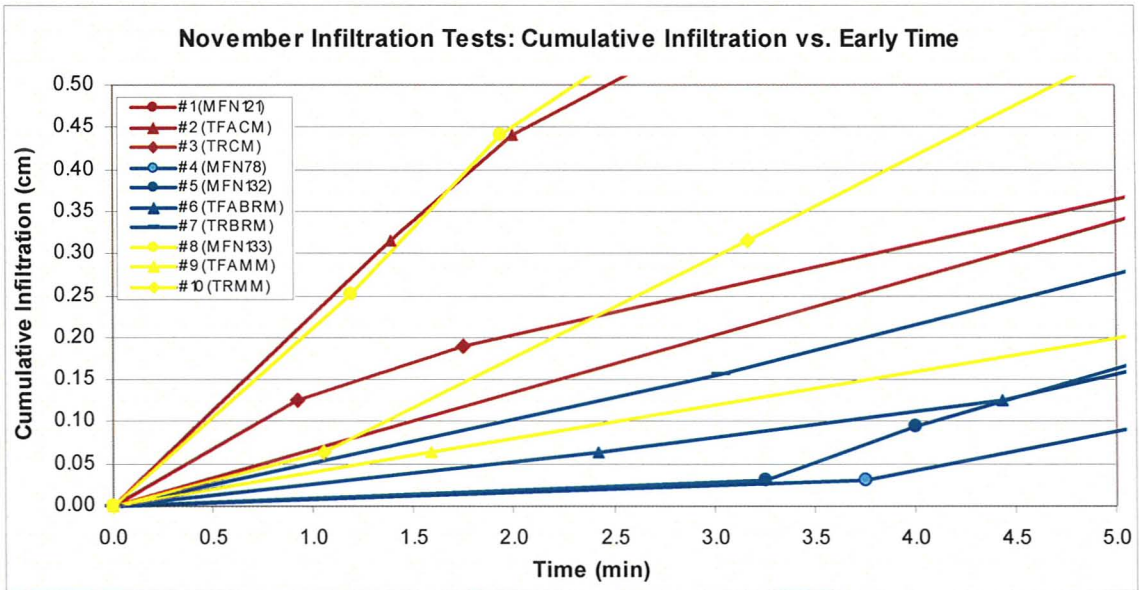

Fig. 4.33 Early time Cumulative Infiltration (cm) vs. Time (min) for November infiltration tests. Blue indicates Char Material (CM) surface, Orange indicates Mixed Material (MM) surface, and Green indicates Brown Material (BRM) surface. Additional symbology: Circle data = Fire Site Low; Triangle data = Fire Site High; Hash Mark data = Transition

The nature of these subsurface materials may not always correlate well with surface material / burn condition. Overall, these data indicate that materials tested in #9 (TFAMM) are more similar to BRM materials than other Mixed Materials.

Infiltration Rate vs. Time for November tests is represented in Fig. 4.34 (for all tests conducted in November). Unlike data from October tests, only two of ten tests in November show the standard infiltration behaviour of wettable materials; where infiltration rates start high and decrease exponentially as soil hydraulic gradients decrease as distance to the wetting front increases. This difference between the two trips may relate to the moisture condition at the surface (i.e. top 0.5 cm) created by the presence of a thawed frozen crust in October and lack of one in November.

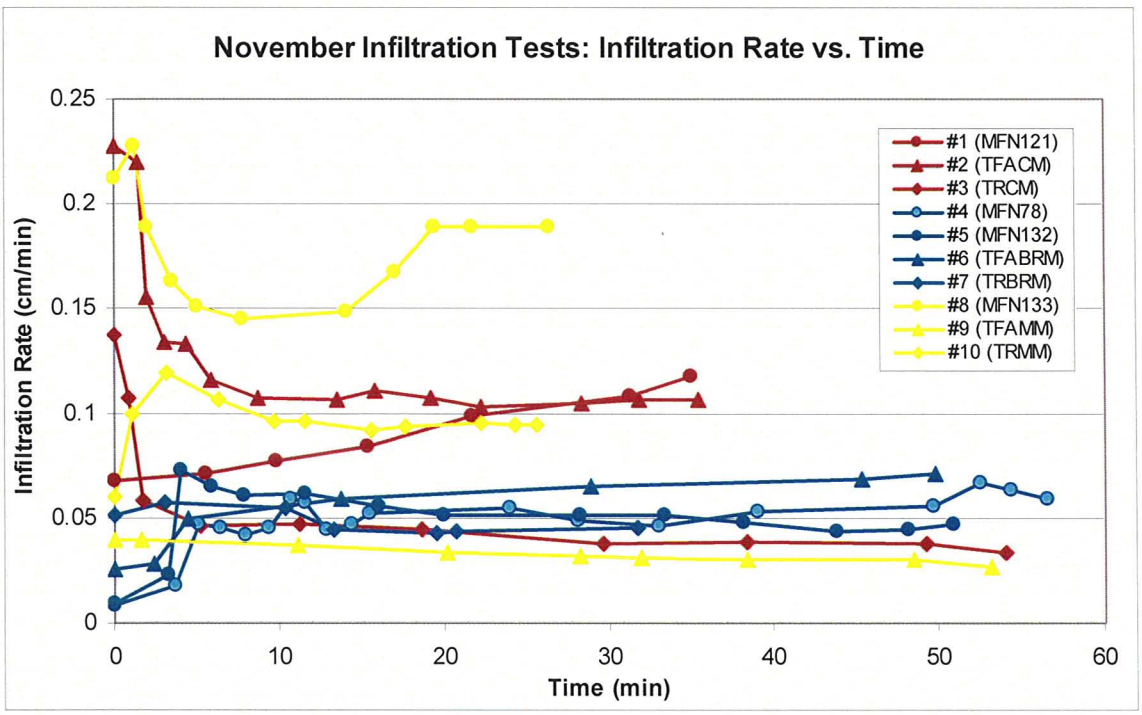

Fig. 4.34 Infiltration Rate (cm/min) vs. Time (min) for November infiltration tests. Blue indicates Char Material (CM) surface, Orange indicates Mixed Material (MM) surface, and Green indicates Brown Material (BRM) surface. Additional symbology: Circle data = Fire Site Low; Triangles data = Fire Site High; Hash Mark data = Transition

Infiltration rate data reveal that hydrophobic behaviour is present in all material types / burn conditions. Brown materials tend to have relatively low infiltration rates regardless of moisture content, and more variable behaviour – particularly in the first 20 minutes of testing. Char materials behave the most wetting of the materials observed here, with higher infiltration rates that drop off within the first 5 minutes of testing. The one exception to this being test #1, which has a slowly steadily increasing infiltration rate for the entirety of the test. Mixed materials exhibit a range of wetting behaviours, including wetting and non-wetting. Overall, Mixed materials behave more similarly to Char materials than Brown materials in infiltration rates and overall response.

While similarities in materials exist between sites, it is difficult to gauge the infiltration response / subsurface conditions based on visual inspection criteria for Char and Mixed materials. Noticeable differences existed in these materials, but the magnitude of infiltration rates was similar in these two materials across all tests. Brown materials on the other hand, were more easily distinguished from Char and/or Mixed materials in terms of visual cues (Fig. 4.2- Fig. 4.4), infiltration response, and time to first bubble. While definitive relationships between burn condition and infiltration response are difficult to draw for these materials, these tests do inform us in a way that drop tests alone are unable to.

Overall, there appears to be a strong relationship to moisture content in both non-wetting and wetting materials, which is not always directly linked to the surface material or water repellency. That is, Char and Mixed materials do not always have higher moisture contents than Brown materials (and vice versa); and all material types / burn conditions exhibit repellency. However, greater proportions of tests exhibit repellent behaviour in the order of Char < Mixed < Brown. For Char and Mixed materials, lower moisture contents tended to result in hydrophilic responses during early time. However, the highest moisture content of these two groups also showed hydrophobic behaviour at the beginning of the test (i.e. #10 (TRMM)). For non-wetting (hydrophobic) materials, increased

moisture contents were associated with higher initial infiltration rates. These results agree with the conclusions of Imeson et al. (1992), Clothier et al. (2003), and Debano, (1975). This indicates that distinct differences exist between lightly / mildly burned materials, and those with more obvious combustion. It also shows that the tension disc infiltrometer method is sensitive to differences in wettability and can be effective in measuring it over more reasonable time periods than other methods (e.g. WDPT) in even relatively wet soils.

Time to first bubble data were presented in Fig. 4.19 (page 114). These data agree well with expectation that more hydrophobic materials (i.e. Brown materials > Mixed Materials > Char Materials) exhibit greater delays to infiltration. The relationship, however, between water repellency as observed in infiltration tests and as observed in time to first bubble data is not always well correlated. It appears that antecedent moisture content of surface materials plays a role in time to first bubble, and that volumetric moisture contents as measured via 20 cm TDR probes are a coarse measure relative to the volume sampled in infiltration tests and not necessarily the best indicator of near-surface (0cm-5cm) moisture conditions.

The longest time to first bubble (TTFB) was observed in materials that had decreasing infiltration rates with time over the long term (i.e. #5 (MFN132)). Most significant is the fact that substantial increases in infiltration rate are observed in more wettable Char materials (#1 (MFN121)); time to first bubble data identify these materials quite easily from other hydrophilic char material tests. If the identification of hydrophobic materials is to be observed in only increases in infiltration rate with time, it might appear as though #1 (MFN121) was more repellent than the Brown materials tested in #5 (MFN132). In conjunction with TTFB data, what becomes obvious is that the repellency of #5 is better expressed at the outset of the infiltration test and in time to first bubble data and the repellency of test #1 is better expressed throughout the duration of the infiltration test. If only TTFB data are considered, the most persistently repellent

surface is that of #5 (MFN132) (with TTFB of >1min). When measures of initial hydrophobic persistence (i.e. TTFB) and infiltration rate data observed over the lengths of tests are combined, valuable infiltration information becomes available and highlights the complex nature of dynamics in these systems. It then seems appropriate when investigating hydrophobic persistence in these dynamic systems to consider the combined behaviours observed in both short (e.g. <5 minutes) and longer time scales (i.e. >20 minutes).

It is hypothesised here that time to first bubble is most sensitive to surface moisture conditions, and less so to overall moisture content (as measured via TDR probes). We recommend that surface moisture content samples be collected at the time of testing. Volumetric moisture contents as measured here, while providing valuable moisture content information, have proven too coarse a measure for the time and spatial scale of tests using the Mini Disc Infiltrometer.

4.6 Summary and Conclusions

In this chapter we report upon *in situ* tests conducted on fire-affected repellent materials approximately 1.5 years post-fire. Water Drop Penetration Time and Volumetric Ethanol Percentage tests were coupled with moisture content data to identify coarse differences in the wettability and temporal dependence of repellence on three different materials / burn conditions within the burn perimeter. Infiltration tests using tension disc infiltrometers captured short term (time to first bubble) and longer term (infiltration ≤1 hour) behaviour of static conditions and dynamic processes in these materials.

We found that time to first bubble as a measure of infiltration initiation was longer in more repellent media indicating that smaller fractions of initially wettable materials existed at the surfaces of these (BRM) materials. This measure was also an indication of the dynamics of contact angle change in surface materials as infiltration would not occur until materials became wettable with prolonged exposure to water (since water was held at the surface under a (constant) negative pressure head). These hydrologic controls (i.e. initial fraction of wettable materials at the surface and contact angle dynamics) are inextricably linked and have a key role in hydrological processes in water repellent media.

Time to first bubble data (TTFB) agree well with expectation that more hydrophobic materials show longer delays in infiltration initiation than wettable materials, but this relationship is complicated by antecedent moisture content and fractional wettability across different tests on the same material type. Further, time to first bubble data did not always relate well to initial infiltration rates indicating that the measure is most relevant to earlier time data – data that is finer than the coarser graduated markings (i.e. 1ml) on the infiltration apparatus. The effectiveness of the measure has not been completely evaluated here, but it holds promise as a tool for the quick identification of repellent media and we agree with Lewis et al. (2006) that it is a more accurate measure of repellency and infiltration initiation than often used WDPT test; particularly where

significant differences in (single) drop infiltration behaviour can affect how hydrophobicity is measured. We have shown here that when coupled with longer term infiltration rate data, one can better assess the relative importance of the measure (see section 4.5.7).

One of the possible sources of error in using the Tension Disc Infiltrometer to determine time to first bubble is in the initial condition set by the operator. This can vary from person to person. As a matter of curiosity, time to first bubble was extended beyond the first drop for one group of tests. In these tests, time to the first 5 bubbles was collected. The advantage of collecting these data is that following the first bubble, the instrument has effectively re-calibrated itself, independent of the operator. Further, in the series of data collected, early time infiltration rate data can be captured, and time to first bubble can be assessed according to these subsequent early time data points without the limitation of the coarse 1ml markings on the apparatus. One amendment to the method would be to time according to the first bubble(s) observed in the bubble tower and collect gravimetric moisture content samples from adjacent material as a complimentary measure. Unlike the tube that is in the reservoir, the tube in the bubble chamber is easily observed and there is no delay between drop detachment and its appearance to the operator. Also, while TDR provide some indication of moisture conditions over the scale of cm's, the scale of the time to first bubble measure as was observed here is quite small and requires a finer measure of moisture conditions.

All materials showed repellency during testing, although Brown materials were the most consistently hydrophobic as observed in increasing infiltration rates and time to first bubble. More variable behaviour was observed in Char and Mixed materials indicating that these materials are more likely to display a range of infiltration behaviours (i.e. both hydrophilic and hydrophobic) between tests. It is apparent from these tests that while surface condition affects the behaviour of subsurface material response to infiltration events, this behaviour cannot be

predicted based on the visual inspection of surface material / burn condition at fire sites.

For *all* materials, infiltration rates are highly dependent on antecedent moisture conditions and the initial wettability of surfaces. While a higher fraction of initially wettable surfaces is well related to an increased initial infiltration rate in all material types, moisture content affects hydrophobic and hydrophilic systems differently. Where high moisture contents reduce initial and overall infiltration rates in hydrophilic systems, high moisture contents in water repellent systems *increase* infiltration.

Water repellent surface materials (i.e. Brown materials) found at Halfway Lake Provincial Park exhibit strong similarities in rates and overall infiltration behaviour that relate well to differences in moisture content. Moisture contents for these materials suggest that for these water repellent materials, increases in moisture content contribute to higher initial infiltration rates. This is in accordance with Huffman et al. (2001) who found that in shallow depths (i.e. 0-6cm), increases in soil moisture best explained decreases in water repellency, even more so than burn severity. Imeson et al. (1992), Clothier et al., (2003) and Imeson et al. (1992) also identified this moisture content – infiltration rate relationship in hydrophobic materials.

Infiltration in hydrophobic materials occurs at rates substantially lower than near-field capacity hydrophilic materials. In contrast to the belief that repellency 'disappears' under some critical moisture content (Doerr et al., 2000), our data indicate that this moisture content–conductivity relationship is complicated by time dependent changes in contact angle and thus, not as simple a relationship as stated. Further, hydrophobicity does not disappear under the time frame observed in infiltration tests. These data suggest that while moisture conditions may play a substantial role in determining the dynamics of these materials, the presence of an increased wettable fraction (i.e. increased surface charring) also largely affects system dynamics by facilitating fluid transport along wettable pore

networks and serving as a more dominant control on infiltration processes (i.e. over system dynamics). When a smaller wettable fraction exists (i.e. as was the case in BRM materials), it is the dynamics of the system that were found to dominate infiltration processes.

We found the tension infiltrometer was a useful tool in discerning differences in hydrophobicity when sufficiently long tests were conducted even in relatively wet soils. Because of the pressure condition (i.e. negative pressure head) applied at the soil surface, changes in wettability due to contact angle dynamics and differences in initial wettability due to fractional wettability can be monitored using the instrument. The apparatus is however limited in the field because of heterogeneity in field hydraulic conductivity and 3D geometrical effects of the expanding wetting bulb. In hydrophobic media, infiltration in 3D can dampen the effects of hydrophobicity on infiltration rates. Only once horizontal gradients are sufficiently small such that repellency has the greater effect on infiltration can infiltration rates reflect the dynamic nature of these systems beyond time to first bubble. Over the durations of some tests, repellency did not appear until 20 minutes of infiltration had occurred. While the 40ml / 40 minute applied limit was the most appropriate balance of practicality and data capture for hydrophobic materials at Halfway Lake Provincial Park, it seems that relevant time scales for hydrophobic media be considered at each site relative to the initial fractional wettability / dynamic contact angle relationship. Given the dynamic and heterogeneous nature of these systems and the variability that exists within them, it is essential that investigations employ techniques and tests that are sensitive to the dynamics (and fractionally wetting component) of these systems and apply *time scales* defined by system properties and not arbitrarily defined standards.

Chapter 5: Fractional Wettability and Contact Angle Dynamics in Water Repellent Porous Media – Conceptual Models

5.1 Introduction

In this chapter, we scale up from the physicochemical level to present a conceptual model that clarifies the roles of fractionally wettable surfaces and dynamic contact angles with respect to wetting in water repellent media. At the physicochemical level, Bayer and Schaumann (2007) and Schaumann et al. (2005) propose that (temporal) differences between water wettable and water repellent materials are controlled by 1) the thickness of the layers of water molecules on hydrophobic materials and 2) heterogeneity in soil surface characteristics. They use a conceptual model to explain the nature of repellency in response to increasing moisture and the physiochemical changes that it elicits in water repellent materials. They examine the role of wetting with respect to conformational changes in polar groups due to increased moisture contents, noting that slow changes in water repellency occur even after constant moisture contents are reached. From this fundamental understanding of physiochemical relationships and behaviours, we present models that explain wetting in water repellent soils at the pore and bulk scales so that the roles of fractional wettability and contact angle dynamics can be better understood relative to more observable hydrologic processes.

5.2 Conceptual Framework for Fractional Wetting and Dynamic Contact Angle Behaviour at the Pore Scale

The following discussion is summarized in Fig. 5.1. Consider a pore that is bordered by both wettable (<90°) and non-wettable soil particles (>90°). For simplicity, in this situation we assume that each particle has a singular surface chemistry and value of contact angle that is either wetting or non-wetting prior to the introduction of water and that the pore space contained within is completely dry. Further, we will consider a pore that is large enough to accommodate both

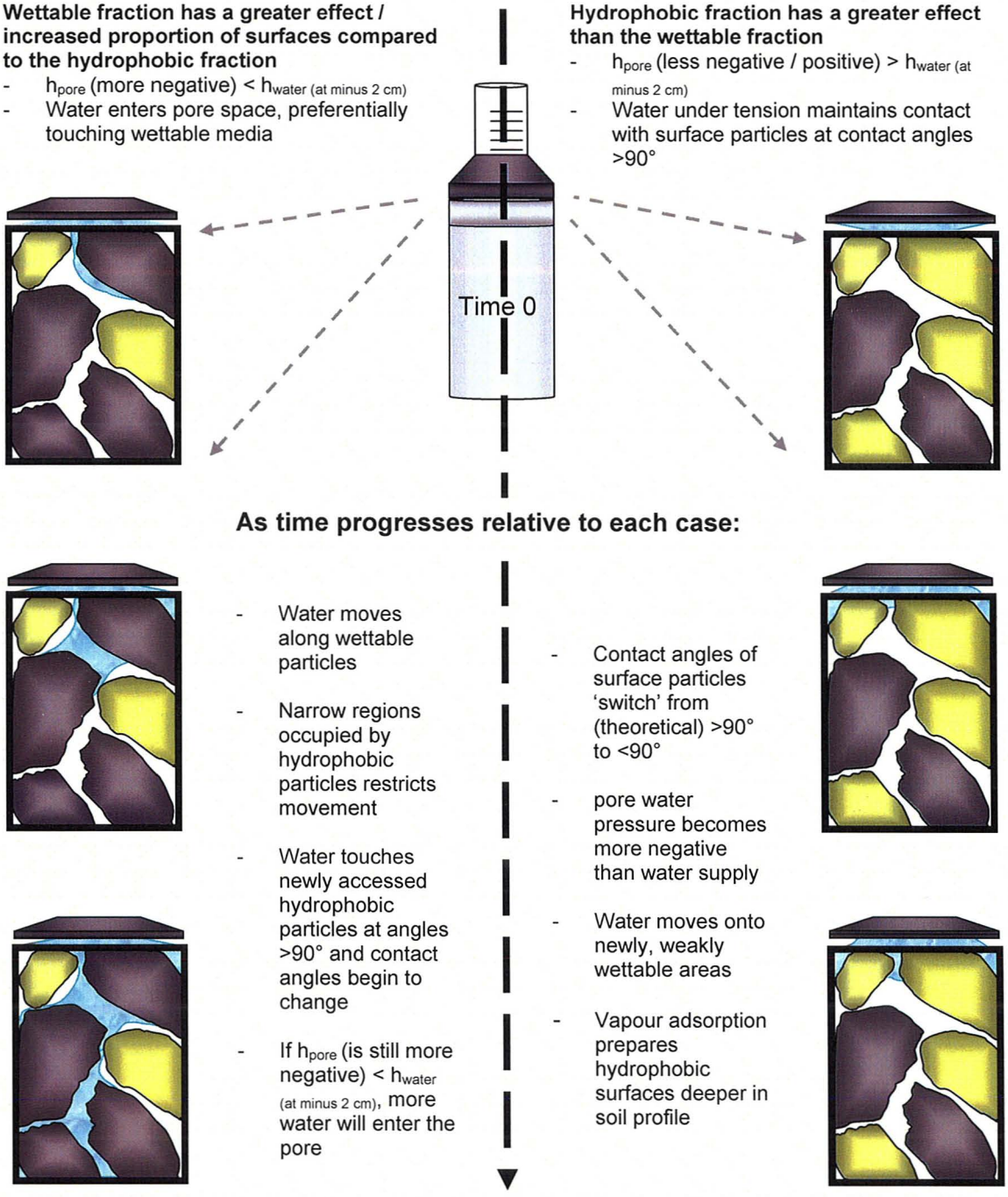

Fig. 5.1 Schematic representation of wetting at the pore scale in variable pores bordered by wettable and hydrophobic particles (i.e. fractionally wetting). Hydrophobic particles have dynamic contact angles with prolonged exposure to water. Yellow particles = initially hydrophobic particles; Grey particles = initially hydrophilic particles.

water and air. Upon the introduction of water supplied at a negative pressure head at the surface of this pore, one of two spontaneous things will occur: water will enter the pore space, or water will remain outside the pore space. In either case water will preferentially touch wettable (<90°) particles. If the overall wettability of the pore space is such that the wettable fraction plays a dominant role either through an increased surface area relative to the non-wettable fraction or that the contact angle effect of the wettable media is sufficiently strong compared to that of the non-wettable particles, the pore will have a sufficiently more negative pressure head condition than the pressure head at which water is being held. Under these conditions, water will enter the pore. Conversely, if the non-wettable fraction is sufficiently strong compared to the wettable fraction in terms of contact angle and/or the surface area of the non-wettable fraction, water will not enter the pore as its pressure head is less negative than the pressure head condition of the infiltrating fluid. The pore pressure head may even be positive, but in both cases (i.e. 'less negative' or 'positive'), water will maintain contact at the surface with whatever fractions of materials are exposed. In the event that the wettable fraction is not exposed at the surface, water will also not enter the pore, but maintain contact with surface materials at some angle greater than (theoretical) 90°.

Under a spontaneous wetting condition (i.e. sorption), capillary pressures will dictate that for a fractionally wettable pore, water entering a pore will preferentially remain in the narrower regions of the pore until fluid pressures are sufficient such that the pore becomes filled. This is consistent with traditional theory describing the distribution of wetting fluids in variable pore spaces (Bear, 1988). However, due to the non-wetting fraction of particles bordering the pore and respective contact angles, there will be an increased resistance to wetting overall (i.e. a less negative pore pressure head); particularly so if non-wetting particles border these narrower regions where water has the greatest tendency to situate. The presence of non-wettable pore walls may even force water into

larger regions of the pore, but this depends on the relationship between the contact angles of water repellent and wettable fractions. In any case, water will adsorb onto wettable materials preferentially. At low (i.e. residual) moisture contents water may only be adsorbed to wettable materials at some maximum (negative) pressure head value (e.g. a minus 2 cm pressure head was applied at the surface in Phase I tests outlined in chapter 3). However, water will come into contact with non-wetting particles should the wettable fraction be able to accommodate greater amounts of water (i.e. the pressure head of the pore is still more negative than the pressure head condition of the water supply). If water remains in narrower regions of the pore that non-wettable particles may be bordering (and not be 'forced' into larger regions due to contact angle effects of the non-wetting fraction), it is without question that water will contact the non-wetting fraction at contact angles <180°. Flow of water *between* fractionally wettable pores will also be governed by these same capillary conditions.

For non-wetting pores where water is held at the surface under tension, increased exposure of water repellent materials to water will contribute to the conformational changes described by Bayer and Schaumann (2007). These changes may contribute to changes in contact angle with time (Diehl and Schaumann, 2007), or put another way, may lead to the breakdown of repellency over time (Doerr et al., 2000; Clothier et al., 2000). While water may not enter the pore for some time, changes in contact angle will occur as time of contact with water increases for these surface materials. The rate of change is largely dependent on the origin of repellency of non-wettable materials and the resistance of surface chemistries and physical properties to surface energy changes with increased exposure to water (Diehl and Schaumann, 2007). Further, the resistance to change is also related to the actual measure of repellency. It may be expected that a high contact angle hydrophobic material will take longer to reach a wetting angle than a low contact angle hydrophobic material. However, the *rate* of contact angle change ultimately dictates the time

at which materials become wetting. So, a high contact angle hydrophobic material that is less resistant to change (i.e. has a fast rate of change) can become wetting before a low contact angle hydrophobic material that is more resistant to change. This has profound implications on the distribution of water in pore spaces since changes in contact angle during infiltration are magnified by the size of the infiltrating region of a pore. This type of non-correlated relationship between the actual measure of contact angles (e.g. Molarity of Ethanol tests) and the rate of change of contact angles (e.g. Water Drop Penetration Time tests) has been expressed in other investigations (Doerr et al., 2005; Doerr and Thomas, 2003).

Only once completely non-wetting surface materials reach wetting contact angles and/or the surface tension of the infiltrating fluid decreases substantially, will water begin to enter the hydrophobic pore. However, due to vapour adsorption, new material onto which water can move will be 'prepared' differently than in the former case where the pore was completely dry. When water does begin to enter the pore, the same aging process will have to occur for newly accessed materials before water moves 'freely' into the pore space. Upon entry into the pore space however, in contrast to the assumption made by many that water will enter larger areas, water will *only* go into those regions if narrow regions remain completely non-wetting. Even if only weakly wetting, water will still preferentially move to narrow regions within a pore when water is held under tension as formulated in traditional theory by eq. 3.2. However, larger areas of pores may inadvertently become weakly wetting prior to narrow regions based solely on proximity to accessible amounts of water and differing rates of contact angle change. This conceptually extends to differences in a bulk media where changes in contact angles elicit greater (for small pores) or lesser (for large pores) changes in capillary response due to differences in pore sizes. Considering two identical but differently size pore spaces that change contact angles at the same rate, upon transition from a wetting to non-wetting pore (i.e.

contact angles switch from >90° to <90°), the smaller pore will have the greater negative pressure head due entirely to its effective radius. This means that the presence of a wettable fraction in a porous medium with dynamic contact angles can play a significant role in the determination of wetting rates and the distribution of water in pore spaces, particularly at the onset of an infiltration event (i.e. because rates are contingent upon the availability of water as facilitated by the wettable fraction (Bachmann et al., 2007) *in addition to* contact angle dynamics and effective pore sizes).

5.3 Conceptual Model of Fractional Wetting and Contact Angle Dynamics in Bulk Media

Here we extend dynamic-fractional wetting concepts at the pore scale to the scale of observation and influence measured in infiltration tests. The following images depict fractionally dynamic wetting through hydrophobic organic layers (i.e. Brown materials) and breakthrough into subsurface (B Horizon) hydrophilic media throughout tests (Fig. 5.2 – Fig. 5.4). It can be seen in these images that small scale pathways develop over the course of infiltration in organic layers. Here, we present three mechanisms by which this occurs: 1) wettable materials facilitate the transport of water to non-wettable materials through wettable pore networks 2) compounds that lower the surface tension of infiltrating water are dissolved during infiltration through wettable media such that water delivered to deeper hydrophobic materials has a lower surface tension compared to that of the original infiltrating fluid and 3) sufficiently small wettable materials may dissolve into infiltrating water and become translocated to deeper regions the soil profile. These do not take into account the role of heating in the chemical alteration of hydrophobic surfaces i.e. materials showing higher contact angles may change contact angle more readily than lower (hydrophobic) contact angle materials that were heated less. Increases in storage occur throughout tests and are expressed as a darkening and expansion of these wetted areas. As the test progresses, the lateral expansion of distributed wetting perturbations can be

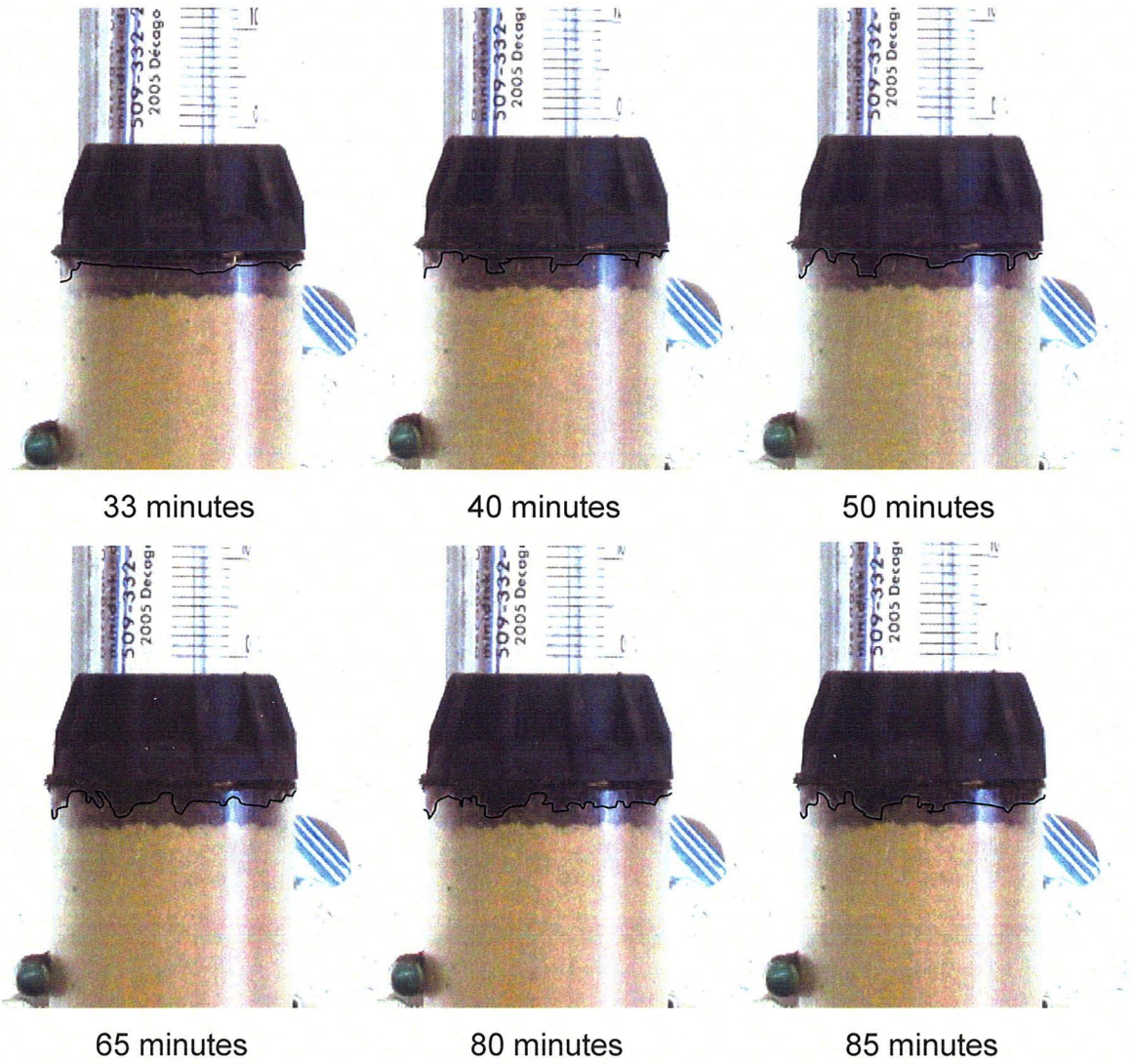

Fig. 5.2 Wettable pore network development in hydrophobic organic materials during 1D (Phase I) column experiment (30-90 minutes). Images correspond to Brown over Mineral (BOM4) and show hydrophilic B Horizon mineral soil overlain by hydrophobic organic cap material. Increases in storage indicated by widening and darkening of wet (organic) areas and highlighted with a black line.

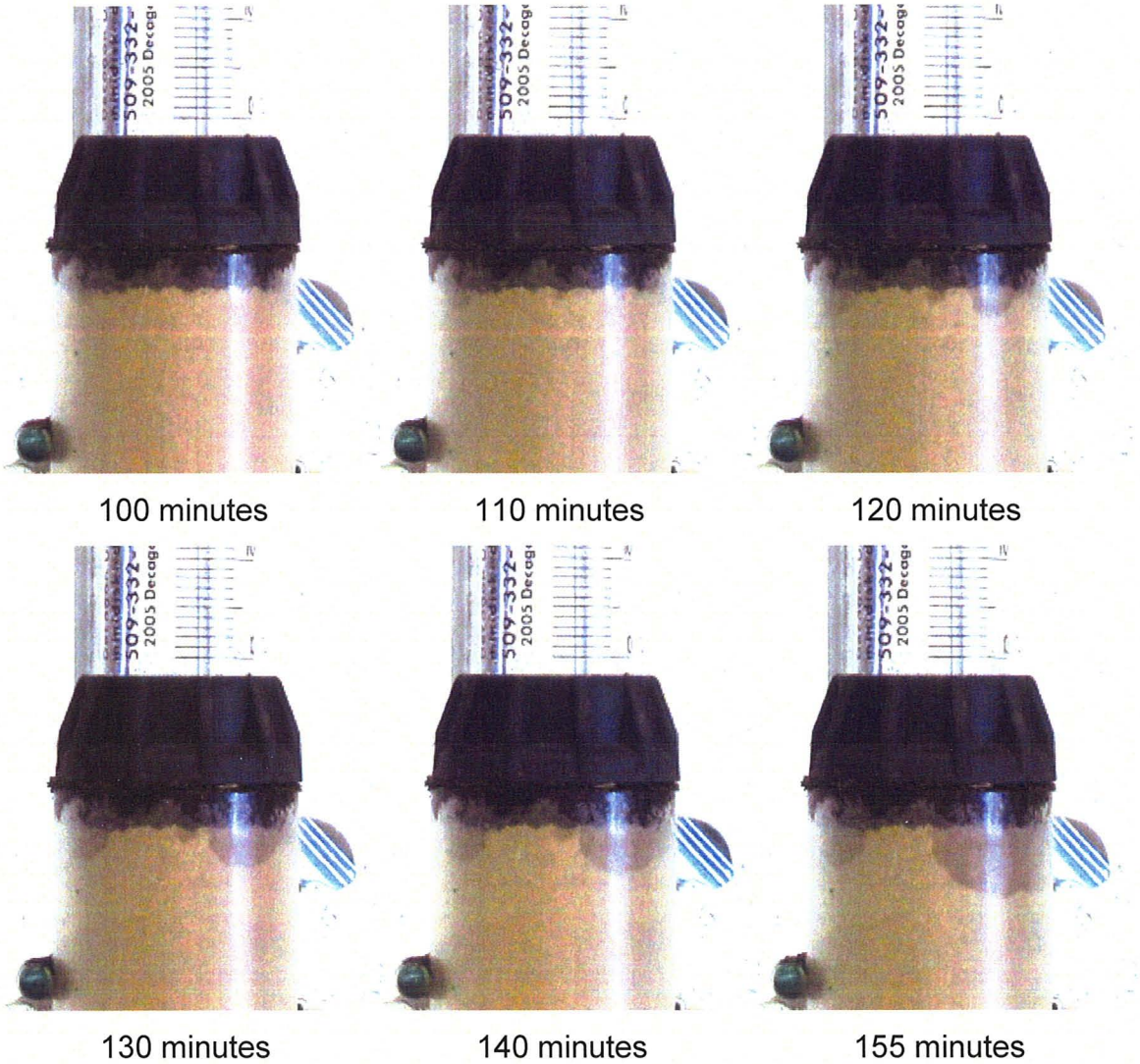

Fig. 5.3 Wettable pore network development in hydrophobic organic materials during 1D (Phase I) column experiment (90-160 minutes). Images correspond to Brown over Mineral (BOM4) and show hydrophilic B Horizon mineral soil overlain by hydrophobic organic cap material. Increases in storage indicated by widening and darkening of wet (organic) areas.

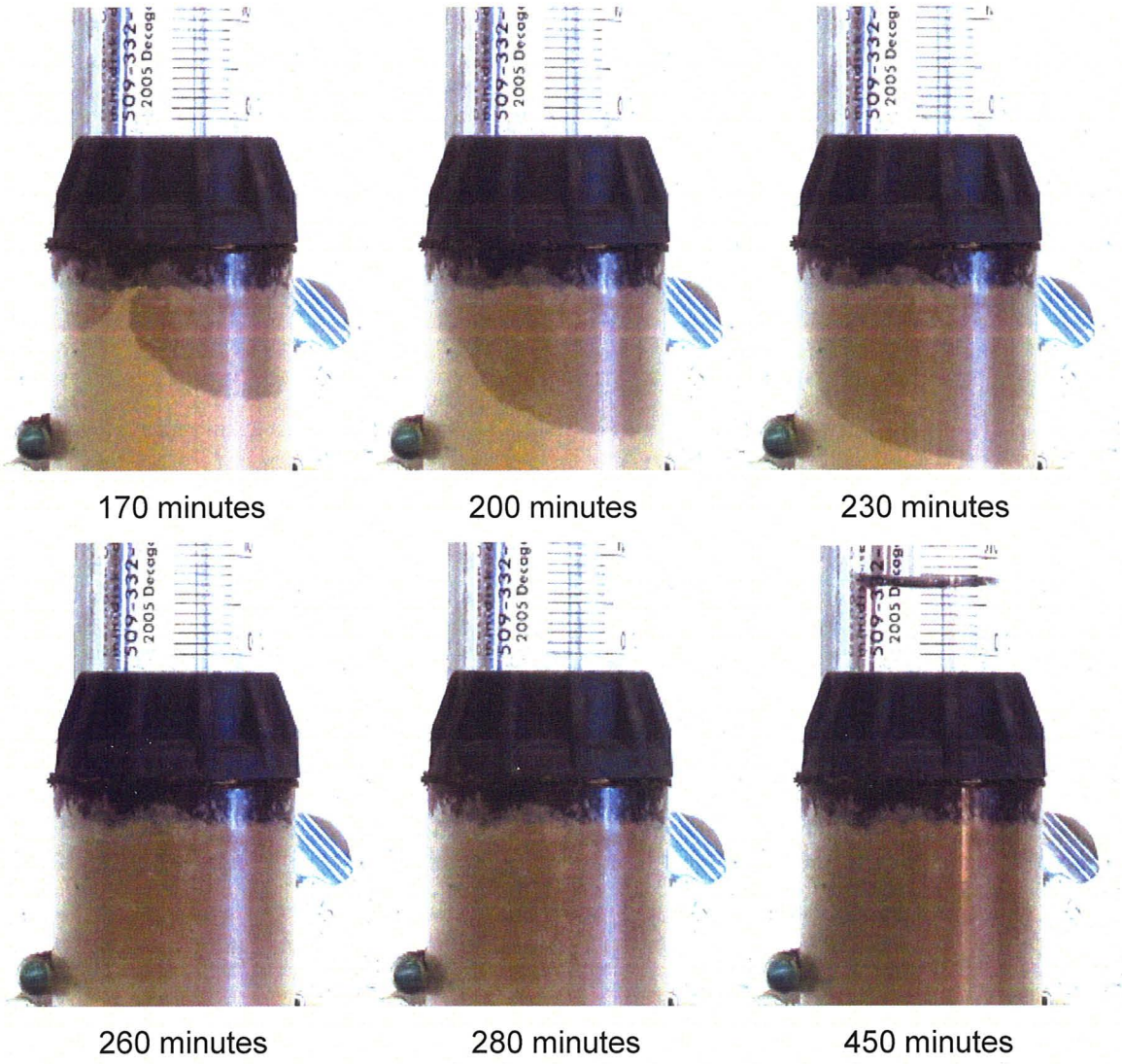

Fig. 5.4 Wettable pore network development in hydrophobic organic materials during 1D (Phase I) column experiment (160-460 minutes). Images correspond to Brown over Mineral (BOM4) and show hydrophilic B Horizon mineral soil overlain by hydrophobic organic cap material. Increases in storage indicated by widening and darkening of wet (organic) areas.

seen in the organic material, even after breakthrough into underlying hydrophilic B Horizon materials. From these observations it appears that while preferential flow paths develop in these materials along wettable pore networks, time dependent changes in contact angle via increased moisture contents contribute to changes in the delivery of water through these flow paths, *and* through adjacent areas. Further, 'new' weakly wettable fractions that were once hydrophobic can now participate in infiltration and contribute to changes in contact angle in adjacent materials at later time by providing access routes for water to travel and make contact with fresh non-wettable surfaces. For these materials, preferential flow does not appear to persist on the scale (centimetres) and durations (minutes, hours) of column experiments carried out here.

The process of wetting and the relationship between increased moisture contents and increased infiltration rates with time are presented in the following conceptual model (Fig. 5.5). In case A, we consider media where contact angle dynamics are significantly more influential on changes in overall system response than the *initially* wettable fraction. Respective of the materials investigated here, these materials have lower hydrophobic contact angles (e.g. 90-100°), but a higher fraction of hydrophobic particles (e.g. lower variability and standard deviation in contact angle measures). While water is held under a constant negative pressure head, initially, a small wettable fraction found at the surface (i.e. 0-0.1cm depth) contributes to the sorption of water into surface (wettable) materials (i.e. has a more-negative pore water pressure head than the water being held under tension at the surface). This elicits movement *along* the pore water pressure head curve (i.e. case A: from CI0 to CI1). Following the resultant initial decrease in infiltration rate due to the wetting up of the small portion of initially wettable particles at the surface, no changes in infiltration rate are observed. We gather that at this time changes (increases) in infiltration rate are proportionally equal to or less than the effect of a decreasing gradient caused by the slow advance of the discontinuous wetting 'front'. However, the supply of

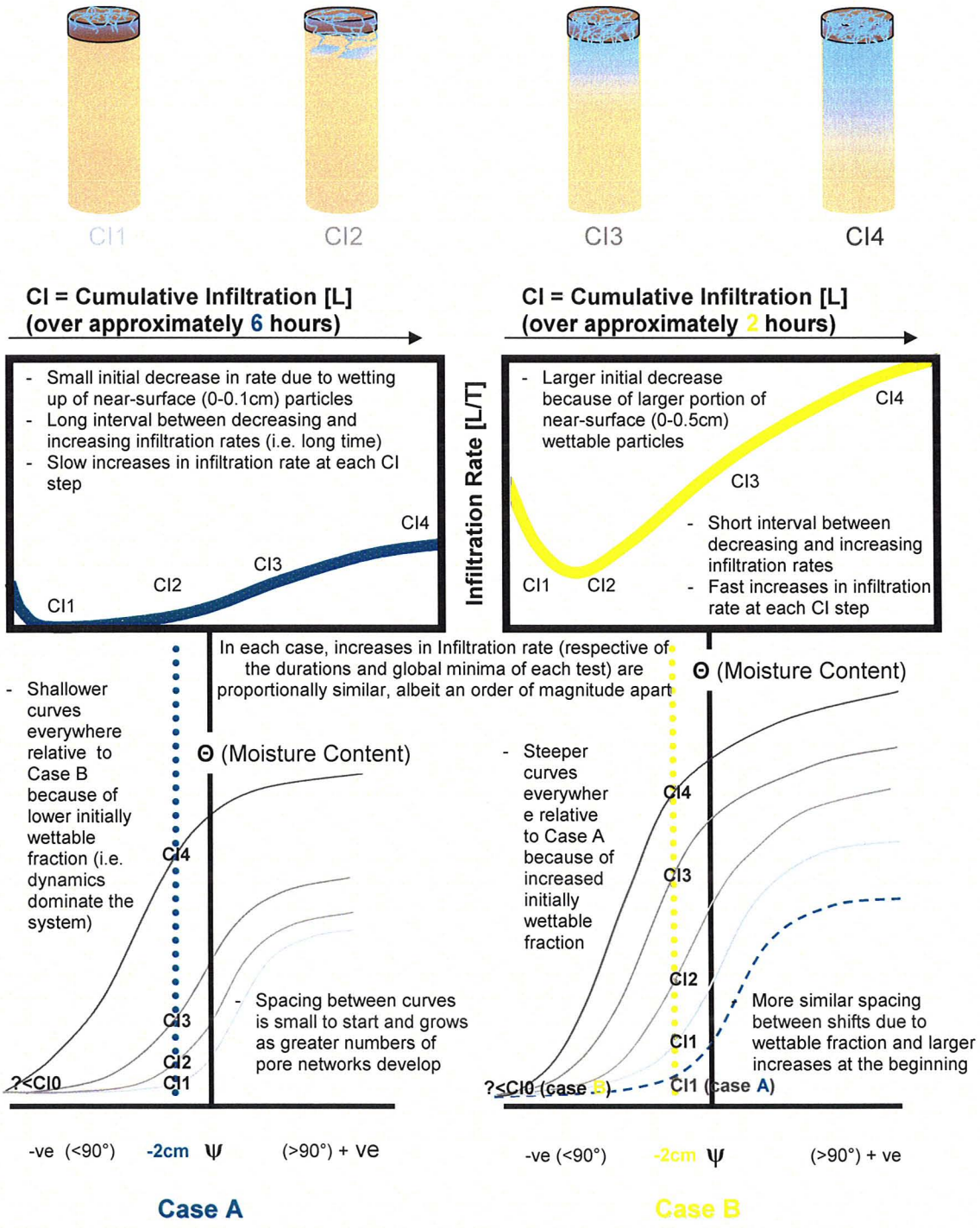

Fig. 5.5 Conceptual model of fractional wetting and dynamic contact angle change in two different cases. Case A (green) describes a system with a small (initially) wettable fraction such that the role of contact angle change is the dominant process throughout an infiltration event. Case B (yellow) describes a system with a large (initially) wettable fraction such that the role of fractional wettability is the dominant control on infiltration.

water contributes to contact angle changes in subsurface water repellent materials which consequently contribute to small increases in moisture content with time. As time progresses, variable pore networks grow towards subsurface B Horizon hydrophilic mineral materials (i.e. deeper into the soil profile) as a result of changing contact angles in overlying organic hydrophobic materials at the pore scale. At this time, contact angles in the (organic) hydrophobic porous media are continually decreasing which *shifts* the capillary – pressure head relationship as shown by Bradford et al. (1997) in proportion to $\cos(\theta)$ (as found by Arye et al. (2007)). These continual decreases in contact angle also affect the fractional wettability of the bulk media such that greater fractions of the bulk media are becoming more wettable. In this system, the proportion of wettable materials is ever increasing, but the wettability of new weakly-wettable materials is also increasing.

At breakthrough into subsurface hydrophilic materials (case A: CI2), infiltration rates begin to increase noticeably. At this particular breakthrough point, changes in the wettability of adjacent materials occur, ever increasing the rate of delivery to hydrophilic subsurface mineral B Horizon materials from this entry point. However, at the same time, additional points of entry into subsurface hydrophilic B materials develop as moisture contents increase in hydrophobic materials; this also contributes to an increasing infiltration rate. Throughout, shifts in the pore water pressure head relationship occur as moisture contents increase. When the pressure head condition is held constant at the surface, increases in moisture content following early times can essentially only be attributed to shifts in pore water pressure head curves, and not to movement along curves caused by changes in the pressure head condition at the surface. At later time, the wetting front is evenly distributed around (across) the column at some depth (case A: CI3). At this point, no further increases should be observed in infiltration rate if a static wettable fraction was affecting infiltration since rates are being increasingly dampened as gradients approach 1 (i.e. $dh/dz \rightarrow 1$) and

wetting is now evenly distributed in the hydrophilic B Horizon material. However, increases in infiltration rate still occur even after this point. This can only be attributed to dynamic contact angles and the increasing fraction of wettable materials that are becoming more wettable with prolonged exposure to water.

In case B, we consider media where the initial wettable fraction is *much* more influential on contact angle dynamics and system response. Relative to the materials discussed previously (case A), consider hydrophilic mineral B Horizon materials overlain by hydrophobic organic materials that consist of a larger fraction of wettable materials at the surface (e.g. 0-0.5cm), and with higher contact angle hydrophobic materials (e.g. CA=115-130°) subsurface. Overall, the conceptual model behaves similarly in case B to case A, except that fractional wettability changes the nature of the shifting pore water pressure head relationship in an infiltration event. Similar to case A, an initial decrease in infiltration rate can be attributed to the sorption of water in hydrophilic surface media, or movement *along* an initial capillary-pressure head curve (i.e. case B: from CI0 to CI1). Since there is a greater fraction of wettable materials at the surface (compared to case A), it might be expected that movement along the curve will be the same, albeit the trajectory of the curves will be different in the two cases. Many authors have identified that differences in the initial position and shape of saturation curves existed between materials with increased non-wettable fractions using synthetically hydrophobised granular materials (e.g. Bradford et al., 1997; Hwang et al., 2006; O'Carroll et al., 2005; Bachman et al., 2007). In relation to what is being presented in this conceptual model, for materials with increased fractions of wettable materials (i.e. case B), we could expect the initial position of the pore water pressure head curve to be above the curve of a material with a smaller wettable fraction material (e.g. case A) (i.e. comparing green dashed of theoretical case A line to initial grey line of case B in Fig. 5.5). The position of the curve in case B, however, will depend on the relative influence of 1) the proportion of wettable surfaces *and* 2) the initial

magnitude of contact angles in hydrophobic media. This is in contrast to case A where bulk media contact angles largely governed the initial position of the capillary-pressure head relationship and fractional wettability *influenced* its position.

In case B, the rate of supply (under the same pressure head condition) is much quicker than in case A, but the overall response of the system is not as dependent on the supply since 1) supply is not being restricted and 2) the greater fraction of wettable particles facilitates transport through wettable pore networks without the requisite of changing contact angles. The first case may appear as somewhat of a self referential statement, but for hydrophobic materials whose rates of contact angle change are largely dependent on the thickness of the film of water, when water is freely available, rates are then only subject to the (temporal constraints of the) physicochemical structure of solid surfaces. In the previous case (i.e. case A), these factors (i.e. changing contact angles, moisture content, and supply) were inextricably linked to one another because moisture content governed contact angle dynamics and contact angle dynamics governed supply. In this case however, the rate of supply is less associated with moisture content (and contact angle dynamics) because there is an increased wettable fraction that does not need to wet-up and undergo contact angle changes in order to transmit water. This means that water gets to non-wettable regions more quickly and that contact angle changes are accelerated in those regions (because water is more freely available).

As a result of these effects, wettable pore networks develop more quickly such that much shorter time intervals are required before 1) infiltration rates quickly rebound and begin to increase steeply 2) there are steep increases in moisture content and 3) breakthrough into underlying hydrophilic mineral B Horizon materials occurs (CI2). The rate of rebound will be substantially quicker than in the previous case because wettable pore networks across the entire medium are developing in quick succession and breaking through into hydrophilic

mineral (B Horizon) materials. Similar to the previous case (A), entry points and materials adjacent to entry points are undergoing changes in contact angle with time, albeit at a much faster rate. This means that the capillary-pressure head curve of case B is shifting (in proportion to $\cos(\theta)$) more quickly as contact angles change more readily. It is possible the increased influence of the initially wettable fraction amplifies the magnitude of these shifts; which is why increases in infiltration rate occur faster in these materials.

Similar to case A, infiltration rates continue to increase at later time, even when the wetting front is evenly distributed in the hydrophilic B Horizon material and (presumably) infiltration rates are dampened by a hydraulic gradient approaching 1 (CI3). It should be noted that these increases in infiltration rate would not be observed in normal, wettable soils which exhibit *decreasing* infiltration rates under similar soil layer geometries (Hillel, 1982). While the initially wettable fraction of materials has a dominant role in this system, contact angle dynamics are still an integral component of the overall response of hydrophobic and weakly wetting materials. At some point, however, the initially wettable fraction will no longer continue to dominate the system (i.e. when all pores are at least weakly wettable, albeit not completely saturated). When this occurs, the system will continue to change *only* according to changes in contact angle; shifts will reflect this in much smaller distances between subsequent curves as time progresses (e.g. CI4).

5.4 Conceptual Model – Conclusions

In this chapter we presented pore scale and bulk scale conceptual models to facilitate better understanding of infiltration processes in fractionally wetting and dynamically changing water repellent media. The temporal changes represented in each of the model scenarios explain increasing infiltration rates with time with respect to the concerted roles of fractional wettability and dynamic contact angles. Considering either fractional wettability or dynamic contact angles alone is insufficient to explain hydrologic processes in these systems. We assert that the complex interplay between the relative fraction of wettable and non-wettable materials and how those proportions shift over time with dynamic contact angles is the fundamental nature of these systems. The unique instrumentation and investigative approach presented in this thesis facilitated the systematic observance of this complex relationship and its affect on infiltration. This provided the means to develop sufficient system insight and understanding to generate this conceptual model which provides a strong foundation for understanding hydrologic processes in these hydrophobic materials.

Chapter 6: Conclusions and Contributions

6.1 Conclusions

Contact angle measurements and lab and field infiltration experiments on hydrophobic media provided new insights into the concerted roles of fractional wetting and dynamic contact angles in naturally occurring water repellent materials. Fractionally wettable surfaces were identified in the initial advancing contact angles of hydrophobic and hydrophilic materials using Axisymmetric Drop Shape Analysis. In both hydrophilic and hydrophobic materials, wetting (<90°) and non-wetting (>90°) angles were observed. A sufficiently large number of measures allowed us to generate a number of statistics that facilitated a more reliable characterization of these materials with respect to existing theory and determine that variable amounts of hydrophilic and hydrophobic surfaces existed in both (bulk) wetting and non-wetting materials. We further identified that the fractional wettability identified in these measures had a substantial impact on temporal wetting processes in these hydrophobic materials during infiltration.

Through visual observations and systematic measures using tension infiltrometers and volumetric moisture content in water infiltration experiments, we conclude that fractional wetting is a primary control on dynamic wetting and contact angle change in these materials. We concluded that differences in *fractional wettability* between hydrophobic materials are best reflected in the overall magnitudes of infiltration rates. In contrast, *contact angle related changes* (i.e. dynamic contact angles) are best reflected in the rate of change of infiltration rates (i.e. delay to observed increases) at later times when less heterogeneous materials deeper in the soil profile are accessed by the wetting front. We found that more fractionally wettable materials (i.e. materials with the greatest variability in CA measures / those that cross the 90° threshold) experienced greater overall infiltration rates *and* rates of change in contact angles as expressed in tension disc infiltration experiments. We therefore conclude that an increased portion of wettable materials in overlying materials can not only influence, but accelerate

the rate of wetting in underlying hydrophobic materials. This highlights the complexity of these systems and the interplay between complimentary controls on wetting in hydrophobic media. In systems that exhibit greater fractional wettability, infiltration rates appear largely governed by fractional wettability. Where a smaller fraction of wettable particles exists, moisture content requirements are much higher before increases in infiltration rates happen; in these instances contact angle dynamics appears to be the rate limiting mechanism. The implications of this finding are quite substantial for systems where a wettable hydrophilic layer is often found above a hydrophobic layer (e.g. Debano, 2003; Doerr et al., 2006; Martin and Moody, 2001).

Under field conditions, many of these relationships are muted and convoluted by the geometry of divergent flow from tension infiltrometers and the natural variability in field moisture conditions. However, the tension infiltrometer holds promise as a reliable tool in the identification and characterization of water repellent media since it is sensitive to changes in wettability over temporal and spatial scales more applicable to infiltration events. Because water is held under tension, it is a requisite that the system 'switch' from the hydrophobic to the hydrophilic state before infiltration occurs. The tension disc infiltrometer can measure the onset of infiltration caused by even a small fraction of wettable material or by the dynamic change in wettability with time. The ability of the tension disc infiltrometer to more sensitively measure the initial and eventual behaviour of infiltration rates in the presence of dynamic contact angles and fractionally wettable media distinguishes it from other methodologies that mute these system dependencies; thus providing valuable insight into hydrophobic system behaviours when used in sufficiently long infiltration tests.

6.2 Contributions and Recommendations

In this study, a number of systematic and complimentary investigations provided the foundation upon which we came to better understand and explain the *combined* roles of fractional wetting and contact angle dynamics in naturally occurring hydrophobic soils. Since these two variables are often studied separately and without thorough explanation, the unique approach we took gave us better insight into the essence of these systems which allowed us to better explain temporal processes in these systems. While it has been suggested that certain measures (i.e. Critical Surface Tension test) provide the most consistent measures of hydrophobicity (Scott, 2003), we find that longer term system behaviour does not always relate to the magnitude of initial contact angles measures i.e. higher hydrophobic initial contact angle materials had *faster* rates of change than lower hydrophobic (initial) contact angle materials and thereby exhibited faster infiltration rates over periods of minutes to hours. The reliability of initial contact angle and dynamic contact angle measures is complicated by scalar dependencies related to fractional wettability. We suspect that fractional wettability is likely to be the rule rather than the exception in water repellent systems. In accordance with these insights, we recommend that measures of both initial contact angles and temporal changes in wetting are captured across 1) pertinent spatial scales (i.e. mm to cm) and 2) pertinent time scales (i.e. 10's minutes to hours). While the spatial scale of measure is largely defined by the apparatus used and intent of research, time scales should be defined by system properties. Even though arbitrarily defined (yet pragmatic) temporal scales may be more convenient, the fundamental expression of repellency-affected hydrologic processes only becomes apparent in sufficiently long duration tests. Further, we conclude that it is advisable in future research that 1) fractional wettability is considered and evaluated with respect to its role in system behaviour during testing and 2) complimentary measures of hydrophobicity be

captured since initial contact angles do not always relate to the rate of contact angle change (i.e. temporal dependence).

We found with a large number of measurements Axisymmetric Drop Shape Analysis on apparent advancing contact angles to be a useful and consistent measure of initial advancing contact angle on post-fire organic soil materials. In contrast to other methodologies, ADSA is able to measure contact angles on new surfaces using water and without the temporal limitations of other methods such as the capillary rise method. The level of insight gained from this technique is directly related to the statistically informative number of measures captured and the number of materials tested; the insights we gained were possible because of the large number of measurements taken. Until a more comprehensive understanding of contact angles (in general) develops, we recommend that multiple (i.e. greater than 20) measures be taken on samples so that more informative statistics and relationships can be drawn within and between materials.

The tension infiltrometer is a useful instrument in the measure of temporal changes in water repellency. In time to first bubble measures, the initial condition of the apparatus appeared to affect measures, but provided coarse differences between materials. For future research, it might prove useful to measure time to first bubble, *and* time to additional bubbles (i.e. 5 bubbles). Following the initial calibration done by the user, the instrument would provide standardized measures of early time infiltration since bubble rate is related to the flow rate.

We found that in 1D, the tension infiltrometer is a useful tool that can be used to discern differences in materials with different degrees of fractional wettability and differences in contact angle dynamics. In 3D field applications, measures from the tension disc infiltrometer are affected by field heterogeneity and geometry of the wetting bulb. While the apparatus was able to provide insight in field systems, the greatest amount of insight, and the greatest hydrophobic distinction between materials was found in systematic laboratory

experiments using natural material configurations that mimicked the field system. When the tension disc infiltrometer is to be used in the field on hydrophobic materials, we suggest that moisture content information is collected relevant to the wetting bulb area. Based on our observations, gravimetric moisture content is a simple and effective way to capture this information.

The limits of the tension disc infiltrometer are reached towards the ends of tests, which are largely defined by the capacity of the reservoir. For hydrophobic soil investigations, the development of a small disc-large capacity infiltrometer would prove to be a useful instrument. While we can estimate the behaviour of hydrophobic materials towards the ends of tests, we found that infiltration behaviour was still changing in these materials up to the point of cessation. The ends of tests in the lab were only defined by the capacity of the infiltrometer and not arbitrary time limits. Further, we found that repellency (fractional wettability and contact angle dynamics) never 'disappeared' in these materials (Doerr et al., 2000) and continued to affect infiltration rates over longer periods. In order to quantify the nature of infiltration up to this point (for these materials), an apparatus that can accommodate its measure over even longer periods must be developed.

While hydrophobic systems may be complex, we have presented a robust and systematic approach to studying these systems. Through this approach, we have identified and quantified key controls in hydrologic processes and have also developed more completely our conceptual understanding of moisture distribution and transport in hydrophobic media that are fractionally wetting and dynamically changing. We anticipate that the reliance on drop tests (i.e WDPT and CST) may not change in future research, but we do hope that the understanding provided here will contextualize the limited information that these tests provide and encourage future research to consider alternative methods to understanding hydrological processes and their associated implications. While the ideas of fractionally wettability and dynamic contact angles are commonly

mentioned, and their presence in hydrophobic media is often recognized, until now these two interrelated controls have not been evaluated together and respective of each other, nor have they been evaluated in naturally occurring repellent media. The information provided in this study addresses more thoroughly and systematically these “old” ideas, but more importantly presents a new way of looking at and understanding these systems that is more applicable for *many* different hydrophobic scenarios. From this fundamental understanding of these systems, we hope that land managers, agriculturists, and researchers are better able to assess, understand, and ameliorate repellency in natural systems.

Works Cited

Al-Futaisi, A. and T.W. Patzek. 2004. *Secondary Imbibition in NAPL-Invaded Mixed-Wet Systems.* Journal of Contaminant Hydrology 74:61-81.

Ankeny, D.M., M. Ahmed, T.C. Kaspar, and R. Horton. 1991. *Simple Field Method for Determining Unsaturated Hydraulic Conductivity.* Soil Science Society of America Journal 55:467-470.

(Arye) Gilboa, J. Bachman, SK. Woche, Y. Chen. 2006. *Applicability of Interfacial Theories of Surface Tension to Water-Repellent Soils.* Soil Science Society of America Journal 70:1417-1429.

Arye, G., I. Nadav, and Y. Chen. 2007. *Short-term Reestablishment of Soil Water Repellency after Wetting: Effect on Capillary Pressure-Saturation Relationship.* Soil Science Society of America Journal 71:692-702.

Bachmann, J., A. Ellies, and K.H. Hartge. 2000. *Development and Application of a New Sessile Drop Contact Angle Method to Assess Soil Water Repellency.* Journal of Hydrology 231-232:66-75.

Bachmann, J., S.K. Woche, M.-O. Goebel., M.B. Kirkham, and R. Horton. 2003. *Extended Methodology for Determining Wetting Properties of Porous Media.* Water Resources Research 39(12)1353-SBH11:1-14.

Bachmann, J., G. Arye, M. Deurer, S.K. Woche, . Horton, KH hartge, Y. Chen. 2006. *Universality of a Surface Tension-Contact Angle Relation for Hydrophobic Soils of Different Texture.* Journal of Plant Nutrition and Soil Science 169:745-753.

Bachmann, J., M. Deurer, and G. Arye. 2007. *Modeling Water Movement in Heterogeneous Water-Repellent Soil: 1. Development of a Contact Angle-Dependent Water-Retention Model.* Vadose Zone Journal 6:436-445.

Bayer, J. and G. Schaumann. 2007. *Development of Soil Water Repellency in the Course of ilsothermal Drying and Upon pH Changes in Two Urban Soils.* Hydrological Processes 21:2266-2275.

Bauters, T.W.J., T.S. Steenhuis, D.A. DiCarlo, J.L. Nieber, L.W. Dekker, C.J. Ritsema, J. Parlange and R. Haverkamp. 2003. *Physics of Water Repellent Soils.* In: Soil Water Repellency: Occurrence, Consequences, and Amelioration. Eds: C.j. Ritsema and L.W. Dekker. Elsevier. Wageningen, Netherlands.

Bear, J. 1988. *Dynamics of Fluids in Porous Media.* American Elsevier Publishing Company, Inc. Mineola, N.Y.

Bens, O., N.A. Wahl, H. Fische, and R.F. Huttl. 2007. *Water Infiltration and Hydraulic Conductivity in Sandy Cambisols: Impacts of Forest Transformation on Soil Hydrological Properties.* European Journal of Forest Research 126:101-109.

Bisdom, E.B.A., L.W. Dekker and J.F.T. Schoute. 1993. *Water Repellency of Sieve Fractions from Sandy Soils and Relationships with Organic Material and soil structure.* Geoderma 56:105-118.

Bradford, S.A., and F.J. Leij. 1995. *Fractional Wettability Effects on Two-and Three-fluid Capillary Pressure-Saturation Relations.* Journal of Contaminant Hydrology 20:89-109.

Bradford, S.A., L.M. Abriola, and F.J. Leij. 1997. *Wettability Effects on Two- and Three-Fluid Relative Permeabilities.* Journal of Contaminant Hydrology 28:171-191.

Carrillo, M.L.K., J. Letey, and S.R. Yates. 1999. *Measurement of Initial Soil-Water Contact Angle of Water Repellent Soils.* Soil Science Society of America Journal 63:433-436.

Carrillo, M.L.K., J. Letey, and S.R. Yates. 2000a. *Unstable Water Flow in a Layered Soil: I. Effects of a Stable Water-Repellent Layer.* Soil Science Society of America Journal 64:450-455.

Carrillo, M.L.K., J. Letey, and S.R. Yates. 2000b. *Unstable Water Flow in a Layered Soil: II. Effects of an Unstable Water-Repellent Layer.* Soil Science Society of America Journal 64:456-459.

Carter, M.R. 1993. *Soil Sampling and Methods of Analysis.* Canadian Society of Soil Science, Lewis Publishers. Boca Raton, FL. 823p.

Cerdà, A. and S. Doerr. 2007. *Soil Wettability, Runoff and Erodibility of Major Dry-Mediterranean Land Use Types on Calcareous Soils.* Hydrological Processes 21:2325-2336.

Cheng, P., D.L.L. Boruvka, Y. Rotenberg, and A.W. Neumann. 1990. *Automation of Axisymmetric Drop Shape Analysis for Measurements of Interfacial Tensions and Contact Angles.* Colloids and Surfaces 43:151-167.

Chibowski, E. 2007. *On Some Relations Between Advancing, Receding and Young's Contact Angles.* Advances in Colloid and Interface Science 133:51-59.

Clothier, B.E. and I. White. 1980. *Measurement of Sorptivity and Soil Water Diffusivity in the Field.* Soil Science Society of America Journal 45:241-245.

Clothier, B.E., G.N. Magesan, L. Heng, and I. Vogeler. 1996. *In situ Measurement of the Solute Adsorption Isotherm using a Disc Permeameter.* Water Resources Research 32(4):771-778.

Clothier, B.E., I. Vogeler and G.N. Magesan. 2003. *The Breakdown of Water Repellency and Solute Transport through a Hydrophobic Soil.* In: Soil Water Repellency: Occurrence, Consequences, and Amelioration. Eds: C.j. Ritsema and L.W. Dekker. Elsevier. Wageningen, Netherlands.

Cobos, D.R. 2009. *Calibrating ECH$_2$0 Soil Moisture Sensors.* [online] Decagon Devices Application Notes. Available: www.decagon.com/pdfs/app_notes/CalibratingECH2OSoilMoistureProbes.pdf (Accessed: August, 2009).

Cook, F.J. and A. Broeren. 1994. *Six Methods for Determining Sorptivity and Hydraulic Conductivity with Disc Permeameters.* Soil Science 157(1):2-11.

Debano, L.F. 1975. *Infiltration, Evaporation, and Water Movement as Related to Water Repellency* in: Soil Conditioners: Proceedings of a symposium on Experimental Methods and Uses of Soil Conditioners. November 15-16, 1973, Las Vegas, Soil Science Society America Special Publication Series 7, Madison WI: 155-163, 186 p.

Debano, L.F. 1981. *Water Repellent Soils: A State-of-the-Art.* Forest Service General Technical Report: PSW-46. Berkeley, CA: United States Department of Agriculture, Pacific Southwest Forest and Range Experiment Station. 22 p.

DeBano, L.F. 2003. *The Role of Fire and Soil Heating on Water Repellency in Wildland Environments: A review.* In: Soil Water Repellency: Occurrence, Consequences, and Amelioration. 2003. Eds: C.j. Ritsema and L.W. Dekker. Elsevier. Wageningen, Netherlands.

Decker, E.L., B. Frank, Y. Suo, and S. Garoff. 1999. *Physics of Contact Angle Measurement.* Colloids and Surfaces A: Physicochemical and Engineering Aspects 156:177-189.

de Gennes, P.G. 1985. *Wetting: Statics and Dynamics.* Reviews of Modern Physics 57(3):827-863.

Dekker, L., and C. Ritsema. 1994. *How Water Moves in a Water Repellent Sandy Soil 1. Potential and Actual Water Repellency*. Water Resources Research 30(9):2507-2517.

Dekker, L.W. and C. Ritsema. 1996. *Variation in Water Content and Wetting Patterns in Dutch Water Repellent Peaty Clay and Clayey Peat Soils.* Catena 28:89-105.

Dekker, L.W. and C.J. Ritsema. 2003. *Wetting Patterns and Moisture Variability in Water Repellent Dutch Soils.* In: Soil Water Repellency: Occurrence, Consequences, and Amelioration. 2003. Eds: C.j. Ritsema and L.W. Dekker. Elsevier. Wageningen, Netherlands.

Dekker, L.W., S.H. Doerr, K. Oostindie, A.K. Ziogas, and C. Ritsema. 2001. *Water Repellency and Critical Soil Water Content in a Dune Sand.* Soil Science Society of America Journal 65:1667-1674.

del Río, O.I. and A. W. Neumann. 1997. *Axisymmetric Drop Shape Analysis: Computational Methods for the Measurement of Interfacial Properties from the Shape and Dimensions of Pendant and Sessile Drops.* Journal of Colloid and Interface Science 196:136-147.

Deurer, M. and J. Bachmann. 2007. *Modeling Water Movement in Heterogeneous Water-Repellent Soil: 2. A Conceptual Numerical Simulation.* Vadose Zone Journal 6:446-457.

Diehl, D. and G. Schaumann. 2007. *The Nature of Wetting on Urban Soil Samples: Wetting Kinetics and Evaporation Assessed from Sessile Drop Shape.* Hydrological Processes 21:2255-2265.

Dlapa, P., I. Simkovix Jr., S.H. Doerr, I. Simkovic, R. Kanka, and J. Mataix-Solera. 2008. *Application of Thermal Analysis to Elucidate Water-Repellency Changes in Heated Soils.* Soil Science Society of America Journal 72:1-10.

Doerr, S.H. 1998. *On Standardising the "Water Drop Penetration Time" and the "Molarity of an Ethanol Droplet" Techniques to Classify Soil Hydrophobicity: A Case Study Using Medium Textured Soils.* Earth Surface Processes and Landforms 23: 663-668.

Doerr, S.H. and J.A. Moody. 2004.*Hydrological Effects of Soil Water Repellency: On Spatial and Temporal Uncertainties.* Hydrological Processes 18:829-832.

Doerr, S.H. and A.D. Thomas. 2003. *The Role of Soil Moisture in Controlling Water Repellency: New Evidence from Forest Soils in Portugal.* In: Soil Water Repellency: Occurrence, Consequences, and Amelioration. Eds: C.j. Ritsema and L.W. Dekker. Elsevier. Wageningen, Netherlands.

Doerr, S.H., R.A. Shakesby and R.P.D. Walsh. 2000. *Soil Water Repellency: Its Causes, Characteristics and Hydro-Geomorphological Significance.* Earth-Science Reviews 51:33-65.

Doerr, S.H., W.H. Blake, R.A. Shakesby, F. Stagnitti, S.H. Vuurens, G.S. Humphreys, and P. Wallbrink. 2004. *Heating Effects on Water Repellency in Australian Eucalypt Forest Soils and their Value in Estimating Wildfire Soil Temperatures.* International Journal of Wildland Fire 13:157-163.

Doerr, S.H., P. Douglas, R.C. Evans, C.P. Morley, N.J. Mullinger, R. Bryant, and R.A. Shakesby. 2005. *Effects of Heating and Post-Heating Equilibration Times on Soil Water Repellency.* Australian Journal of Soil Research 43:261-267.

Doerr, S.H., R.A. Shakesby, W.H. Blake, C.J. Chafer, G.S. Humphreys, and P.J. Wallbrink. 2006. *Effects of Differing Wildfire Severities on Soil Wettability and Implications for Hydrological Response.* Journal of Hydrology 319:295-311.

Doerr, S.H., C.J. Ritsema, L.W. Dekker, D.F. Scott and D. Carter. 2007. *Water repellence of soils: New insights and emerging research needs.* Hydrological Processes 21:2223-2228.

Douglas, P., K. Mainwaring, C. Morley and S. Doerr. 2007. *The Kinetics and Energetics of Transitions Between Water Repellent and Wettable Soil Conditions: A Linear Free Energy Analysis of the Relationship Between WDPT and MED/CST.* Hydrological Processes 21:2248-2254.

Dussan, E.B.V. 1979. *On the Spreading of Liquids on Solid Surfaces: Static and Dynamic Contact Lines.* Annual Reviews in Fluid Mechanics 11:371-400.

Ellerbrock, R. H., Gerke, H. H., Bachmann, J., Goebel, M.-O. 2005. *Composition of Organic Matter Fractions for Explaining Wettability of Three Forest Soils.* Soil Science Society of America Journal 69:57-66.

Environment Canada. 2009. [online] Canadian Climate Normals 1971-2000: Sudbury A Ontario. Available: www.climate.weatheroffice.ec.gc.ca/climate_normals (Accessed: April, 2009).

Felton, G.K. 1992. *Soil Water Response Beneath a Tension Infiltrometer: Computer Simulation.* Soil Science 154(1):14-24

Feng, G.L., Letey, J., Wu, L. 2001. *Water Ponding Depths Affect Temporal Infiltration Rates in a Water-Repellent Sand.* Soil Science Society of America Journal 65:315-320.

Ferreira, A.J.D., C.O.A. Coelho, R.P.D. Walsh, R.A. Shakesby, A. Ceballos and S.H. Doerr. 2003. *Hydrological Implications of Soil Water-Repellency in Eucalyptus Globulus Forests, North-Central Portugal.* In: Soil Water Repellency: Occurrence, Consequences, and Amelioration. Eds: C.j. Ritsema and L.W. Dekker. Elsevier. Wageningen, Netherlands.

Fidanza, M.A., J.L. Cisar, S.J. Kostka, J.S. Gregos, M.J. Schlossberg and M. Franklin. 2007. *Preliminary Investigation of Soil Chemical and Ohysical Properties Associated with Type-I Fairy Ring Symptoms in Turfgrass.* Hydrological Processes 21:2285-2290.

Franco, C.M.M., M. E. Tate and J. M. Oades. 1995. *Studies on non-Wetting Sands. I. The Role of Intrinsic Particulate Organic Matter in the development of Water Repellency in non-Wetting Sands.* Australian Journal of Soil Research 33:253-263.

Gerald, C.F. and P.O. Wheatley. 1984. *Applied Numerical Analysis (3rd ed).* Addison-Wesley Publishing Company, Don Mills, ON. 579p.

Goebel, M. J. Bachmann, S.K. Woche, W.R. Fischer, and R. Horton. 2004. *Water Potential and Aggregate Size Effects on Contact Angle and Surface Energy.* Soil Science Society of America Journal 68:383-393.

Goebel, M., S.K. Woche, J. Bachmann, A. Lamparter and W.R. Fischer. 2007. *Significance of Wettability-Induced Changes in Microscopic Water Distribution for Soil Organic Matter Decomposition.* Soil Science Society of America Journal 71:1593-1599.

Good, R. J. 1992. *Contact Angle, Wetting, and Adhesion: A Critical Review.* Journal of Adhesion Science and Technology 6(12)1269-1302.

Hallett, P.D., N. Nunam, J.T. Douglas, and I.M. Young. 2004. *Millimeter-Scale Spatial Variability in Soil Water Sorptivity: Scale, Surface Elevation, and Subcritical Repellency Effects.* Soil Science Society of America Journal 68:352-358.

Hillel, D. 1982. *Introduction to Soil Physics.* Academic Press. Toronto, ON. 364p.

Hoofar, M. and A.W. Neumann. 2004. *Axisymmetric Drop Shape Analysis (ADSA) for the Determination of Surface Tension and Contact Angle*. Journal of Adhesion 80:727-743.

Hoofar, M. and A.W. Neumann. 2006. *Recent Progress in Axisymmetric Drop Shape Analysis (ADSA).* Advances in Colloid and Interface Science 121:25-49.

Horne, D.J. and McIntosh. 2003. *Hydrophobic Compounds in Sands from New Zealand.* In: Soil Water Repellency: Occurrence, Consequences, and Amelioration. Eds: C.j. Ritsema and L.W. Dekker. Elsevier. Wageningen, Netherlands.

Huffman, E.L., L.H. MacDonald and J.D. Stednick. 2001. *Strength and Persistence of Fire-Induced Soil Hydrophobicity Under Ponderosa and Lodgepole Pine, Colorado Front Range.* Hydrological Processes 15:2877-2892.

Hwang, S.I., K. P. Lee, D.S. Lee, and S.E. Powers. 2006. *Effects of Fractional Wettability on Capillary Pressure-Saturation-Relative Permeability Relations of Two-Fluid Systems.* Advances in Water Resources 29:212:216.

Imeson, A.C., J.M Verstaten, E.J. van Mulligen, and J. Sevink. 1992. *The Effects of Fire and Water Repellency on Infiltration and Runoff under Mediterranean Type Forest.* Catena 19:345-361.

Johnson, R.E. Jr. and R.H. Dettre. 1964. *Contact Angle Hysteresis I. Study of an Idealized Rough Surface. In:* R.F. Gould (ed.) Contact Angle, wettability and adhesion.Advances in Chemistry Series 43, American Chemical Society. Washington, DC.

Keizer, J.J., S.H. Doerr, M.C. Malvar, A.J.D. Ferreira and V.M.F.G. Pereira. 2007. *Temporal and Spatial Variations in Topsoil Water Repellency Throughout a Crop-Rotation Cycle on Sandy Soil in North-Central Portugal.* Hydrological Processes 21:2317-2324.

King PM. 1981. *Comparison of Methods for Measuring Severity of Water Repellence of Sandy Soils and Assessment of Some Factors that Affect its Measurement.* Australian Journal of Soil Research 19:275–285.

Kobayashi, M. and T. Shimizu. 2007. *Soil Water Repellency in a Japanese Cypress Plantation Restricts Increases in Soil Water Storage During Rainfall Events.* Hydrological Processes 21:2356-2364.

Kwok, D.Y., T. Gietzelt, K. Grundke, H.-J. Jacobasch, and A.W. Neumann. 1997. *Contact Angle Measurements and Contact Angle Interpretation. 1. Contact Angle Measurements by Axisymmetric Drop Shape Analysis and a Goniometer Sessile Drop Technique.* Langmuir 13:2880-2894.

Kwok, D.Y., C.N.C. Lam, A. Li, A. Leung, R. Wu, E. Mok, and A.W. Neumann. 1998. *Measuring and Interpreting Contact Angles: A Complex Issue.* Colloids and Surfaces A: Physicochemical Engineering Aspects 142:219-235.

Leelamanie, D.A.L. and J. Karube. 2007. *Effects of Organic Compounds, Water Content and Clay on the Water Repellency of a Model Sandy Soil.* Soil Science and Plant Nutrition 53:711-719.

Leighton-Boyce, G., S.H. Doerr, R.A. Shakesby and R.P.D. Walsh. 2007. *Quantifying the Impact of Soil Water Repellency on Overland Flow generation and erosion: A New Approach Using Rainfall Simulation and Wetting Agent on* in situ *Soil.* Hydrological Processes 21:2337-2345.

Letey, J. 2001. Causes and Consequences of Fire-Induced Soil Water Repellency. Hydrological Processes 15:2867-2875.

Letey, J., M.L.K. Carrillo and X.P. Pang. 2003. *Approaches to Characterize the Degree of Water Repellency.* In: Soil Water Repellency: Occurrence, Consequences, and Amelioration. 2003. Eds: C.j. Ritsema and L.W. Dekker. Elsevier. Wageningen, Netherlands, p 51-57.

Lewis, S.A., J.Q. Wu, and P. Robichaud. 2006. *Assessing Burn Severity and Comparing Soil Water Repellency, Hayman Fire, Colorado.* Hydrological Processes 20:1-16.

Lewis, S.A. P.R. Robichaud, B.E. Frazier, J.Q. Wu, D.M Laes. 2008. *Using Hyperspectral Imagery to Predict Post-Wildfire Water Repellency.* Geomorphology 95:192-205.

Lichner, L., P.D. Hallett, D.S. Feeney, O. Dugova, M. Sir, and M. Tesar. 2007. *Field measurement of Soil Water Repellency and its Impact on Water Flow Under Different Vegtation.* Biologia 62/5:537-541.

Likos, W.J. and N Lu. 2004. *Hysteresis of Capillary Stress in Unsaturated Granular Soil.* Journal of Engineering Mechanics 130(6): 646-655.

Logsdon, S.D. 1997. *Transient Variation in the Infiltration Rate During Measurement with Tension Infiltrometers.* Soil Science 162(4):233-241.

MacDonald, L.H. and Edward L. Huffman. 2004. *Post-fire Soil Water Repellency: Persistence and Soil Moisture Thresholds.* Soil Science Society of America Journal 68:1729-1734.

Marmur, A. 2006. *Soft Contact: Measurement and Interpretation of Contact Angles.* Royal Society of Chemistry: Soft Matter 2:12-17.

Martin, D.A. and J.A. Moody. 2001. *Comparison of soil infiltration rates in burned and unburned mountainous watersheds.* Hydrological Processes 15:2893-2903.

Mataix-Solera, J., V. Arcenegui, C. Guerrero, A.M. Mayoral, J. Morales, J. González, F. García-Orenes and I. Gómez. 2007. *Water Repellency Under Different Plant Species in a Calcareous Forest Soil in a Semiarid Mediterranean Environment.* Hydrological Processes 21:2300-2309.

McHale, G., N.J. Shirtclifee, and Mi.I. Newton. 2004. *Contact-angle Hysteresis on Super-Hydrophobic Surfaces.* Langmuir 20:10146-10149.

McHale, G., N.J. Shirtcliffe, M.I. Newton, B. Pyatt, and S.H. Doerr. 2007. *Self-Organization of Hydrophobic Soil and Granular Surfaces.* American Institute of Physics: Applied Physics Letters 90, 0541110:1-3.

McNabb, D.H., F. Gaweda, and H.A. Froehlich. 1989. *Infiltration, Water Repellency, and Soil Moisture Content after Broadcast Burning a Forest Site in Southwest Oregon.* Journal of Soil and Water Conservation 44(1):87-90.

Merion, T.S., A. Marmur, and I.S. Saguy. 2004. *Contact Angle Measurement on Rough Surfaces.* Journal of Colloid and Interface Science 274:637-644.

Miyata, S., K. Kosugi, T. Gomi, Y. Onda and T. Mizuyama. 2007. *Surface Runoff as Affected by Soil Water Repellency in a Japanese Cypress Forest.* Hydrological Processes 21:2365-2376.

Murray, M.D. and B.W. Darvell. 1990. *A Protocol for Contact Angle Measurement.* Journal of Physics D: Applied Physics 23:1150-1155.

Naasz, R., J.-C. Michel, and S. Charpentier. 2008. *Water Repellency of Organic Growing Media Related to Hysteretic Water Retention Properties.* European Journal of Soil Science 59:156-165.

National Wildlife Coordinating Group (NWCG). 2001. *Fire Effects Guide.* [online] National Interagency Fire Center publication: NFES 2394. Boise, ID. Available: http://www.nwcg.gov/pms/RxFire/FEG.pdf (Accessed: June, 2009).

O'Carroll, D.M., L.M. Abriola, C.A. Polityka, S.A. Bradford, and A.H. Demond. 2005. *Prediction of Two-Phase Capillary Pressure-Saturation Relationships in Fractional Wettability Systems.* Journal of Contaminant Hydrology 77:247-270.

Ontario Ministry of Natural Resources: Sudbury District Ministry of Natural Resources. 2008. *Halfway Lake Provincial Park Natural Disturbances* [map]. Version 1.0. 1:30,000. Sudbury, ON: Queen's Printer for Ontario 2008.

Ontario Ministry of Natural Resources: Ontario Parks, Northeast Zone. 2009. *Halfway Lake Landscape Disturbances* [digital map]. Version 1.0. Sudbury, ON: Queen's Printer for Ontario 2009.

Orfanus, T., Z. Bedrna, L., Lichner, P.D. Hallet, K. Kňava, and M. Sebíň. *Spatial Variability of Water Repellency in Pine Forest Soil.* Soil and Water Research 3(1):S123-S129.

Pierson, F.B., P.R. Robichaud, C.A. Moffet, K.E. Spaeth, C.J. Williams, S.P. Hardegree, and P.E. Clark. 2008. *Soil Water Repellency and Infiltration in Coarse-Textured Soils of Burned and Unburned Sagebrush Ecosystems.* Catena 74:98-108.

Quyum, A., G. Achari, and R.H. Goodman. 2002. *Effect of Wetting and Drying and Dilution on Moisture Migration Through Oil Contaminated Hydrophobic Soils.* Science of the Total Environment 296:77-87.

Regalado, C.M. and A. Ritter. 2009. *A Soil Water Repellency Empirical Model.* Vadose Zone Journal 8:136-141.

Reynolds, W.D. 2006. Tension Infiltrometer Measurements: Implications of Pressure Head Offset due to Contact Sand. Vadose Zone Journal 5:1287-1292.

Reynolds, W.D. and Elrick, D.E. 1991. *Determination of Hydraulic Conductivity Using a Tension Infiltrometer.* Soil Science Society of America Journal 55:633-639.

Ritsema, C. and L. Dekker. 1994. *How Water Moves in a Water Repellent Sandy Soil 2. Dynamics of Fingered Flow.* Water Resources Research 30(9):2519-2531.

Robichaud, P.R. 2003. *Fire Effects on Infiltration Rates after Prescribed Fire in Northern Rocky Mountain Forests, USA.* In: Soil Water Repellency: Occurrence, Consequences, and Amelioration. Eds: C.j. Ritsema and L.W. Dekker. Elsevier. Wageningen, Netherlands.

Robichaud, P.R., S.A. Lewis, and L.E. Ashmun. 2008. *New Procedure for Sampling Infiltration to Assess Post-fire Soil Water Repellency.* Res. Note. RMRS-RN-33. Fort Collins, CO: U.S. Department of Agriculture, Forest Service, Rocky Mountain Research Station. 14 p.

Rodríguez-Alleres, M., E. Benito and E. deBlas. 2007. *Extent and Persistence of Water Repellency in North-Western Spanish Soils.* Hydrological Processes 21:2291-2299.

Rodríguez-Valverde, M.A. Caberizo-Vílchez, P. Rosales-López, A. Páez-Dueñas, R.Hidalgo-Álvarez. 2002. *Contact Angle Measurements on Two (Wood and Stone) non-Ideal Surfaces.* Colloids and Surfaces A: Physicochemical Engineering Aspects 206:485-495.

Rosso, R., M.C. Rulli, and D. Bocchiola. 2007. *Transient Catchment Hydrology after Wildfires in a Mediterranean Basin: Runoff, Sediment, and Woody Debris.* Hydrological Earth Systems Science 11(1):125-140.

Roy, J.L., W.B. McGill. 2002. *Assessing Soil Water Repellency Using the Molarity of Ethanol Droplet (MED) Test.* Soil Science 167:83-97.

Schaumann, G.E., E. Hobley, J. Burraß, and W. Rotard. 2005. *H-NMR Relaxometry to Monitor Wetting and Swelling Kinetics in High-Organic Matter Soils.* Plant and Soil 275:1-20.

Schaumann, G., B. Braun, D. Kirchner, W. Rotard, U. Szewzyk and E. Grohmann. 2007. *Influence of Biofilms on the Water Repellency of Urban Soil Samples.* Hydrological Processes 21:2276-2284.

Scott, D.F. 2000. *Soil Wettability in Forested Catchments in South Africa; as Measured by Different Methods and as Affected by Vegetation Cover and Soil Characteristics.* In: Soil Water Repellency: Occurrence, Consequences, and Amelioration. 2003. Eds: C.j. Ritsema and L.W. Dekker. Elsevier. Wageningen, Netherlands

Shakesby, R.A., S.H. Doerr and R.P.D. Walsh. 2003. *The Erosional Impact of Soil Hydrophobicity: Current Problems and Future Research Directions.* Journal of In: Soil Water Repellency: Occurrence, Consequences, and Amelioration. Eds: C.j. Ritsema and L.W. Dekker. Elsevier. Wageningen, Netherlands.

Soil Moisture Systems (SMS). 2006. Tension Infiltrometer. [online] Available: http://www.soilmeasurement.com/tension_infil.html. (Accessed: May, 2009).

Taumer, K., H. Stoffregen and G. Wessolek. 2005. *Determination of Repellency Distribution Using Soil Organic Matter and Water Content.* Geoderma 125:107-115.

Tillman, R.W., D.R Scott, M.G. Wallis, and B.E. Clothier. 1989. *Water-Repellency and its Measurement by Using Intrinsic Sorptivity.* Australian Journal of Soil Research 27:637-644.

Valat, B., C. Jouany, and L.M. Riviere. 1991. *Characterization of the Wetting Properties of Air-Dried Peats and Composts.* Soil Science 152 (2):100-107

van Dam, J.C., J.H.M. Wösten, A. Nemes. 1996. *Unsaturated Soil Water Movement in Hysteretic and Water Repellent Soils.* Journal of Hydrology 184:153-173.

Verheijen, F.G.A. and L.H. Cammeraat. 2007. *The Association Between Three Dominant Shrub Species and Water Repellent Soils along a Range of Soil Moisture Contents in Semi-Arid Spain.* Hydrological Processes 21:2310-2316.

Wallach, R. and E.R. Graber. 2007. *Infiltration into Effluent Irrigation-Induced Repellent Soils and the Dependence of Repellency on Ambient Relative Humidity.* Hydrological Processes 21:2346-2355.

Wang, Z., L. Wu, C.J. Ritsema, L.W. Dekker and J. Feyen. 2000. *Effects of Soil Water Repellency on infiltration Rate and Flow Instability.* Journal of Hydrology 231-232:265-276.

Woodward, R.P. 2008a. *Contact Angle Measurements Using the Drop Shape Method.* [online] First Ten Angstroms, Portsmouth, VA. Available: http://firsttenangstroms.com/pdfdocs/CAPaper.pdf (Accessed: January, 2008).

Woodward, R.P. 2008b. *Surface Tension Measurements Using the Drop Shape Method.* [online] First Ten Angstroms, Portsmouth, Va. Available: http://firsttenangstroms.com/pdfdocs/STPaper.pdf (Accessed: January, 2008).

Yeh, YK., LJ. Chen, and JY. Chang. 2008. *Contact Angle Hysteresis on Regular Pillar-like Hydrophobic Surfaces.* Langmuir 24:245-251.

Young, T. 1805. *An Essay on the Cohesion of Fluids.* Philosophical Transactions of the Royal Society of London 95:65-87.